CRISPR-Cas9 Engineering for Improvement and Development of Blood Cell-Based Gene Therapy

Dissertation
der Mathematisch-Naturwissenschaftlichen Fakultät
der Eberhard Karls Universität Tübingen
zur Erlangung des Grades eines
Doktors der Naturwissenschaften
(Dr. rer. nat.)

vorgelegt von
Guillermo Ureña Bailén
aus Jaén, Spanien

Tübingen
2023

Gedruckt mit Genehmigung der Mathematisch-Naturwissenschaftlichen Fakultät der Eberhard Karls Universität Tübingen.

Tag der mündlichen Qualifikation: 06.07.2023
Dekan: Prof. Dr. Thilo Stehle
1. Berichterstatter: Prof. Rupert Handgretinger
2. Berichterstatter: Prof. Alexander Weber

INDEX

1. Abbreviations

A

Acetoxymethyl ester (AM)
Acute myeloid leukemia (AML)
Adeno-associated virus (AAV)
Adoptive cell transfer (ACT)
Adult hemoglobin (HbA)
American Society for Bone Marrow Transplant (ASBMT)

B

B-cell lymphocytic leukemia (B-ALL)
B-cell lymphoma/leukemia 11A (BCL11A)
β-globin gene (HBB)

C

Casitas B-lineage lymphoma proto-oncogene-b (CBLB)
Chimeric antigen receptor (CAR)
Clustered regulatory interspaced short palindromic repeats (CRISPR)
Colony forming unit (CFU)
CRISPR-associated protein 9 (Cas9)
CRISPR RNA (crRNA)
Cytokine release syndrome (CRS)

D

Double-stranded break (DSB)
Deoxyribonucleic acid (DNA)

E

Effector-to-target cell ratio (E:T)

F

Fetal hemoglobin (HbF)

G

Good manufacturing practice (GMP)
Graft-versus-host disease (GvHD)
Genome-wide, Unbiased Identification of DSBs Enabled by Sequencing (GUIDE-seq)

H

Hematopoietic stem and progenitor cell (HSPC)
Hematopoietic stem cell transplantation (HSCT)
High-performance liquid chromatography (HPLC)
Homology direct repair (HDR)
Host-versus-graft (HvG)

I

Insertions and deletions (InDel)
Immunoreceptor tyrosine-based inhibitory motif (ITIM)

K

Killer cell lectin-like receptor C1 (KLRC1)
Knock-out (KO)

N

Natural killer (NK)
Non-homologous end joining (NHEJ)
Non-transfected control (NTC)

P

Protospacer adjacent motif (PAM)
Peripheral blood mononuclear cell (PBMC)

R

Ribonucleic acid (RNA)
Ribonucleoprotein (RNP)

S

Sickle cell disease (SCD)

Sickle hemoglobin (HbS)

Single-chain variable fragment (ScFv)

Single guide ribonucleic acid (SgRNA)

T

T cell immunoreceptor with Ig and ITIM domains (TIGIT)

T cell Engineering (TCE)

Test-cuvette adaptor (TCA)

Trans-activating crRNA (trcrRNA)

Transfusion-dependent thalassemia (TDT)

Tumor-associated antigen (TAA)

2. Summary

In the past few years, the CRISPR-Cas9 system has emerged as one of the most valuable and versatile technologies for efficient gene editing. Its advantageous features offer a wide range of applications, including the development of human therapy for the treatment of cancer and genetic diseases. In this context, blood cells are ideal candidates for CRISPR modification as their isolation is less invasive than the procedures required for other tissues. These cells can be suitably expanded and engineered *ex vivo*, then subjected to careful analysis in standardized conditions to ensure successful genetic modification and cellular fitness, and finally, infused into the patient.

In the first project of this thesis, CRISPR-Cas9 was employed to enhance the effector function of NK-92 cells for leukemia treatment (AML and B-ALL) in combination or absence of a chimeric antigen receptor (CD19-CAR and CD276-CAR). Up to three different inhibitory checkpoints (CBLB, NKG2A, and TIGIT) were knocked out in the NK-92 cell lines. These targets were selected given the relevance of their inhibitory pathways in cancer immunotherapy and the fact that both receptors and ligands are highly expressed in NK-92 and cancer cells, respectively. The resulting knock-out cells were further tested by *in vitro* assays against malignant cell lines to corroborate the potential anticancer benefit derived from the corresponding genetic modification. While NKG2A knock-out did not boost the killing performance, CBLB and TIGIT knock-outs showed promising enhanced cytotoxicity against AML. Future experiments in animal models would conclude whether the implementation of these genetic improvements can boost NK-92 cell-based immunotherapy against leukemia *in vivo*.

In the second project, the main objective was the generation of a protocol for the automation of efficient CRISPR-Cas9 gene editing of HSPCs in the GMP-compatible device CliniMACS® Prodigy for the treatment of β-hemoglobinopathies following the same gene editing strategy as the CTX001 treatment. Together with our partners from Miltenyi Biotec, we pursued a thorough protocol optimization to achieve efficient gene editing, and it led to a clinical-scale proof-of-concept study that resulted in suitable BCL11A editing and restoration of HbF expression. The generated protocol will support the development of novel treatments for patient care as it can be easily transferred to other genetic diseases, and will potentially increase the accessibility of gene therapy in the near future.

3. Zusammenfassung

In den letzten Jahren hat sich das CRISPR-Cas9-System als eine der wertvollsten und vielseitigsten Technologien für effizientes Gene Editing erwiesen. Seine vorteilhaften Eigenschaften bieten eine breite Palette potenzieller Anwendungen, einschließlich der Entwicklung menschlicher Therapien für die Behandlung von Krebs und genetischen Krankheiten. In diesem Zusammenhang sind Blutzellen ideale Kandidaten für die CRISPR-Veränderung, da ihre Isolierung weniger invasiv ist als die für andere Gewebe erforderlichen Verfahren. Diese Zellen können in geeigneter Weise expandiert und ex vivo modifiziert werden. Anschließend werden sie unter standardisierten Bedingungen einer sorgfältigen Analyse unterzogen, um eine erfolgreiche genetische Veränderung und zelluläre Fitness sicherzustellen, und schließlich dem Patienten infundiert.

Im ersten Projekt dieser Arbeit wurde CRISPR-Cas9 eingesetzt, um die Effektorfunktion von NK-92-Zellen für die Leukämiebehandlung (AML und B-ALL) in Kombination oder in Abwesenheit eines chimären Antigenrezeptors (CD19-CAR und CD276-CAR) zu verbessern. In den NK-92-Zelllinien wurden bis zu drei verschiedenen hemmenden Immun-Checkpoints (CBLB, NKG2A und TIGIT) ausgeschaltet. Diese Targets wurden aufgrund der Relevanz ihrer Hemmwege für die Krebsimmuntherapie und der Tatsache ausgewählt, dass sowohl die Rezeptoren als auch die Liganden in NK-92-Zellen bzw. Krebszellen stark exprimiert sind. Die resultierenden Knock-out-Zellen wurden in In-vitro-Tests gegen bösartige Zelllinien getestet, um den potenziellen Nutzen der entsprechenden genetischen Veränderung für die Krebsbehandlung zu bestätigen. Während der Knock-out von NKG2A die Abtötungsleistung nicht erhöhte, zeigten die Knock-outs von CBLB und TIGIT eine vielversprechende erhöhte Zytotoxizität gegen AML. Zukünftige Experimente in Tiermodellen werden zeigen, ob die Implementierung dieser genetischen Verbesserungen die Immuntherapie mit NK-92-Zellen gegen Leukämie in vivo verbessern kann.

Im zweiten Projekt bestand das Hauptziel darin, ein Protokoll für die Automatisierung der effizienten CRISPR-Cas9-Gene-Editierung von HSPCs im GMP-konformen CliniMACS® Prodigy-Gerät für die Behandlung von β-Hämoglobinopathien zu erstellen, wobei dieselbe Gene-Editierungsstrategie wie bei der Behandlung mit CTX001 angewandt wurde. Gemeinsam mit unseren Partnern bei Miltenyi Biotec haben wir eine gründliche Optimierung des Protokolls durchgeführt, um eine effiziente Gen-Editierung zu erreichen. Das Ergebnis war eine Proof-of-Concept-Studie im klinischen Maßstab, die zu einer angemessenen BCL11A-Editierung und Wiederherstellung der HbF-Expression führte. Das entwickelte Protokoll wird die Entwicklung neuartiger Behandlungen für die Patientenversorgung unterstützen, da es leicht auf andere genetische Krankheiten übertragen werden kann, und es wird möglicherweise die Zugänglichkeit der Gentherapie in naher Zukunft verbessern.

4. Publications

4.1 Accepted publications

1. **Ureña-Bailén G***, Block M*, Grandi T, et al. Automated Good Manufacturing Practice-Compatible CRISPR-Cas9 Editing of Hematopoietic and Progenitor Stem Cells for Clinical Treatment of β-hemoglobinopathies. *The CRISPR Journal*. 2023. DOI:10.1089/crispr.2022.0086

2. Mohammadian Gol T, **Ureña-Bailén G**, Hou Y, et al. CRISPR medicine for blood disorders: Progress and challenges in delivery. *Frontiers in Genome Editing*. 2023. DOI: 10.3389/fgeed.2022.1037290

3. Hou Y, **Ureña-Bailén G**, Mohammadian Gol T, et al. Challenges in Gene Therapy for Somatic Reverted Mosaicism in X-Linked Combined Immunodeficiency by CRISPR/Cas9 and Prime Editing. *Genes*. 2022:13;2348. DOI: 10.3390/genes13122348

4. **Ureña-Bailén G**, Dobrowolski JM, Hou Y, et al. Preclinical Evaluation of CRISPR-Edited CAR-NK-92 Cells for Off-the-Shelf Treatment of AML and B-ALL. *International Journal of Molecular Sciences*. 2022;23. DOI: 10.3390/ijms232112828

5. **Ureña-Bailén G**, Antony JS, Hou Y, et al. CRISPR Medicine: Advance, Progress and Challenges In: CRISPR-/Cas9 Based Genome Editing for Treating Genetic Disorders and Diseases. (Vaschetto LM; ed). CRC Press, Boca Raton. 2022.

6. Hou Y, Gratz HP, **Ureña-Bailén G,** et al. Somatic Reversion of a Novel IL2RG Mutation Resulting in Atypical X-Linked Combined Immunodeficiency. *Genes*. 2021;13. DOI: 10.3390/genes13010035

7. Antony JS, Daniel-Moreno A, Lamsfus-Calle A, et al. A Mutation-Agnostic Hematopoietic Stem Cell Gene Therapy for Metachromatic Leukodystrophy. *The CRISPR Journal*. 2022:66-79. DOI: 10.1089/crispr.2021.0075

8. Grote S, **Ureña-Bailén G**, Chan KC, et al. In Vitro Evaluation of CD276-CAR NK-92 Functionality, Migration and Invasion Potential in the Presence of Immune Inhibitory Factors of the Tumor Microenvironment. *Cells*. 2021;10. DOI: 10.3390/cells10051020

9. Lamsfus-Calle A, Daniel-Moreno A, **Ureña-Bailén G,** et al. Universal Gene Correction Approaches for β-hemoglobinopathies Using CRISPR-Cas9 and Adeno-Associated Virus Serotype 6 Donor Templates. *The CRISPR Journal*. 2021;4:207-222. DOI: 10.1089/crispr.2020.0141

10. **Ureña-Bailén G**, Lamsfus-Calle A, Daniel-Moreno A, et al. CRISPR/Cas9 technology: towards a new generation of improved CAR-T cells for anticancer therapies. *Briefings in Functional Genomics*. 2020;20:191-200. DOI: 10.1093/bfgp/elz039

11. Lamsfus-Calle A, Daniel-Moreno A, **Ureña-Bailén G,** et al. Hematopoietic stem cell gene therapy: The optimal use of lentivirus and gene editing approaches. *Blood Reviews*. 2020;40. DOI: 10.1016/j.blre.2019.100641

4.2 Manuscripts in preparation

1. **Ureña-Bailén G**, Rupprecht J, Malenke E, et al. BCL11A CRISPR-Cas9 editing is stable and maintained along various blood cell subpopulations in β-hemoglobinopathies patients treated with CTX001.

4.3 Poster presentations

1. **Ureña-Bailén G**, Lamsfus-Calle A, Daniel-Moreno A, et al. Establishing a Cell and Gene Therapy Platform for the Treatment of Various Diseases in Pediatrics. Poster presented at Forschungskolloquium der Medizinischen Fakultät; 17th October 2022; CRONA Klinik, Tübingen, Germany.

2. **Ureña-Bailén G**, Lamsfus-Calle A, Daniel-Moreno A, et al. Generation of CRISPR-improved T cells for production of more efficient and safer CAR-T cells. Poster presented at Retreat der Forschungsgruppen; 15th November 2019; Schloss Reisensburg, Günzburg, Germany.

4.4 Contribution to the publications that comprise this thesis

4.4.1 Preclinical evaluation of CRISPR-edited CAR-NK-92 cells for off-the-shelf treatment of AML and B-ALL

For this manuscript, I proposed and performed the experimental design for CBLB, NKG2A, and TIGIT knock-outs (Figure 4). The original idea was conceptualized by Dr. Justin S. Antony, Dr. Markus Mezger, and me, and was initially investigated and explored by Dr. medic. Jérôme-Maurice Dobrowolski and M.Sc. Alicia Dirlam. I performed all CRISPR-Cas9 gene-editing experiments shown in this publication, including parental and CAR-NK-92 electroporation in the Neon® Transfection System and the MaxCyte GTx™ electroporator. Dr. Alicia Roig-Merino aided in the optimization of the CRISPR-Cas9 transfection efficiency and supported all protocols performed with the MaxCyte GTx™ electroporator. Additionally, I performed gene editing assessment by ICE and flow cytometry analyses, contributed to the receptor characterization of effector and target cell lines, which was mainly performed by Dr. medic. Jérôme-Maurice Dobrowolski, and carried out Western blot analyses of CBLB together with Dr. Tahereh Mohammadian Gol. I performed all luciferase and calcein-based assays using AML and B-ALL cell lines (Figure 3, Figure 5, and Figure 6) counting with the help of M.D. Yujuan Hou. CAR transductions were performed by Dr. Judith Feucht and Dr. Sabine Schleicher. Generation of luciferase-expressing leukemic cell lines was performed by M.Sc. Daniel Atar, Dr. Christian Seitz and Dr. Judith Feucht. I performed the statistical analyses with the aid of M.D. Yujuan Hou and Dr. Tahereh Mohammadian Gol, and presented the data in tables and figures. I wrote the complete first draft of the manuscript, which was further improved and revised by Dr. Markus Mezger, Dr. Justin S. Antony, and Dr. Rupert Handgretinger.

4.4.2 Automated good manufacturing practice-compatible CRISPR-Cas9 editing of hematopoietic and progenitor stem cells for clinical treatment of β-hemoglobinopathies

In this manuscript, I share the first authorship with M.Sc. Milena Block. I was involved in the experimental design of the conducted research, which was mainly proposed by Dr. Markus Mezger, Dr. Rupert Handgretinger, and Dr. Stefan Wild, and performed HSPCs erythroid differentiations and marker characterizations besides ICE assessments of BCL11A gene editing, including PCR and samples preparation. I aided in the optimization of the electroporation conditions and the CliniMACS® Prodigy large-scale production of edited HSPCs, which was mainly performed by M.Sc. Milena Block and M.Sc. Tommaso Grandi. The small-scale and upscale experiments were performed by M.Sc. Milena Block, M.Sc. Tommaso Grandi, M.Sc. Faidra Aivazidou, M.Sc. Jona Quednau, M.Sc. Dariusz Krenz, Dr. Alberto Daniel-Moreno, and Dr. Andrés Lamsfus-Calle. I analyzed the hemoglobin HPLC data generated by Dr. Thomas Epting, performed the freezing/thawing gene editing and viability assessments (Figure 3), and substantially contributed to the writing of the manuscript, which was prepared together with M.Sc. Milena Block, and eventually reviewed and improved by Dr. Stefan Wild, Dr. Markus Mezger, and Dr. Rupert Handgretinger. I organized the data in all tables and figures shown in the manuscript.

4.5 Declaration according to § 5 Abs. 2 No. 8 of the Ph.D. regulations of the Faculty of Science for Collaborative Publications

For Cumulative Thesis Only!

Last name, First name: Ureña-Bailén, Guillermo

List of publications:

1. **Guillermo Ureña-Bailén**, Jérôme-Maurice Dobrowolski, Yujuan Hou, Alicia Dirlam, Alicia Roig-Merino, Sabine Schleicher, Daniel Atar, Christian Seitz, Judith Feucht, Justin S. Antony, Tahereh Mohammadian Gol, Rupert Handgretinger and Markus Mezger. Preclinical Evaluation of CRISPR-Edited CAR-NK-92 Cells for Off-the-Shelf Treatment of AML and B-ALL. International Journal of Molecular Sciences. 2022;23. DOI: 10.3390/ijms232112828

2. **Guillermo Ureña-Bailén*,** Milena Block*, Tommaso Grandi, Faidra Aivazidou, Jona Quednau, Dariusz Krenz, Alberto Daniel-Moreno, Andrés Lamsfus-Calle, Thomas Epting, Rupert Handgretinger, Stefan Wild† and Markus Mezger†. Automated Good Manufacturing Practice-Compatible CRISPR-Cas9 Editing of Hematopoietic and Progenitor Stem Cells for Clinical Treatment of β-hemoglobinopathies. The CRISPR Journal. 2023. DOI:10.1089/crispr.2022.0086

EBERHARD KARLS
UNIVERSITÄT
TÜBINGEN

Mathematisch-Naturwissenschaftliche Fakultät

Nr.	Accepted publication?	Author list	Candidate position in author list	Scientific ideas by the candidate (%)	Data generation by the candidate (%)	Analysis and interpretation by the candidate (%)	Paper writing done by the candidate (%)
1	Yes	**Guillermo Ureña-Bailén**, Jérôme-Maurice Dobrowolski, Yujuan Hou, Alicia Dirlam, Alicia Roig-Merino, Sabine Schleicher, Daniel Atar, Christian Seitz, Judith Feucht, Justin S. Antony, Tahereh Mohammadian Gol, Rupert Handgretinger and Markus Mezger	First	80%	70%	90%	90%
2	Yes	**Guillermo Ureña-Bailén***, Milena Block*, Tommaso Grandi, Faidra Aivazidou, Jona Quednau, Dariusz Krenz, Alberto Daniel-Moreno, Andrés Lamsfus-Calle, Thomas Epting, Rupert Handgretinger, Stefan Wild† and Markus Mezger†	First shared	40%	30%	60%	60%

I confirm that the above stated is correct

_____

Date, signature of the candidate

I/We certify that the above stated is correct

_____

Date, signature of the doctoral committee or at least one of the supervisors

5. Introduction

5.1 CRISPR-Cas9 system

The well-known clustered regularly interspaced short palindromic repeat (CRISPR) was identified as an adaptive immune system of bacteria against bacteriophages. The system comprises CRISPR-associated proteins (Cas proteins) which cut foreign DNA into small pieces that will be concatenated in a CRISPR array.[1-3] When transcribed, the resulting RNA is processed and the individual CRISPR RNAs (crRNAs) are separated with the aid of a trans-activating crRNA (trcrRNA).[1, 4-6] Both crRNA and trcrRNA associate with the Cas protein to generate double-stranded breaks (DSBs) and cut invasive DNA molecules when a suitable protospacer adjacent motif (PAM) is present.[7]

The biotechnology derived from the CRISPR/Cas system allows for targeted gene editing with the help of a guide RNA (gRNA) that combines both crRNA and trcrRNA in the same sequence.[8] When delivering the system into the cells, the selective cutting produces a DSB in the target sequence that has to be repaired to avoid cellular death.[9-11] The break is very likely to be solved by the non-homologous end joining (NHEJ) repair mechanism, leading to insertions and deletions (InDel) of random nucleotides in the sequence (Figure 1A).[10, 12] Under certain circumstances, homology-directed repair (HDR) pathway is available when a donor template is present, resulting in a precise correction of the DSB by homologous recombination (Figure 1A).[3, 13]

These features suitably allow the addition, correction, and/or knock-out of genes of interest, opening boundless possibilities for the treatment of genetic human diseases (Figure 1B). However, this technology is not infallible as the off-target effect (the CRISPR-related cuts occurring elsewhere in the genome except the intended target) is still a major concern and undesired chromosomal rearrangements derived from DSBs can lead to unwanted modifications and oncogenesis.[14-16] Improved CRISPR-based technologies such as more precise Cas proteins or the novel prime editing approach can help optimizing the specificity and safety of the gene therapy while maintaining or increasing the editing efficiency.[17, 18]

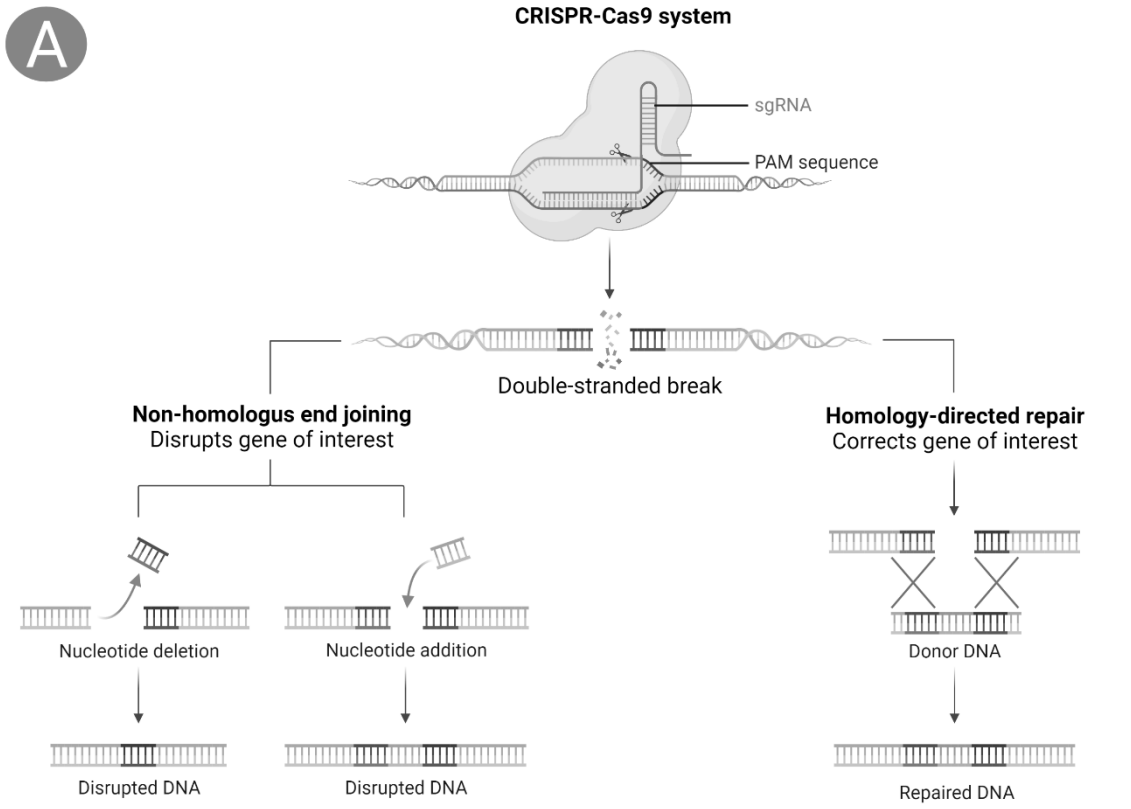
A
CRISPR-Cas9 system
sgRNA
PAM sequence
Double-stranded break
Non-homologus end joining
Disrupts gene of interest
Homology-directed repair
Corrects gene of interest
Nucleotide deletion
Nucleotide addition
Donor DNA
Disrupted DNA
Disrupted DNA
Repaired DNA

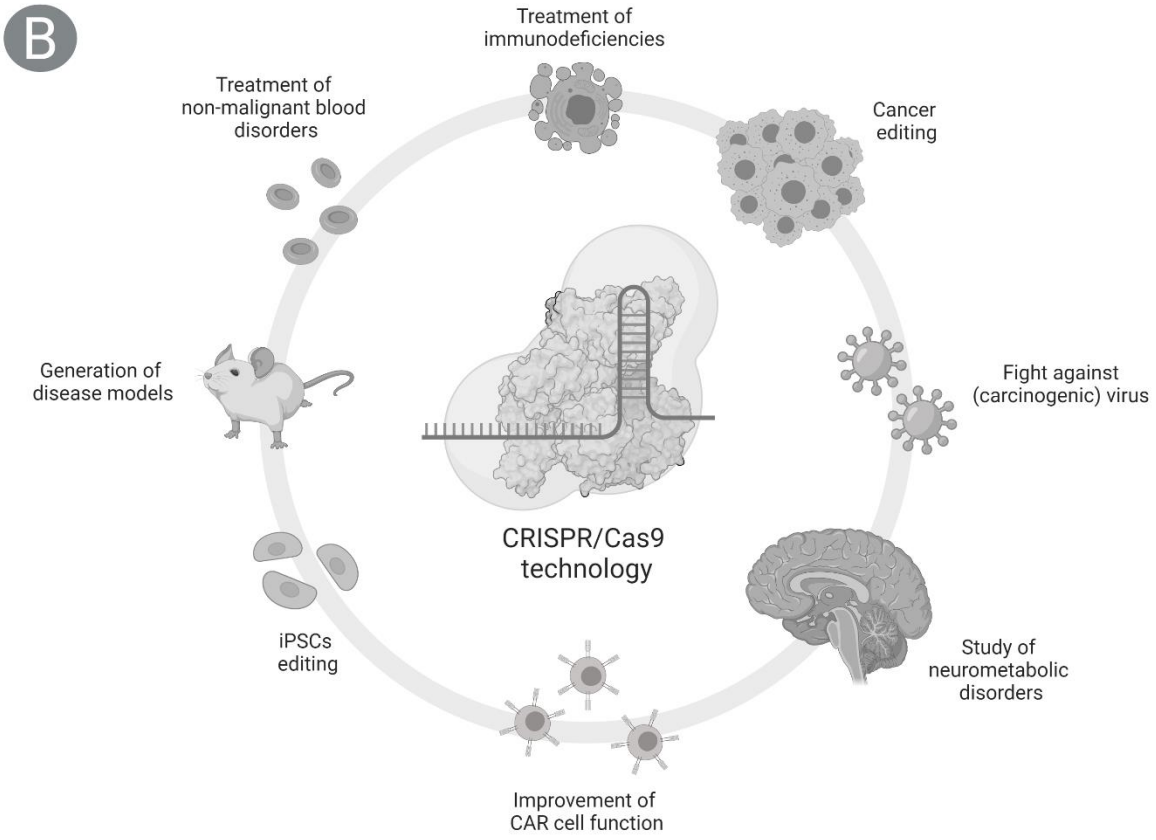
B
Treatment of immunodeficiencies
Treatment of non-malignant blood disorders
Cancer editing
Generation of disease models
Fight against (carcinogenic) virus
CRISPR/Cas9 technology
iPSCs editing
Study of neurometabolic disorders
Improvement of CAR cell function

Figure 1: A) CRISPR-Cas9 system molecular mechanism and its main applications. When the sgRNA anneals to its target sequence and a protospacer adjacent motif (PAM) is recognized, the Cas9 protein generates a double-stranded break (DSB) in the DNA sequence that needs to be solved to continue with the cell cycle. Non-homologous end joining (NHEJ) pathway repairs the DSB by random insertions and deletions of nucleotides and favors the disruption of the gene of interest, whereas homology-directed repair (HDR) leads to gene correction in the presence of a donor DNA template. This figure was created with BioRender.com. B) Fields of application of the CRISPR-Cas9 technology in human medicine include the treatment of blood disorders, cancer immunotherapy, and improvement of CAR therapies, among others. This figure was generated with Biorender.com by the thesis author and was published in *CRISPR-/Cas9 Based Genome Editing for Treating Genetic Disorders and Diseases* book by CRC Press. The figure is reproduced in this thesis with permission of the licensor through PLSclear.

5.2 Gene therapy for cancer and blood disorders

5.2.1 NK-92 immunotherapy for cancer treatment

5.2.1.1 Cancer disease and conventional treatments

Cancer disease is one of the most devastating pathologies worldwide, annually causing millions of deaths, and is expected to increase its incidence in the coming years.[19] It is a complex disorder generated by genetic predisposition, mutagenic agents (ionizing radiation, viral infections, and carcinogens, among others), or spontaneous mutations that disrupt the proper control of the cell cycle and leads to unrestrained proliferation, replicative immortality, resistance to cell death, avoidance of immune destruction and many other features known as the hallmarks of cancer (Figure 2).[20, 21] As a result, the immune system is unable to constrain the malignancy and the normal functions and homeostasis of the surrounding tissues are progressively affected (being distant healthy tissues also affected in the case of metastasis), which ultimately leads to the systemic collapse of the organism and consequent death. There are many different types of cancer depending on the genes mutated and the kind of cells involved in the development of the disease. Such heterogeneity conforms the main challenge for the establishment of universal treatment, even for the same type of malignancy.[22]

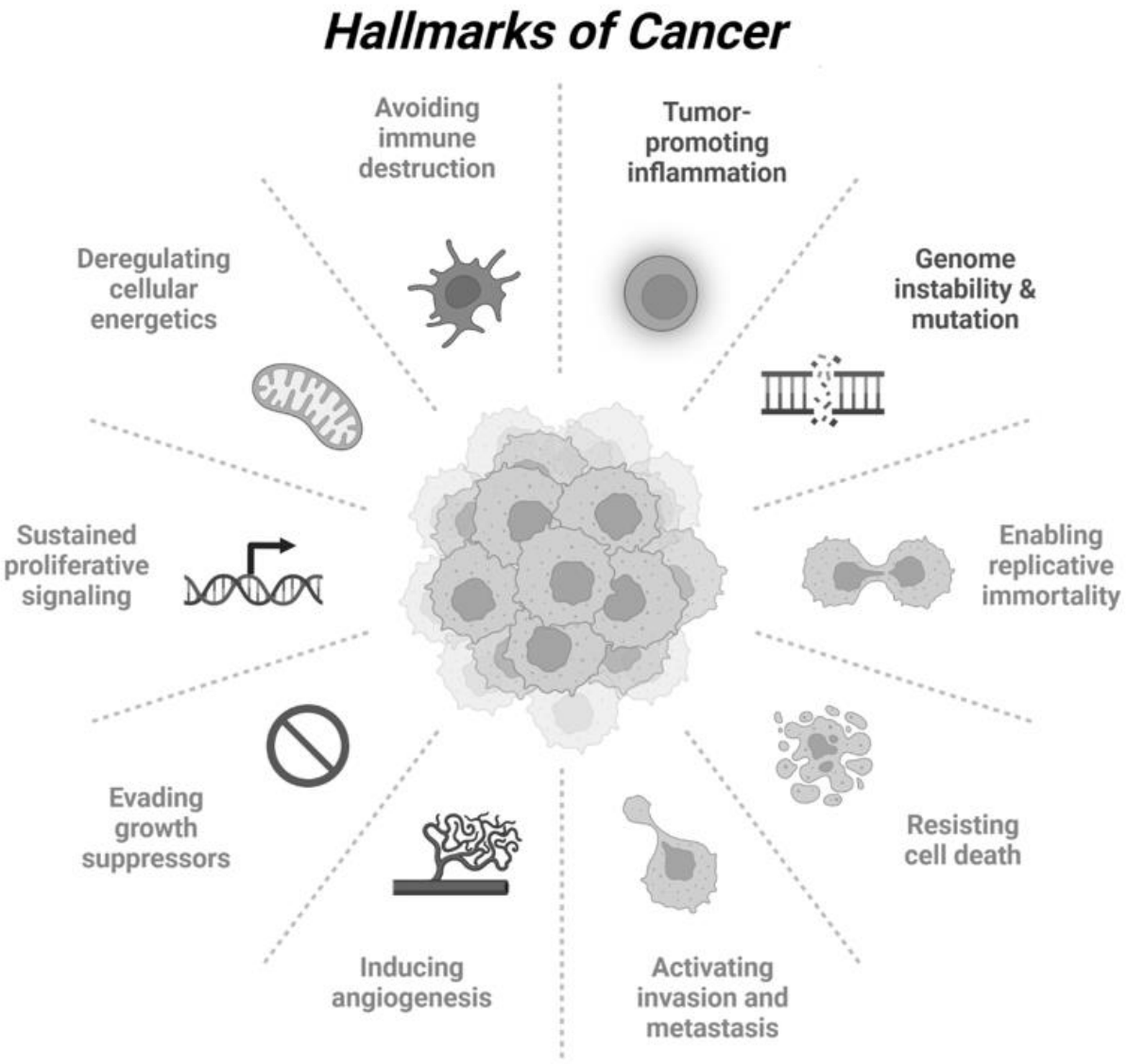

Figure 2: The hallmarks of cancer include all features and events leading to the development of the malignancy. The main characteristics include unrestrained proliferation, uncontrolled growth, angiogenesis induction, invasion and metastasis, resistance to cellular death, and replicative immortality. The enabling factors leading to cancer progression involve the avoidance of immune destruction and deregulation of the energetic metabolism. Additionally, tumor-promoting inflammation and genome instability favor cancer development. This figure was created with BioRender.com.

Leukemia is a heterogeneous group of clonal disorders caused by the uncontrolled proliferation of blood progenitor cells arrested in a certain stage of their development. A proportion greater than 20% of blasts in the peripheral blood or bone marrow leads to acute leukemia, the most aggressive form of the disease that results in a rapid onset of symptoms.[23-25] The disease is classified attending to the cellular lineage of the malignant blasts. This work investigates B-ALL, leukemia involving B-cell precursor blasts, and AML, consisting of the

malignant proliferation of stem cell precursors of the myeloid lineage.[25, 26] ALL is the most frequent malignancy in children, whereas AML is the most prevalent blood cancer in adults, accounting for 80% of all cases.[23-25]

Traditional treatments for leukemia include chemotherapy, radiation, monoclonal antibodies, or allogeneic HSCT.[27] The lack of specificity for chemotherapy and radiation approaches results in higher risks of relapse and suffering from severe side effects which can drastically reduce the quality of life of the patient.[28, 29] Allogeneic HSCT brings GvHD and derived toxicities which can be life-threatening.[30, 31] Consequently, more effective and safer targeted strategies have been studied and developed to enhance and use the immune system against leukemia.

5.2.1.2 CAR therapy: T cells or NK cells?

CAR immunotherapy is based on the transgenic expression of specific membrane chimeric receptors able to recognize an overexpressed antigen in the malignant cells by an extracellular single-chain variable fragment (ScFv). The recognition strongly activates the effector function of the immune cell through the activation of an intracellular domain, with no further need for additional activator signals. CARs enhance tumor-associated antigen (TAA) recognition by enabling the identification of intact cell surface proteins, meaning that cancer targeting would not be restricted to MHC recognition or antigen presentation. This fact avoids common escape mechanisms such as HLA loss or altered processing mechanisms.[32, 33] Additionally, different TAAs not susceptible to being presented in the MHC can be properly recognized by the CAR.

As the main orchestrators of the immune system, T cells have important effector functions against cancer including clonal expansion, tissue migration, immunomodulation, cytotoxicity, and long-lasting T cell memory.[34] As a result, autologous and heterologous CAR-T cells have been extensively studied for the treatment of cancer, reaching very promising milestones for the treatment and cure of leukemia.[35, 36] The persistence of the CAR-T cells in the organism can last for decades, functioning as a surveillance mechanism to prevent potential relapses.[37] However, there are important severe side effects to consider, such as CRS, neurotoxicity, graft rejection, and iatrogenic responses, that might hinder the safe clinical application.[38, 39]

Despite not offering the persistence of T cells, NK cells are suitable CAR carriers and mighty cancer killers unable to generate severe systemic immune responses that could lead

to CRS and neurotoxicity.[40] As they are inherently cytotoxic against cancer cells, they are still effective when the CAR target is downregulated as an escape mechanism from resistant cancer cells.[41] Moreover, they can be obtained from unmatched MHC donors, but isolating clinically-relevant numbers from primary sources can be challenging since they represent a small population in the blood (circa 10% of isolated PBMCs).[42]

5.2.1.3 Off-the-shelf NK-92 immunotherapy

NK-92 is an NK cell line originally isolated from the peripheral blood of a 50-year-old male patient with rapidly progressive non-Hodgkin's lymphoma. Interestingly, the NK-92 cell line, like other NK cell lines such as NK-101 or KHYG-1, maintains the cytotoxic function against cancer cells and can be cultured indefinitely with a periodic supplementation of interleukin 2. Their use for clinical treatment was considered by irradiating the cells at 10 Gy to induce chromosomal damage that would stop their unrestrained proliferation. Therefore, the infused cells are not able to persist in the body, but their cytotoxic function remains active.[43, 44] This fact makes the use of a single dose for effective treatment unlikely, but the need for multiple administrations can help to determine the optimal dosage according to the observed outcome in the patient after each infusion.[45]

The use of cell lines such as NK-92 for immunotherapy brings substantial benefits. This IL-2 dependent cell line exhibits high cytolytic activity, lacks the majority of KIR inhibitory receptors, and provides an unlimited source of effector cells, offering valuable options when autologous transplantations are not possible and it is hard to find a suitable donor.[42, 45, 46] The everlasting availability of the effector cells can translate into faster treatment implementations compared to the weeks or months needed for primary cell-based therapy, being ideal for off-the-shelf and ready-to-use approaches. Moreover, cell line-based therapies are more affordable to produce, as the whole manufacturing process can cost ten times less while producing multiple infusions.[42] Consequently, clinical and preclinical research with NK-92 and other cell lines can lead to more accessible personalized cancer therapy for patient care.

5.2.1.4 NK cell inhibitory checkpoint knock-out for enhancing immunotherapy by CRISPR-Cas9

The disruption of immune checkpoints was previously explored with blocking antibodies that would occupy the target receptor without transducing the corresponding inhibitory signal to the cell. As a result, the communication between cancer and immune cells is suppressed and the immune function is maintained.[47] Following a similar strategy, the gene knock-out of the immune inhibitory receptor to abolish the pathway permanently was proposed as a feasible

alternative. This approach avoids the potential immune adverse events related to the systemic administration of blocking antibodies that could interfere with other immune functions in the organism (i.e. on-target off-tumor effect) while preventing immunosuppression, but also presents the disadvantage of potential autoimmunity derived from the disruption of the immune cell checkpoint.[48, 49] To reduce such risk, it is crucial to combine this strategy with a CAR-targeted approach to ensure the specificity of the treatment or with short-lasting infusion-based treatments, such as NK cell immunotherapy, where the effector cells do not persist for a long time in the organism of the patient and pertinent adjustments can be made for subsequent doses to avoid severe autoimmune reactions. Alternatively, researchers have also considered the implementation of inducible suicide mechanisms for the controllable shutdown of the therapy.[50, 51]

The inhibitory checkpoint molecules studied in this thesis are listed below. They are known to play a key role in cancer immunotherapy and are targets of interest for the effective treatment of leukemia.[52-58]

- Casitas B-lineage lymphoma proto-oncogene-b (CBLB) is a non-redundant negative regulator of immune activation which functions as an E3 ubiquitin ligase. Like other ligases from its family, CBLB interacts with protein tyrosine kinases via protein–protein interaction domains. It is mostly expressed in peripheral lymphoid organs, suggesting a prominent role in the regulation of adaptive immune responses and the maintenance of peripheral tolerance.[59] Its ablation has been shown to improve T cell anticancer function.[60, 61] In NK cells, its regulatory function is associated with the TAM receptor family (Tyro3, Axl, and Mer).[62] When the TAM receptor binds to its ligand Gas6, it phosphorylates CBLB and blocks NK cell activation by ubiquitylation of LAT1.[63] This blockage can be surpassed by two synergistic activating signals such as NKG2D and CD244.[64] CBLB KO improved NK cell cytotoxicity in leukemic models and its knock-down enhanced the expression of perforin, granzyme B, and IFN-γ.[52, 53]

- NKG2A is a single-pass type 2 membrane glycoprotein that belongs to the C-type lectin superfamily. It is found to associate in a heterodimer with CD94, forming a receptor of non-classical MHC class I molecules such as HLA-E (normally overexpressed in cancer cells).[65] The ligand interaction leads to the phosphorylation of ITIMs in NKG2A, which actively recruit and activate SHP-1 and SHP-2 phosphatases, thus suppressing the activation signals generated by activating receptors such as NKG2D.[66] NKG2A KO enhanced NK cell cytotoxicity against multiple myeloma.[67] Similarly, NKG2A downregulation increases the effectivity of NK cell antitumor infusions.[68]

- T cell immunoreceptor with Ig and ITIM domains (TIGIT) is a receptor of the Ig superfamily. It takes part in a complex regulatory network involving multiple inhibitory receptors, one competing costimulatory receptor (DNAM-1/CD226), and multiple ligands such as CD155 and CD112.[69] TIGIT/CD155 interaction between NK and cancer cells leads to the downregulation of CD226.[70, 71] As a result, TIGIT expression is a marker of NK cell exhaustion in many cancer models and reduces NK cell functionality in humans.[71-73] Its blockade in combination with other inhibitory checkpoints proved to boost NK-92 cytotoxicity against AML.[56]

5.2.2 HSPCs editing for the treatment of β-hemoglobinopathies

5.2.2.1 B-hemoglobinopathies and conventional treatments

B-hemoglobinopathies are among the most widely spread genetic diseases in the world.[74] They are the result of β-globin gene mutations that lead to insufficient (β^+) or absent (β^0) production of β-globin chains, needed for the conformation of the adult hemoglobin and the normal function of erythrocytes (Figure 3). The most common disorders in this group are sickle cell disease (SCD) and β-thalassemia. In SCD, a single amino acid substitution in the β-globin gene (p.E6V) leads to the formation of abnormal HbS that tends to form pathogenic aggregates in hypoxic conditions, conferring fragility and stickiness to the red blood cells. As a result, vessel obstruction, hemolysis, and anemia are reported in SCD patients.[75] Therapies with hydroxycarbamide, erythrocyte transfusion, and HSPC transplantation are contemplated for patient treatment.[76] Concerning β-thalassemia, it is classified under three types depending on the phenotype and severity of the disease: thalassemia minor (heterozygous β-thalassemia with mild, microcytic hypochromic anemia), thalassemia intermedia (mild homozygous or mixed heterozygous β-thalassemia of moderate severity, with a varying need for transfusions) and thalassemia major (severe homozygous or mixed heterozygous β-thalassemia with long-term, transfusion-dependent anemia). Blood transfusions are usually needed to keep healthy hemoglobin levels in the patients. In the case of thalassemia major, HSPC transplantation is additionally considered for the cure of the disease, but the often-challenging search for a matching donor and the side effects of the supportive treatment with lifelong regular transfusions make this approach suboptimal.[77]

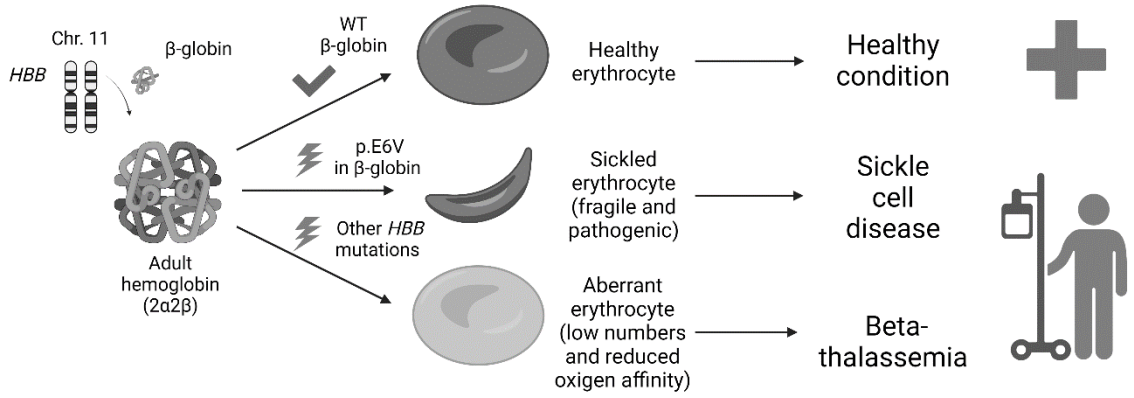

Figure 3: The β-globin takes part in the formation of adult hemoglobin. Healthy erythrocyte accounts for fully functional hemoglobin, whereas pathogenic conditions may be originated from aberrant β-globin subunits, including sickle cell disease and beta-thalassemia. This figure was created with BioRender.com.

5.2.2.2 Gene therapy for β-hemoglobinopathies

Novel gene therapy approaches were developed to avoid donor cells' scarcity, GvHD, and graft failure associated with allogeneic HSPC transplantation. The most straightforward strategy is based on the transfer of a copy of the healthy human β-globin gene into the autologous HSPCs of the patient by means of a lentiviral vector. The lentiviral delivery is quite efficient and suitable to achieve a therapeutic effect, showing clinical remission and remediation of the disease in two of the three treated patients with SCD, and reduced the frequency of transfusions in the third patient (clinical trials NCT02151526, NCT02633943, and NCT04628585).[78] On the other hand, the potential integration of the lentiviral construct in the genome increases the risk of oncogenesis.[79, 80] In this context, CRISPR-Cas9-directed repairs in combination with AAV vectors were investigated, leading to notable editing efficiencies and re-storage of HbA expression in patient cells in preclinical studies.[81]

Other strategies were based on the knock-out of fetal hemoglobin (HbF) repressors to emulate the benign condition of HbF persistence reported in some carriers of the β-globin mutation who did not suffer from β-hemoglobinopathies. Two hemoglobin switches occur during human development: from embryonic to fetal globins and later from fetal to adult.[82] To ensure the last hemoglobin switch, the repression of γ-globin expression is promoted in adult-stage erythroblasts.[82, 83] For the aforementioned individuals, the repression of γ-globin is disrupted and HbF expression is thereby reactivated. Recent clinical trials NCT03655678 and NCT03745287 have shown promising results using CTX001 treatment for the resurgence of HbF expression in the patients (Figure 4).[84] The strategy consists of the *ex vivo* editing of

patients' HSPCs inducing the disruption of the *BCL11A* enhancer by CRISPR-Cas9. This way, the expression of BCL11A is avoided and the production of HbF is restored as BCL11A is not suppressing the expression of γ-globin anymore (Figure 4). Patients treated with this strategy have been cured of the disease and increased their quality of life as they are now transfusion independent.[84]

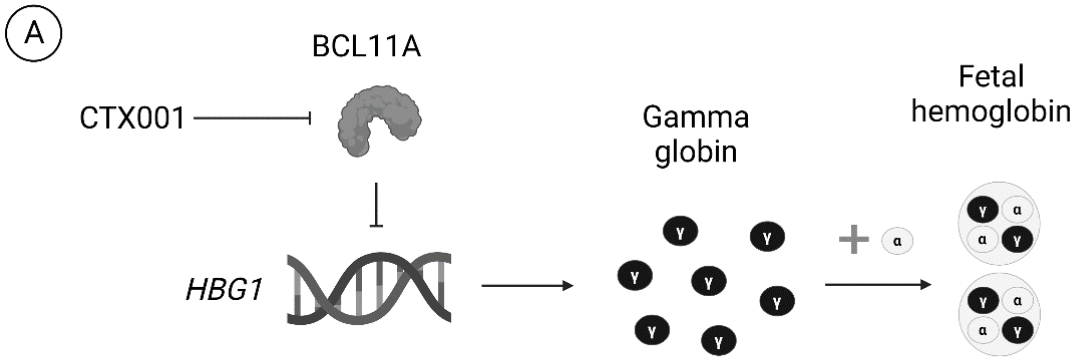

B

	Adult hemoglobin	Fetal hemoglobin
Healthy	Active and functional	Inactive
Patient	Active but aberrant	Inactive
Patient +CTX001	Active but aberrant	Reactivated and functional

Figure 4: A) CTX001 treatment relies on the CRISPR-induced knock-out of the BCL11A repressor to re-activate the expression of gamma-globin and consequently fetal hemoglobin. B) Status of adult and fetal hemoglobin in healthy and beta-hemoglobinopathies patients with or without CTX001 treatment. This figure was created with BioRender.com.

5.2.2.3 Automated CliniMACS® Prodigy with electroporator for gene therapy development

The development and production of cellular products for therapy can be automated in innovative closed systems such as the CliniMACS® Prodigy from Miltenyi Biotec (Figure 5).[85] Sterility is achieved thanks to a closed tubing circuit consisting of interconnected plastic bags, tubes, and containers that are installed on the system, such as the TS-520 (Miltenyi Biotec). Each tube connection is set between automatic pumps that control the flow of the cells, media, and reagents along the process. The tubing set provides a CentriCult Unit (CCU) to culture the cells which can additionally be centrifuged thanks to its rotor, allowing the change of mediums and reformulations needed for suitable cell culture. It also has a magnetic holder where a column for magnetic separation can be placed to facilitate the isolation of the target cells. All processes are controlled from the activity matrix of the software, which is defined by an external operator. Supplementary modules such as the CliniMACS® Electroporator and its EP-2 tubing set (Miltenyi Biotec) can be incorporated into the device, enabling the performance of additional processes like electroporation and CRISPR transfections.

These features make the CliniMACS® Prodigy a valuable technology as it can manufacture cellular products on its own while fulfilling GMP-grade standards. Relevant protocols using this equipment have already been developed for HSPC isolation for clinical application and the generation of CAR-T cells.[86, 87] Furthermore, economic analyses estimate CAR-T cell production costs to be affordable for low and middle-income pricing in developing countries using the CliniMACS Prodigy.[88]

The CliniMACS® Electroporator offers two electroporation set-ups. A test-cuvette adapter (TCA) is useful for the screening of different electroporation parameters at a small-scale that will aid in the search for the most efficient conditions (Figure 6A). It is ideal for initial pre-optimization experiments as it does not require the installation of the tubing set to be performed. On the other hand, the electroporation chamber of the EP-2 tubing set allows the cell processing of large-scale amounts of cells by means of cyclic electroporations (Figure 6B). The electroporation process is defined by 2 consecutive pulses: the first one, usually involving a higher voltage, is involved in the disruption of the cell membrane and opening of the pores, whereas the second one, of lower voltage but longer duration, is suited for facilitating the delivery of the transfection components into the cytoplasm and nucleus. Pulses can be delivered in a single pulse (*square* mode) or many pulses of short duration (*burst* mode). Depending on the change of the electric field, bipolar pulses are also available (*flip* pulse). An overview of different pulse combinations using the CliniMACS® Electroporator is depicted in Figure 6C.

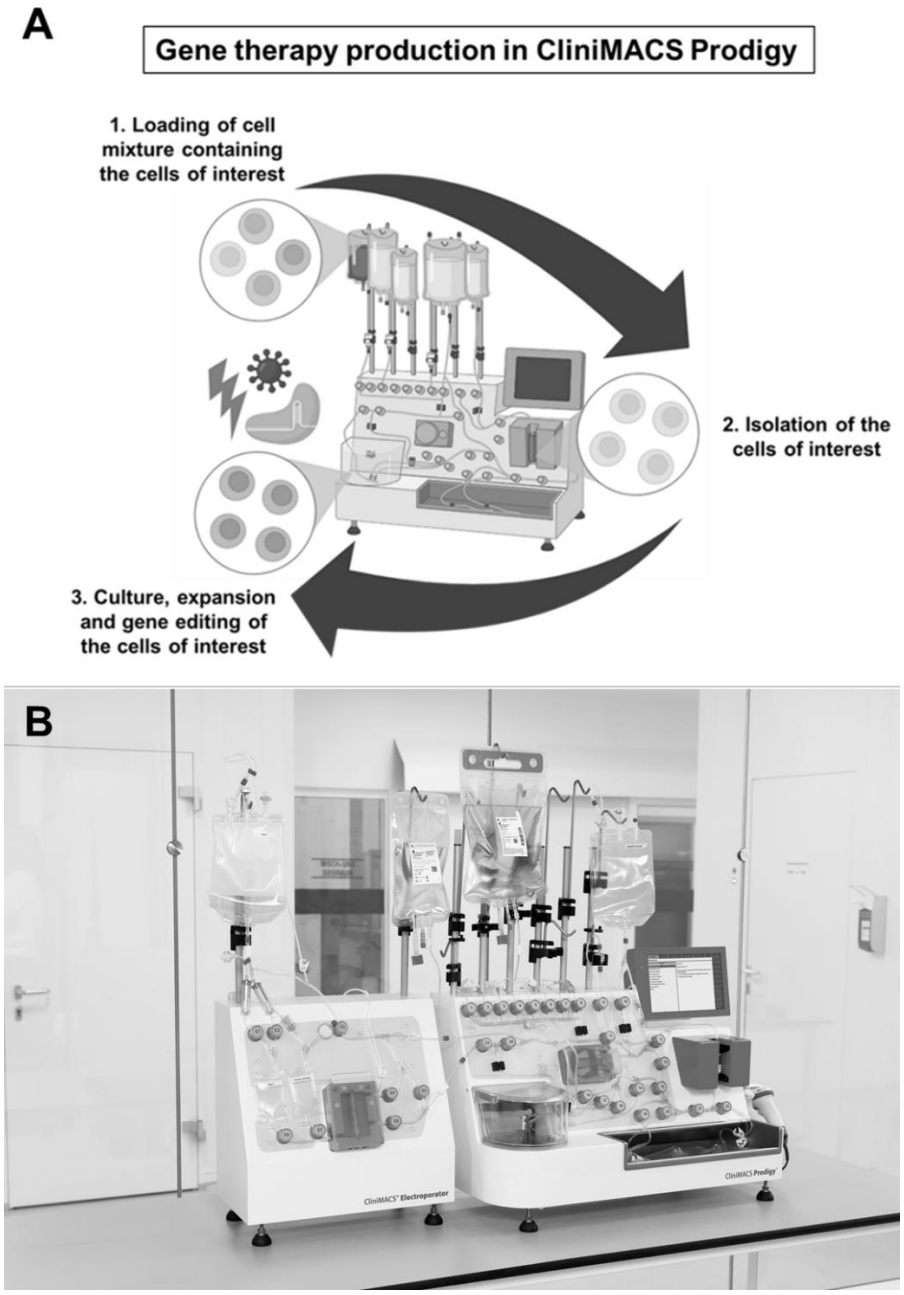

Figure 5: A) Schematic overview of the automated process on the CliniMACS® Prodigy® developing a blood-derived cellular product. Firstly, the cell mix is loaded in the cellular bag. The isolation of the cells of interest is performed in the cell separation column. In the next step, cells are transported back into the cell cultivation chamber inside the CentriCult Unit (CCU) for further culture and expansion. Additional modules, such as the CliniMACS® Electroporator (not depicted in the scheme), can as well be used for further downstream processes like cell electroporation and gene editing protocols. This figure was created with BioRender.com. B) CliniMACS® Prodigy instrument (right) connected to the CliniMACS® Electroporator (left). This figure was included for illustration and academic reasons. Copyright © 2023 Miltenyi Biotec B. V. & Co. KG. All rights reserved.

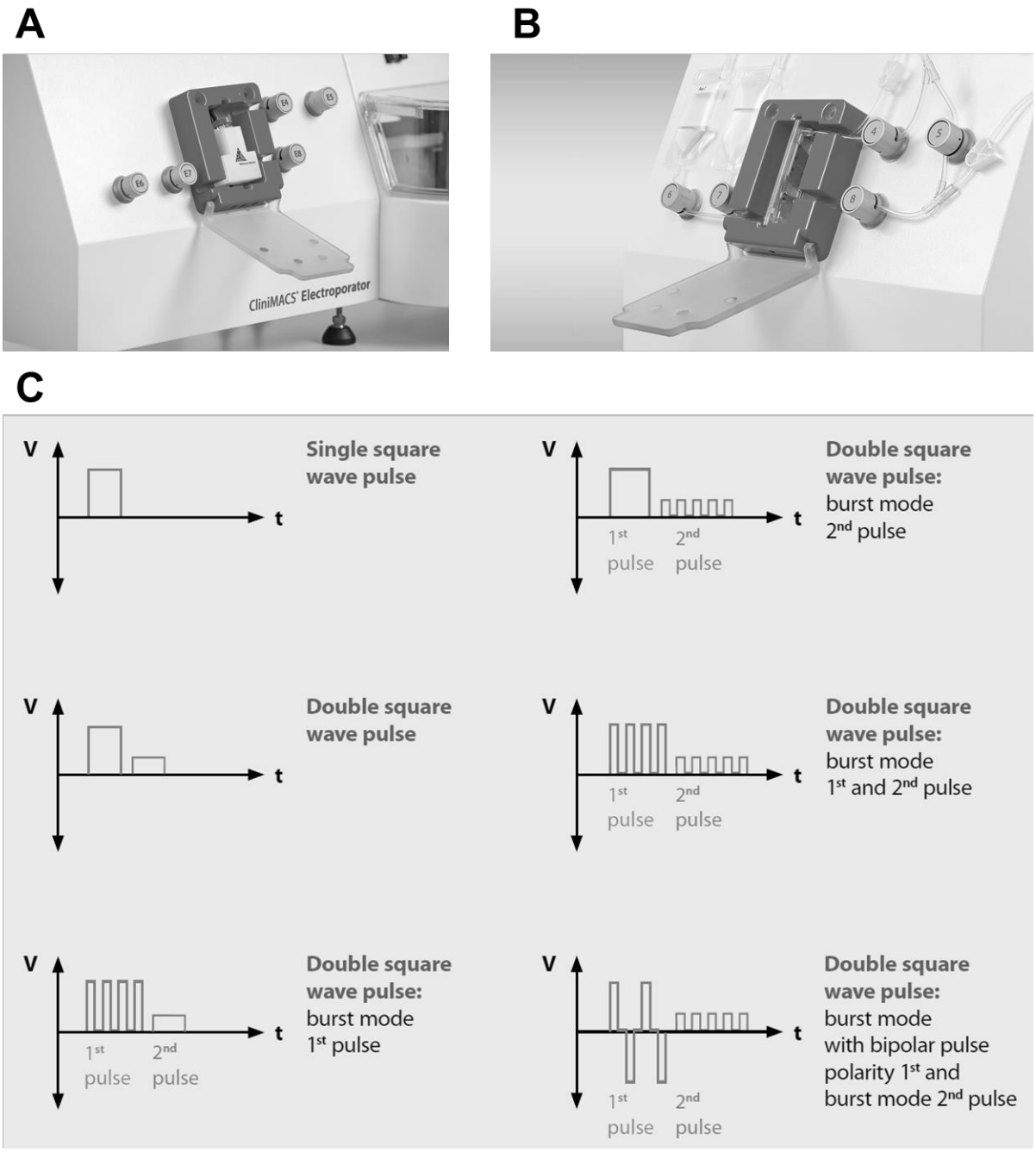

Figure 6: A) The Test-Cuvette Adaptor (TCA) placed in the electroporation unit of the CliniMACS® Electroporator for small-scale screenings. B) Electroporation unit housing the electroporation cuvette of the the CliniMACS® Prodigy® EP-2 Tubing Set for upscale and clinical-scale experiments. C) Different pulse combinations are available on the CliniMACS® electroporator. This figure was included for illustration and academic reasons. Copyright © 2023 Miltenyi Biotec B. V. & Co. KG. All rights reserved.

6. Objectives

In this Ph.D. thesis, two different projects were pursued.

- The objective of the first project focused on improving NK-92 cancer immunotherapy by disrupting different inhibitory checkpoints (CBLB, NKG2A, and/or TIGIT) using the CRISPR-Cas9 system. This approach was implemented alone or in combination with specific CARs (CD19-CAR or CD276-CAR) to boost cytotoxic activity against leukemia (B-ALL and AML).

- The main goal of the second project was the establishment of a standard transfection protocol for efficient CRISPR-Cas9 gene editing of HSPCs in the automated GMP-compliant CliniMACS® Prodigy for the treatment of β-hemoglobinopathies. To this aim, different optimization experiments were designed to discern the most suitable conditions for efficient CRISPR-Cas9 transfection in a clinical-scale scenario using the same gene editing strategy that was set up for the CTX001 treatment (studied in clinical trials NCT03655678 and NCT03745287) but reducing the number of open steps. This strategy is based on the *BCL11A* knock-out to rescue HbF expression to restore functional erythrocytes.

7. Results and discussion

7.1 Preclinical evaluation of CRISPR-edited CAR-NK-92 cells for off-the-shelf treatment of AML and B-ALL

7.1.1 CAR target and inhibitory ligand screening in leukemic target cell lines

The expression of different molecules across several leukemia cell lines was assessed in flow cytometry stainings for the identification of potential CAR targets and inhibitory pathways. For B-ALL, the cell lines KOPN-8, MHH-CALL-4, Nalm-6, and Nalm-6 GFP/Luc were analyzed. As expected, the expression of CD19 was high for all tested cell lines since they all derive from the B-cell lineage (95 – 100%).[89] This receptor is mostly targeted in CAR therapies against B-cell malignancies,[90] so it was reasonable to select an anti-CD19 CAR for this study. B-ALL cell lines also exhibited expression of inhibitory ligands, being Gal-9 the most abundantly expressed (50 – 100%). HLA-E and CD86 expression were highly expressed in KOPN-8 and MHH-CALL-4 cells (HLA-E: 98.8% and 60.8%, CD86: 70.5% and 62.8%, respectively). Other inhibitory ligands such as CD155, CD273, and CD274 were almost absent in all B-ALL cell lines (0 – 20%).

Regarding the AML cell lines, NOMO-1, THP-1, U-937, and U-937 CD19tag/Luc were studied. The CAR target in this type of leukemia is not as evident as for B-ALL, but some receptors were found to be upregulated and represent suitable CAR target candidates. In this context, CD276 expression, abnormally high in most solid tumors,[91] also proved to be upregulated in AML,[92] as corroborated by the staining of all studied AML cell lines in this work (80 – 100%). Additionally, AML cell lines express a wider range of inhibitory ligands, being CD155, Gal-9, and HLA-E the ones with the highest expression (30 – 100%, 80 – 100%, and 60 – 80%, respectively). CD86 was also highly expressed in NOMO-1 and THP-1 (64.9% and 100%, respectively) whereas CD273 and CD274 expression was extremely low for all tested cell lines (0 – 5%). CD66a expression seemed to be upregulated for THP-1 (81.2%).

7.1.2 Inhibitory receptor screening in NK-92 effector cell lines

The expression of CAR and inhibitory receptors were studied in CD19-CAR, CD276-CAR, and parental NK-92 cell lines, revealing high levels of PD1, NKG2A, and TIGIT in flow cytometry stainings (90 – 100%, 99 – 100%, and 95 – 100%, respectively) as well as high expression levels of CD34 in CD276-CAR$^+$ NK-92 cells and CD271 in CD19-CAR$^+$ NK-92 as

expected given the transduced construct design (98% and 100%, respectively). Low levels of TIM-3 and CTLA-4 were reported (5 – 20% and 20 – 45%, respectively).

In line with our previous observations, NKG2A and TIGIT were considered relevant KO targets since their matching ligands (HLA-E and CD155, respectively) were present in all AML and some B-ALL cell lines. TIM-3 was excluded from this study given its low expression in the effector cells despite its ligand (Gal-9) being widely expressed in the leukemic cell lines. Similarly, CTLA-4 was not eligible although CD86 expression was upregulated in some of the target cell lines. Instead, CBLB was considered as its knock-out was previously known to enhance cytotoxicity in NK cells.[52]

7.1.3 Generation of CRISPR-KO NK-92 cell lines

Besides single KO cell lines for each target gene, multiple KO NK-92 and CAR-NK-92 cell lines were implemented to identify potential additive or synergic effects that could be a result of the disruption of all three of them, as suggested by previous research that found enhanced cytotoxicity when targeting several inhibitory checkpoints at the same time.[56] For this purpose, NKG2A KO cells were sequentially transfected with CRISPR CBLB RNP, then expanded for two weeks, and finally transfected again with CRISPR TIGIT RNP. This method was envisioned to avoid or reduce the harmful effects of a single-step multiplex transfection such as undesired chromosomal rearrangements due to simultaneous DSBs induced by different CRISPR RNPs.[93]

A screening of all NK cell electroporation protocols available in the MaxCyte GTx device (NK-3, NK-4, and NK-5) using DsRed mRNA expression as an efficiency readout was carried out in order to select the protocol leading to the highest transfection efficiencies. In brief, DsRed mRNA was generated by *in vitro* transcription as previously described [94] and 5 µg were employed in the electroporation of 2.5 x 10^6 NK-92 cells, then the DsRed expression was measured as a transfection efficiency reporter one day after transfection in a flow cytometer. As all tested conditions proved to efficiently transfect the NK-92 cells and similar efficiencies were attained (98.6 – 99.3%, Figure 7), this screening was excluded from our published work, where we described the exact settings used for the CRISPR-Cas9 transfections (NK-4 protocol).

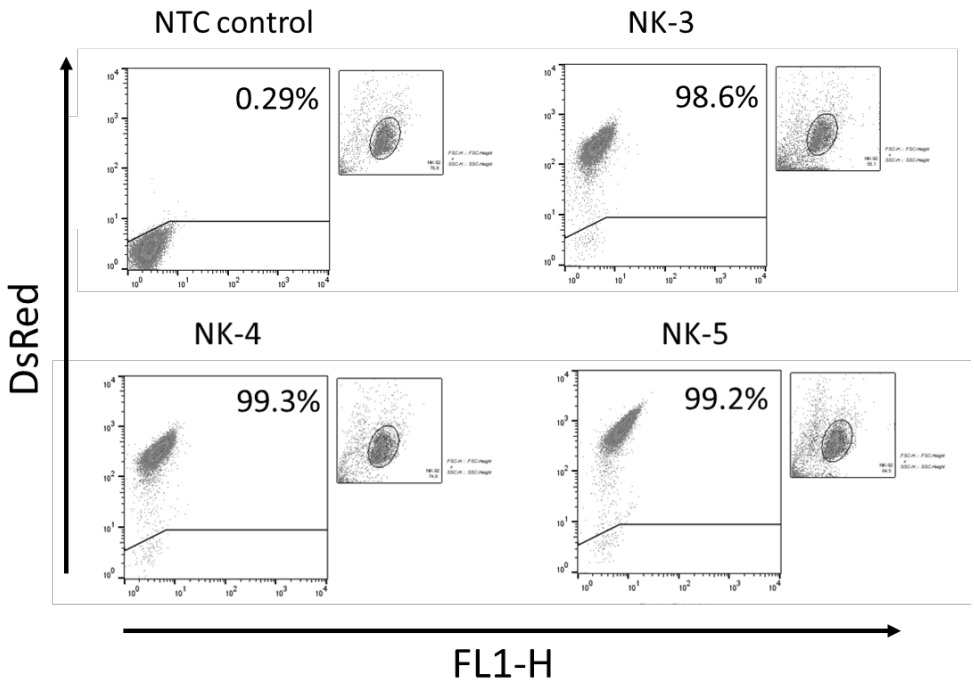

Figure 7: Flow cytometry plots of NTC control and NK-92 samples transfected with DsRed mRNA using NK-3, NK-4, or NK-5 electroporation protocols in MaxCyte GTx. Each fluorescence plot presents the gating strategy in SSC/FSC channels on the right side, selecting the NK-92 population.

The InDel frequency after CRISPR transfection was optimal for all single KO cell lines as well as for the triple KO (CBLB: 71 – 90%, NKG2A: 84 – 94%, TIGIT: 80 – 83%). Subsequent protein analyses revealed a pronounced downregulation of the inhibitory receptors (85 – 100% reduction for NKG2A and 60 – 75% for TIGIT in flow cytometry analyses and 60 – 100% reduction in CBLB expression in immunoblots). DNA studies were also performed on day 5 after transfection to ascertain that the genetic and translational fingerprints of the KO populations were the same for both analyses, although they could have been performed earlier since CRISPR-induced modifications are expected to occur in the first hours after the electroporation.

7.1.4 Outperformance of CAR-NK-92 for the treatment of AML and B-ALL compared to parental NK-92

To test the antileukemic activity of the NK-92 cell lines, two types of cytotoxicity assays were performed: calcein release assays and live-cell-based luciferase assays. While these assays are standard for the study of cellular cytotoxicity, it was relevant to corroborate that similar outcomes could be obtained using both methodologies to determine consistently observable effects.

Calcein-based cytotoxicity assay consists of the passive diffusion of calcein AM through the target cells' membrane after an incubation period, then the intracellular esterases cleave the AM group and produce fluorescent calcein. The substrate excess is removed in consecutive washing steps and the labeled cells are ready for the assay.[95] When the target cell dies, the calcein is released to the medium and can be recovered in the supernatant. Consequently, calcein fluorescence in the supernatant is directly proportional to target cell lysis. As calcein can be actively pumped out by the target cells via multidrug resistant channels at prolongated time points,[96] the time of the study was limited to 2 hours and different E:T ratios were seeded (10:1, 5:1, and 2.5:1) to study a concentration-dependent effect.

On the other hand, live cell-based luciferase assays require the transduction and constitutive expression of the luciferase construct in the target cells. When D-luciferin is provided to the medium, the target cells uptake the substrate and the luciferase will produce light only in a metabolically active cell, as the luciferase enzymatic reaction requires ATP and different cofactors.[97] Thus, the light emitted by the luciferase reaction is inversely proportional to target cell lysis. To pursue time-course studies in the luciferase set-up, sample replicates were prepared for each time point, so the luciferin could be added at the exact time of the measurement (0, 2, 4, and 6 hours). Extended time points such as 24 hours were not considered in the readout as the lysis of the target cells could also be due to other factors such as nutrient deprivation or competition with the effector NK-92 cells, which were seeded at 5:1 E:T ratio.

The significant difference between parental and CAR-NK-92 cell lines antileukemic cytotoxicity was observable in both AML and B-ALL cytotoxicity experiments, where CD19-CAR and CD276-CAR cell lines greatly outperformed their parental counterpart. In calcein assays that lasted for 2 hours, CD19-CAR NK-92 cells were able to lyse up to 40 – 60% of the B-ALL leukemic cells employed in the study versus up to 10% lysis when using unmodified NK-92 (10:1 E:T ratio). Concerning CD276-CAR NK-92 cells, up to 30 – 40% of AML cells were lysed compared to less than 5% when using parental NK-92 (10:1 E:T ratio). Not surprisingly, a concentration-dependent effect is observable and more effector-specific lysis is reported for the higher E:T ratios, indicating that the increase in the cytotoxic performance is dependent on the effector cells' concentration.

In time-course cytotoxicity studies using luciferase-based assays, the difference between parental and CAR cell lines was even more remarkable: CD19-CAR NK-92 cells and CD276-CAR NK-92 reached 85% and 95% of specific lysis against Nalm-6 GFP/Luc and U-937 CD19tag/Luc cells respectively after 6 hours of co-incubation compared to less than 15%

specific lysis of parental NK-92 against both leukemic cell lines. The CAR activity was specific as CD19-CAR NK-92 and CD276-CAR NK-92 did not exhibit enhanced cytotoxicity activity when their target ligand was absent. As expected, the target cell lysis is increasing with time, reaching almost complete lysis at 6 hours.

When comparing the calcein and luciferase assays directly, comparable results were reported. Taking Nalm-6 5:1 E:T ratio vs. Nalm-6 GFP/Luc 5:1 E:T ratio at 2 hours into consideration, similar results were obtained (33.3 ± 2.5 % vs. 37.6 ± 6.0 % for CD19-CAR and 3.3 ± 4.2 % vs. 13.3 ± 3.3 % for NK-92). For U-937 and U-937 CD19tag/Luc, the reported values were slightly different, but superior CAR-induced lysis was evident (34.8 ± 1.7 % vs. 46.3 ± 1.6 % for CD276-CAR and 1.8 ± 0.6 % vs. 0 % for NK-92). These observations ratify the results and indicate that the CAR enhancement in the cytotoxic performance, compared to the parental NK-92 cell line, is not biased nor dependent on the *in vitro* methodology. Different cytotoxicity values measured in calcein and luciferase assays may indicate different sensitivities, which is not unexpected as they are based on different experimental methodologies.

7.1.5 Cytotoxicity assays revealed CBLB and TIGIT checkpoints as important targets for AML treatment by NK-92 immunotherapy

Concerning the CRISPR KO cell lines, there was no significant and consistent improvement of the cytotoxic performance in both CD19-CAR or CD276-CAR NK-92 cell lines. Nonetheless, a significant cytotoxic enhancement could be observed in single KO CBLB NK-92 against AML, more concretely U-937 and single KO CBLB and TIGIT against U-937 CD19tag/Luc cell line (2.5 to 3-fold improvement compared to parental NK-92). This benefit was probably overshadowed in CAR-NK-92 *in vitro* assays due to the potency of the CAR, which was able to lyse almost all leukemic cells after 6 hours. Since the activation and inhibition of NK cells depends on a tight balance of activator versus inhibitory signals,[98] the rapid destruction of the leukemic cells might have prevented the production of inhibitory molecules in concentrations sufficient to favor the balance towards inhibition. The employment of lower E:T ratios could help to corroborate this hypothesis as the overall cytotoxic activity would occur slower. Additionally, a clear limitation of the present study involves the lack of *in vivo* experimentation. Chamberlain et al. previously reported no benefit of PD1 KO in *in vitro* studies of T cell immunotherapy against cancer cell lines, although its efficacy has extensively been proven in clinical trials.[99] Animal studies would be necessary to assess the efficiency of the CAR CRISPR KO NK-92 cell lines as other key elements of cancer immunosuppression (such as bone marrow niche and leukemic microenvironment) would be involved as well, where the

inhibitory checkpoint KO strategy could properly make a difference and bring therapeutic benefits.

It was surprising not to observe any benefit of the NKG2A KO even though its respective KO or downregulation proved to increase NK cell cytotoxicity in previous publications.[67, 68] Apart from the aforementioned limitations, it might be possible that NKG2A inhibitory pathway is not relevant in the NK-92 cell line functionality. Differences between the receptor profile and lysis mechanisms of NK-92 and NK cells have been reported.[46, 100] Thereby, it seems reasonable to expect differences in their main inhibitory pathways. A side-by-side comparison of both NKG2A KO cells in cytotoxicity assays could test this idea.

One of the most novel ideas in this study involved the combination of CBLB, NKG2A, and TIGIT KO in the same cell line. Unexpectedly, there is no observable additive or synergistic effect in the cytotoxic performance of the triple KO cell lines, despite the fact that CBLB and TIGIT single KOs proved to be valuable against AML. As a matter of fact, the cytotoxic activity was found to be significantly lower than the single KO or unmodified counterparts for some leukemic targets (KOPN-8, MHH-CALL-4, Nalm-6, and NOMO-1). Time analyses at 6 hours in the luciferase assays revealed no difference between CAR and triple KO CAR NK-92 cells, suggesting that the effector function remains but there is a delay in the cytotoxic performance. The extensive genetic manipulations of the triple KO cell lines (three different CRISPR modifications together with the CAR lentiviral semi-random transduction) were hypothesized to result in a substantial loss of cellular fitness and consequent reduction in the effector function. More studies at the genomic level aiming for the detection of CRISPR off-target effects, transcriptomic analyses with RNA arrays, and profile analysis of interleukin production would corroborate this potential negative effect.

Finally, the employment of innovative gene editing techniques such as the prime editing, which does not rely on DSB-mediated gene correction and allows precise modifications of the DNA, may improve the outcome and should be explored in future multiplexing experiments. Nevertheless, as additional cell engineering increases the chances of undesired genetic modifications, it would be worthy to study the combination of the CAR therapy with single CRISPR inhibitory checkpoint KO together with antibody blockades, which could bring similar therapeutic benefits without risking the cellular fitness of the effector NK-92 cells.

7.2 Automated good manufacturing practice-compatible CRISPR-Cas9 editing of hematopoietic and progenitor stem cells for clinical treatment of β-hemoglobinopathies

7.2.1 Transfection protocol optimization for efficient *BCL11A* editing

7.2.1.1 Finding the most suitable electroporation settings

To find the most suitable settings for efficient HSPCs electroporation, a pre-screening of different pulse modes, voltages, and pulse lengths was pursued. DsRed mRNA was transfected in a small-scale setup consisting of an electroporation cuvette placed on the TCA in the CliniMACS® Prodigy electroporator (Figure 6A). This way, the expression of the fluorescent protein was measured as a marker of electroporation efficiency one day after transfection. This initial experiment revealed first pulse *Flip* and *Square* 600V protocols as the most efficient ones (70 – 75% of $DsRed^+$ cells and 90% viability for the screened *Flip* protocols, 70 – 90% of $DsRed^+$ cells and 60 – 100% viability for the screened *Square* protocols) and was selected for posterior CRISPR transfection experiments.

To mimic a large-scale electroporation, the electroporation chamber of the CliniMACS® EP-2 Tubing Set was used instead of the small-scale cuvette (Figure 6B). It was extracted from the EP-2 tubing system and manually filled with syringes, pumping the cellular solutions and the CRISPR reagents inside (450 pmol BCL11A RNP, formed by 450 pmol of Cas9 RNP and 900 pmol sgRNA, were used per million of HSPCs). The moderate editing performance indicated that additional optimization steps were needed to attain superior InDel rates (48 – 54%).

In this context, *Flip* 600V was selected in further optimization experiments as it led to the highest *BCL11A* InDel rates. The length and voltage of the second pulse were studied in addition to the “cold shock” cell culture at 32°C after transfection, which has proven to increase CRISPR modification efficiency.[101] The most efficient conditions were found with a high voltage first pulse (600V 104 µs burst/bipolar, 8 µs burst duration) followed by a low voltage second pulse (200V 5000 µs square) for the electroporation in addition to 32°C “cold-shock” culture in the first hours after transfection (*BCL11A* InDel 82%).

7.2.1.2 Effect of RNP and cell concentrations

Once the transfection conditions were optimized, the rest of the elements involved in the clinical-scale production were revised. It was critical to analyze different reagent concentrations as the cyclical automated electroporation does not always rely on specific electroporation volumes but a certain range, therefore the concentration inside the electroporation chamber could differ in each cycle. For this aim, different RNP and cellular concentrations were tested to find the most suitable combination for efficient electroporation. The amount of 45 pmol RNP (45 pmol Cas9 RNP combined with 90 pmol sgRNA in a 1:2 molar ratio) was already known to lead to effective transfection for 1 x 10^5 HSPCs in previous small-scale investigations,[94] therefore 450 pmol Cas9 RNP for 1 x 10^6 HSPCs was set as a middle point in the screening. The results showed that *BCL11A* editing is effective for a wide range of RNP and cell concentrations (InDel 78 – 85%), being 1 x 10^7 cells/mL and an RNP concentration of 2250 – 6750 pmol/mL (225 – 675 pmol per million cells) the most proper conditions for efficient gene editing. Increasing the RNP concentration to 1350 pmol per million of HSPCs decreased the editing efficiency (InDel 68%). This observation is likely to be a result of CRISPR-derived toxicity and loss of cellular fitness.[102]

7.2.1.3 Effect of different electroporation volumes and thawed material

As the automated electroporation process in the CliniMACS® Prodigy relies on a pumping system that fills the electroporation cuvette within a certain volume range (typically 600 – 650µL), it was important to corroborate whether the editing efficiency could be influenced by different filling volumes of the electroporation chamber. Similar *BCL11A* editing and cellular viability were observed between 200 – 800 µL of filling volume (InDel 64 – 66%, viability 86 – 89%). Despite using 450 pmol RNP per million cells, a reduction was noticeable in the editing efficiency (from InDel 78% to 65%). This decrease is hypothesized to be a consequence of the usage of frozen and thawed HSPCs for this test, as a similar effect was observable in all experiments where frozen cell material was employed (see sections 7.3.1.4 and 7.3.1.6). Consistent with this finding, Zhang et al. previously showed a significant reduction of the electroporation efficiency when using thawed T cells (up to a 2-fold decrease compared to fresh T cells).[103]

7.2.1.4 Study of RNP stability

The automated electroporation in the CliniMACS® Prodigy lasts for a variable duration that depends on the total volume of cells to be processed. Thus, sensitive reagents such as the CRISPR RNP can be affected when stored at room temperature for a long time. A preliminary experiment revealed no difference in the editing efficiency of the remaining RNP of an automated run (stored in the reagent bag at 22 °C for 1 h) and freshly prepared RNP (InDel 85 and 87% respectively). This result is not unexpected as the manufacturer claims that the RNP is stable for up to three days at 23 °C.[104]

7.2.1.5 Study of donor variability in the transfection efficiency

Donor variability is not influencing the experimental outcome when using cell material from healthy donors, as similar editing efficiencies were achieved for four different individuals (InDel 60 ± 7.3). Patient HSPCs could show different editing outcomes because of lower cellular fitness, but it was not possible to pursue a direct comparison as there was no access to patient material in this investigation. Nevertheless, Frangoul et al. showed efficient InDel rates for NCT03655678 and NCT03745287 patients (InDel 68.9% for the TDT patient and 82.6% and 78.7% for the two manufactured lots for the SCD patient), suggesting that donor variability is not a general concern in the development of engineered cellular products for the treatment of β-hemoglobinopathies.[84]

7.2.1.6 CentriCult Unit effect on the editing efficiency

To exclude any detrimental effect of the CCU in the recovery of the transfected HSPCs, the InDel rate of a sample cultured in a conventional incubator after transfection was compared to that of another edited sample cultured in the CCU. Both reached the same editing efficiency (InDel 69%), indicating the suitability of the CCU for the culture and expansion of cellular products.

7.2.2 Proof-of-concept clinical-scale production of *BCL11A* KO HSPCs

7.2.2.1 Clinical-scale production of edited HSPCs is feasible using the CliniMACS® Prodigy

2.1 x 10^8 $CD34^+$ HSPCs were processed in the CliniMACS® Prodigy using the TCE automated process and the electroporation pulses previously optimized in small-scale experiments. On day 2, 1.1 x 10^8 cells were harvested (52% recovery from the initial amount) with suitable viability (80.8% compared to 85% of NTC control cells). The recovery rate was moderate as cell loss can be expected from the transfection and manipulation in the automated process, but it was very similar to the recovery of the NTC sample (52% vs. 56% respectively). Still, the production yielded clinically relevant amounts of edited HSPCs. Following the recommendation of the ASBMT of a minimal dose of 2 x 10^6 $CD34^+$ cells/kg for successful transplantation, the resulting cell product of 1 x 10^8 $CD34^+$ cells would be appropriate for the treatment of a 50 kg patient.[105]

Subsequent genetic analyses showed high rates of *BCL11A* KO (InDel 71 – 74%). The functionality of the resulting cells was analyzed with *in vitro* assays. CFU analyses showed typical myeloid colonies and similar total colony counts as well as distributions of colony types in comparison to the NTC control cells, supporting the maintenance of stemness capability of the CRISPR-edited cells. *In vitro* erythroid differentiation experiments showed upregulation of typical erythroid markers (CD233, CD235a) and loss of stem cell markers (CD34) on day 21 of the differentiation.

Regarding HbF resurgence, both intracellular stainings and HPLC analyses showed upregulation of HbF expression in the treated cells. The levels of HbF measured in flow cytometry for the transfected cells increased from 21% on day 7 of the erythroid differentiation to 83% on day 21, whereas for the NTC control the levels of expression changed from 16% to 67%. The HPLC analysis corroborated these findings with an HbF / (HbF + HbA) ratio of 20.4% for NTC control and 63.8% for the automated processed sample. In this way, it was concluded that the HbF expression resembled the editing rate on the genomic level. These results are similar and consistent with previous investigations involving the same *BCL11A* editing strategy (including the same gRNA), where HbF expression was properly restored in erythrocytes derived from healthy donor-edited HSPCs and no CRISPR-derived off-target effects were found by GUIDE-seq and deep-sequencing analyses.[94, 106]

7.2.2.2 Freezing and thawing of edited HSPCs resulted in the reduction of the editing efficiency

The generated BCL11A KO HSPCs produced at the clinical scale were frozen together with their control samples for 6 months in order to emulate clinical standard procedures. After cell thawing, genetic and viability analyses were performed for up to 24h. The InDel efficiency was found to be reduced in comparison to the freshly edited cells (from 74% to 54%) and it was hypothesized that CRISPR-modified HSPCs were less resilient to freezing and thawing stresses than unmodified HSPCs, leading to the observed reduction in the editing efficiency. Concerning the cellular fitness, high viability (82 – 86%) and consistent cellular numbers were observed during the first few hours after thawing ($9.4 \times 10^5 – 1.12 \times 10^6$ cells/mL at 0 – 4 h) whereas a decline was observed after 24 h (7.6×10^5 cells/mL, 82% viable). It is worth noting that the thawing of the cells was pursued following a conventional laboratory protocol and was not performed according to clinical standards. Together with the lack of repetitions, the true effect of freezing and thawing cycles in the editing efficiency remains to be determined.

7.2.2.3 Final considerations

All in all, the obtained results proved that the clinical-scale production of CRISPR-modified *BCL11A* KO HSPCs can be run in a single closed GMP system using the CliniMACS® Prodigy with Electroporator. Consequently, the number of open steps, which must be minimized to prevent contamination risks, and personnel costs for specialized technicians can be considerably reduced.[107] These facts would aid in the development of therapies such as the CTX001 treatment in a safer, more affordable, and more convenient manner. When employed in NCT03655678 and NCT03745287 clinical trials, the cellular product was generated with a combination of CliniMACS® Prodigy (Miltenyi Biotec) and MaxCyte Gen2 GT electroporator (MaxCyte Inc).[84] Following the methodology described in this thesis, the whole process can be feasibly run in the CliniMACS® platform alone using interconnected closed tubing sets, with no need for open manipulation steps.

As the resulting edited HSPCs from the clinical-scale run proved to be functional, conserved their stemness, and their derived erythrocytes presented increased HbF expression, this transfection protocol constitutes a promising methodology for the treatment of β-hemoglobinopathies, and can be potentially translated to the therapy of other genetic diseases. Besides, the CliniMACS® Prodigy with Electroporator allows on-site production of the cellular product, with no need for external processing of the cells in a specialized center. The availability of the device in the clinical site can accelerate patient treatment and bypass the challenging cryo-chain needed for optimal storage of the product (Figure 8).[108]

The clinical-scale run was performed as a proof-of-concept experiment and more repetitions would be needed to address the reproducibility of the generated protocol for routine use. This aspect should be explored in further investigations. The costs associated with the proof-of-concept clinical-scale production are described in Table 1.

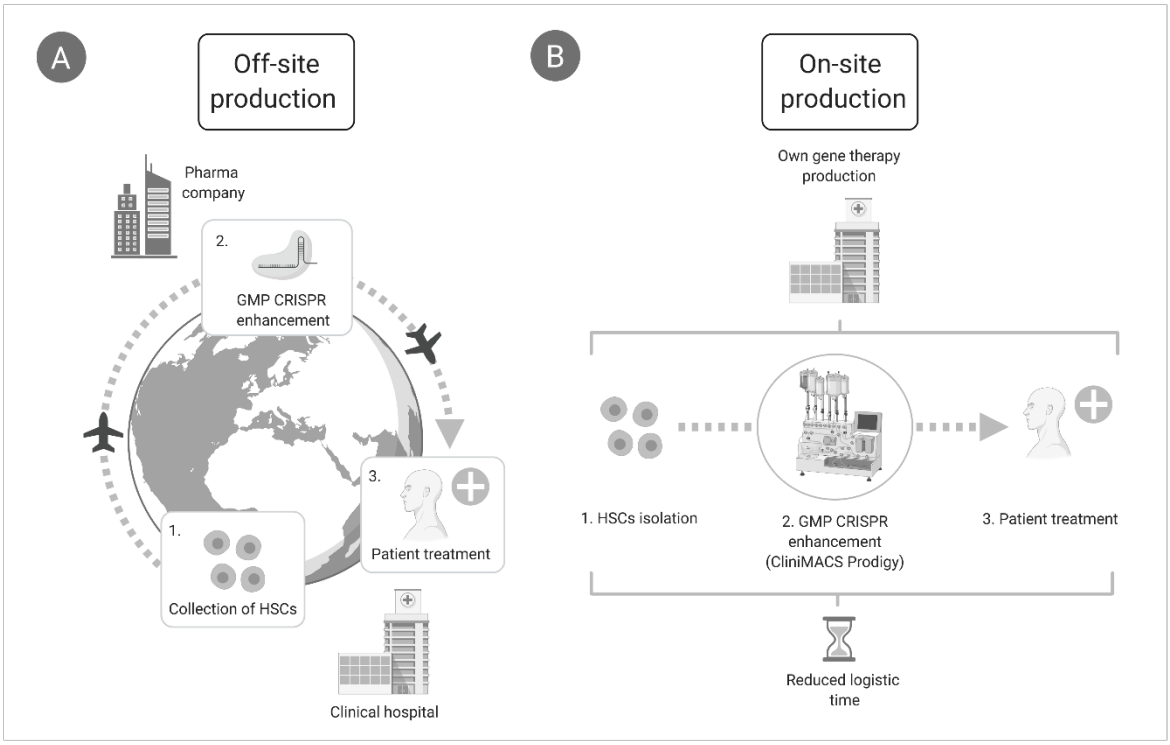

Figure 8: A) Off-site production of HSPC-based gene therapy requires the collection of patient material in the clinical site before shipment to a specialized center from a pharmaceutical partner and proceeding with the GMP production of CRISPR-edited cells. The resulting cells are immediately frozen and delivered to the clinical site to proceed with the treatment. The cryogenic conditions have to be maintained during the whole transportation to ensure proper storage and quality. B) On-site production of gene therapy products by CliniMACS® Prodigy provides a faster treatment implementation as material collection, gene therapy production, and treatment occur in the same location. The scheme was generated with Biorender by the thesis author and was published in *CRISPR-/Cas9 Based Genome Editing for Treating Genetic Disorders and Diseases* book by CRC Press. The figure is reproduced in this thesis with permission of the licensor through PLSclear.

Table 1: Cost calculation of the reagents needed for single clinical-scale production of BCL11A edited HSPCs in the CliniMACS® Prodigy with Electroporator. The costs for clinical therapy production would increase as GMP-grade CRISPR-Cas reagents are more expensive.

	Price (Germany, December 2022)
HSPCs apheresis (with transport, Cytocare)	18.000,00 €
TS310 (Miltenyi Biotec)	1.806,00 €
CD34 Reagent (Miltenyi Biotec)	3.111,00 €
CliniMACS Buffer (Miltenyi Biotec)	273,00 €
NaCl 0,9% (Fresenius)	7,70 €
IgG 10% (Apotheke)	57,00 €
Cas9 (research grade, IDT)	17.534,80 €
gRNA (research grade, IDT)	1.135,00 €
TS520 (Miltenyi Biotec)	2.055,00 €
EP-2 (Miltenyi Biotec)	745,00 €
HSC-Brew GMP medium (Miltenyi Biotec)	1.988,00 €
Cytokines (SCF, TPO, Flt3L)	2.487,00 €
HSA (Octapharma)	740,00 €
Electroporation Buffer (Miltenyi Biotec)	515,00 €
Total	**50.454,50 €**

8. Concluding remarks

In the first project of the thesis, CRISPR-Cas9 was employed for the enhancement of NK-92 immunotherapy for cancer treatment. The number of clinical and preclinical studies including genetic improvement of effector immune cells by the disruption of inhibitory immune checkpoints has increased in the last years and so has the number of promising targets for therapy. However, only a few of them consider direct comparisons of several targets to discern which strategy is more beneficial, or propose the combination of different knock-outs to analyze potential synergistic treatments. This objective was pursued in this thesis by direct comparison of the knock-out of three different inhibitory checkpoints (CBLB, NKG2A, TIGIT) and their combination in NK-92 effector cell lines against leukemia. The results showed cytotoxic upregulation by CBLB and TIGIT KOs for AML treatment whereas NKG2A KO did not improve NK-92 antileukemic activity. The combination of CRISPR-Cas9 improvements with novel CAR approaches will pave the way toward more efficient treatments for many types of cancer. Moreover, the use of off-the-shelf cell lines such as NK-92 was considered with an aim to establish more affordable personalized therapy options against cancer, since their production would be significantly more cost-effective than that of primary cell-based therapies.

In the second project, a close collaboration with Miltenyi Biotec resulted in the optimization and development of a novel protocol in the CliniMACS® Prodigy device for GMP clinical-scale production of CRISPR-Cas9 genetically modified HSPCs for the treatment of β-hemoglobinopathies. The proposed method led to a proof-of-concept study that used the same gene editing strategy as ongoing clinical trials (NCT03655678 and NCT03745287). The experiment resulted in the re-establishment of the HbF expression in the treated HSPCs and yielded sufficient cell numbers for the treatment of a hypothetical patient. The automation of the whole manufacturing process in a single system has very important advantages such as the reduction of personnel costs, contamination risks, and the possibility of in-house production with consequent reductions in delivery times and bypassing of the challenging cryo-chain. All in all, the generated protocol is expected to accelerate β-hemoglobinopathies gene therapy availability in the clinic and support the development of similar therapies in the CliniMACS® Prodigy platform.

9. Acknowledgements

I would first like to thank Dr. Markus Mezger for his kind advice and mentoring, even in the toughest times. Without his priceless guidance, this thesis would have never come into existence. Moreover, I would like to thank Dr. Justin Antony Selvaraj for his assistance and counseling, despite the far distance. I would also like to acknowledge Prof. Rupert Handgretinger and Prof. Alexander Weber for their careful supervision. I am thankful to Stefan Morsch Stiftung for its financial support during these years.

I feel tremendously fortunate to had the opportunity to collaborate with Dr. Stefan Wild and Milena Block from Miltenyi Biotec, I warmly appreciate that they made me feel at home during my days in Bergisch-Gladbach. Similarly, I feel lucky to have investigated alongside AG Feucht, AG Seitz, AG Schleicher, AG Shilbach, and AG André, I will always be grateful for their great support.

I owe my mentors and friends Dr. Andrés Lamsfus Calle and Dr. Alberto Daniel Moreno for their continuous encouragement and precious help in my scientific formation, I will never forget the great memories lived together. My special thanks go to my laboratory fellows and friends Yujuan Hou and Dr. Tahereh Mohammadian Gol who helped me along the way, always with a smile, and gave me confidence and strength when nobody else could. I would like to acknowledge Jérôme Maurice Dobrowolski, Paul Gratz, Hans-Peter Gratz, Ralph Sinn, and Paul Trosien, whom I am proud to have taught one thing or two about the laboratory but from whom I have also learnt very special lessons (and some nice jokes). This section would not be complete without thanking Derya Güngor, Luise Luib, and Janani Raju for the great moments spent together.

I am deeply thankful to my family, especially to my parents, Dolores and Manuel, and my brother, Eduardo, for their unfailing support and affection. And last but not least, I would like to thank my life partner Carmen for enlightening my darkest moments and for her unconditional love.

10. References

1. Mojica FJM, Díez-Villaseñor Cs, García-Martínez J et al. Intervening Sequences of Regularly Spaced Prokaryotic Repeats Derive from Foreign Genetic Elements. *Journal of Molecular Evolution.* 2005;60:174-182. DOI: 10.1007/s00239-004-0046-3
2. Marraffini LA, Sontheimer EJ. CRISPR interference limits horizontal gene transfer in staphylococci by targeting DNA. *Science.* 2008;322:1843-1845.
3. Hille F, Charpentier E. CRISPR-Cas: biology, mechanisms and relevance. *Philosophical Transactions of the Royal Society B: Biological Sciences.* 2016;371:20150496. DOI: 10.1098/rstb.2015.0496
4. Haft DH, Selengut J, Mongodin EF et al. A Guild of 45 CRISPR-Associated (Cas) Protein Families and Multiple CRISPR/Cas Subtypes Exist in Prokaryotic Genomes. *PLOS Computational Biology.* 2005;1:e60. DOI: 10.1371/journal.pcbi.0010060
5. Makarova KS, Grishin NV, Shabalina SA et al. A putative RNA-interference-based immune system in prokaryotes: computational analysis of the predicted enzymatic machinery, functional analogies with eukaryotic RNAi, and hypothetical mechanisms of action. *Biology Direct.* 2006;1:7. DOI: 10.1186/1745-6150-1-7
6. Barrangou R, Fremaux C, Deveau H et al. CRISPR Provides Acquired Resistance Against Viruses in Prokaryotes. *Science.* 2007;315:1709. DOI: 10.1126/science.1138140
7. Swarts DC, Mosterd C, van Passel MWJ et al. CRISPR Interference Directs Strand Specific Spacer Acquisition. *PLOS ONE.* 2012;7:e35888. DOI: 10.1371/journal.pone.0035888
8. Brouns SJJ, Jore MM, Lundgren M et al. Small CRISPR RNAs guide antiviral defense in prokaryotes. *Science (New York, NY).* 2008;321:960-964. DOI: 10.1126/science.1159689
9. Jinek M, Chylinski K, Fonfara I et al. A Programmable Dual-RNA–Guided DNA Endonuclease in Adaptive Bacterial Immunity. *Science.* 2012;337:816. DOI: 10.1126/science.1225829
10. Jiang W, Bikard D, Cox D et al. RNA-guided editing of bacterial genomes using CRISPR-Cas systems. *Nature Biotechnology.* 2013;31:233-239. DOI: 10.1038/nbt.2508
11. Nishimasu H, Ran FA, Hsu Patrick D et al. Crystal Structure of Cas9 in Complex with Guide RNA and Target DNA. *Cell.* 2014;156:935-949. DOI: 10.1016/j.cell.2014.02.001
12. Barnes DE. Non-homologous end joining as a mechanism of DNA repair. *Current Biology.* 2001;11:R455-R457. DOI: https://doi.org/10.1016/S0960-9822(01)00279-2
13. Dudáš A, Chovanec M. DNA double-strand break repair by homologous recombination. *Mutation Research/Reviews in Mutation Research.* 2004;566:131-167. DOI: https://doi.org/10.1016/j.mrrev.2003.07.001
14. Liu M, Zhang W, Xin C et al. Global detection of DNA repair outcomes induced by CRISPR-Cas9. *Nucleic Acids Research.* 2021;49. DOI: 10.1093/nar/gkab686.

15. Liang P, Xu Y, Zhang X et al. CRISPR/Cas9-mediated gene editing in human tripronuclear zygotes. *Protein Cell.* 2015;6:363-372. DOI: 10.1007/s13238-015-0153-5

16. Zhang X-H, Tee LY, Wang X-G et al. Off-target Effects in CRISPR/Cas9-mediated Genome Engineering. *Molecular Therapy - Nucleic Acids.* 2015;4:e264. DOI: https://doi.org/10.1038/mtna.2015.37

17. Vakulskas CA, Dever DP, Rettig GR et al. A high-fidelity Cas9 mutant delivered as a ribonucleoprotein complex enables efficient gene editing in human hematopoietic stem and progenitor cells. *Nat Med.* 2018;24:1216-1224. DOI: 10.1038/s41591-018-0137-0

18. Anzalone AV, Randolph PB, Davis JR et al. Search-and-replace genome editing without double-strand breaks or donor DNA. *Nature.* 2019;576:149-157. DOI: 10.1038/s41586-019-1711-4

19. Upadhyay A. Cancer: An unknown territory; rethinking before going ahead. *Genes Dis.* 2021;8:655-661. DOI: 10.1016/j.gendis.2020.09.002

20. Hanahan D. Hallmarks of Cancer: New Dimensions. *Cancer Discovery.* 2022;12:31-46. DOI: 10.1158/2159-8290.CD-21-1059

21. Hanahan D, Weinberg RA. Hallmarks of cancer: the next generation. *Cell.* 2011;114:646-674. DOI: 10.1016/j.cell.2011.02.013

22. Fisher R, Pusztai L, Swanton C. Cancer heterogeneity: implications for targeted therapeutics. *Br J Cancer.* 2013;108:479-485. DOI: 10.1038/bjc.2012.581

23. Vakiti A, Mewawalla P. Acute Myeloid Leukemia. *StatPearls.* 2022.

24. Seth R, Singh A. Leukemias in Children. *The Indian Journal of Pediatrics.* 2015;82:817-824. DOI: 10.1007/s12098-015-1695-5

25. Shallis RM, Wang R, Davidoff A et al. Epidemiology of acute myeloid leukemia: Recent progress and enduring challenges. *Blood Reviews.* 2019;36:70-87. DOI: https://doi.org/10.1016/j.blre.2019.04.005

26. Terwilliger T, Abdul-Hay M. Acute lymphoblastic leukemia: a comprehensive review and 2017 update. *Blood Cancer Journal.* 2017;7:e577-e577. DOI: 10.1038/bcj.2017.53

27. Davis AS, Viera AJ, Mead MD. Leukemia: an overview for primary care. *Am Fam Physician.* 2014;89:731-738.

28. Debela D, Muzazu SG, Heraro KD et al. New approaches and procedures for cancer treatment: Current perspectives. *SAGE Open Med.* 2021;9. DOI: 10.1177/20503121211034366

29. Behranvand N, Nasri F, Zolfaghari Emameh R et al. Chemotherapy: a double-edged sword in cancer treatment. *Cancer Immunology, Immunotherapy.* 2022;71:507-526. DOI: 10.1007/s00262-021-03013-3

30. Min CK, Eom KS, Lee S et al. Effect of induced GVHD in leukemia patients relapsing after allogeneic bone marrow transplantation: single-center experience of 33 adult patients. *Bone Marrow Transplantation.* 2001;27:999-1005. DOI: 10.1038/sj.bmt.1703021

31. Sweeney C, Vyas P. The Graft-Versus-Leukemia Effect in AML. *Frontiers in Oncology.* 2019 (Review);9. DOI: 10.3389/fonc.2019.01217

32. Vitale M, Pelusi G, Taroni B et al. HLA class I antigen down-regulation in primary ovary carcinoma lesions: association with disease stage. *Clin Cancer Res.* 2005;11:67-72.

33. Kim SK, Cho SW. The Evasion Mechanisms of Cancer Immunity and Drug Intervention in the Tumor Microenvironment. *Frontiers in Pharmacology.* 2022 (Review);13. DOI: 10.3389/fphar.2022.868695

34. Masopust D, Schenkel JM. The integration of T cell migration, differentiation and function. *Nature Reviews Immunology.* 2013;13:309-320. DOI: 10.1038/nri3442

35. Sheykhhasan M, Manoochehri H, Dama P. Use of CAR T-cell for acute lymphoblastic leukemia (ALL) treatment: a review study. *Cancer Gene Therapy.* 2022;29:1080-1096. DOI: 10.1038/s41417-021-00418-1

36. Nair R, Westin J. CAR T-Cells In: *Immunotherapy*. (Naing A and Hajjar J; eds). Springer International Publishing, Cham. 2020; pp. 215-233.

37. Melenhorst JJ, Chen GM, Wang M et al. Decade-long leukaemia remissions with persistence of CD4+ CAR T cells. *Nature.* 2022;602:503-509. DOI: 10.1038/s41586-021-04390-6

38. Ureña-Bailén G, Lamsfus-Calle A, Daniel-Moreno A et al. CRISPR/Cas9 technology: towards a new generation of improved CAR-T cells for anticancer therapies. *Briefings in Functional Genomics.* 2020;19:191-200. DOI: 10.1093/bfgp/elz039

39. Safarzadeh Kozani P, Safarzadeh Kozani P, Rahbarizadeh F et al. Strategies for Dodging the Obstacles in CAR T Cell Therapy. *Frontiers in Oncology.* 2021 (Review);11. DOI: 10.3389/fonc.2021.627549

40. Pan K, Farrukh H, Chittepu VCSR et al. CAR race to cancer immunotherapy: from CAR T, CAR NK to CAR macrophage therapy. *Journal of Experimental & Clinical Cancer Research.* 2022;41:119. DOI: 10.1186/s13046-022-02327-z

41. Mehta RS, Rezvani K. Chimeric Antigen Receptor Expressing Natural Killer Cells for the Immunotherapy of Cancer. *Front Immunol.* 2018;9. DOI: 10.3389/fimmu.2018.00283

42. Klingemann H, Boissel L, Toneguzzo F. Natural Killer Cells for Immunotherapy – Advantages of the NK-92 Cell Line over Blood NK Cells. *Frontiers in Immunology.* 2016 (Review);7.

43. Arai S, Meagher R, Swearingen M et al. Infusion of the allogeneic cell line NK-92 in patients with advanced renal cell cancer or melanoma: a phase I trial. *Cytotherapy.* 2008;10:625-632. DOI: https://doi.org/10.1080/14653240802301872

44. Klingemann HG, Wong E, Maki G. A cytotoxic NK-cell line (NK-92) for ex vivo purging of leukemia from blood. *Biol Bone Marrow Transplant.* 1996;2:68-75.

45. Overview E. Natural killer cells for cancer immunotherapy: a new CAR is catching up. *EBioMedicine.* 2019;39:1-2. DOI: 10.1016/j.ebiom.2019.01.018

46. Maki G, Klingemann H-G, Martinson JA et al. Factors Regulating the Cytotoxic Activity of the Human Natural Killer Cell Line, NK-92. *Journal of Hematotherapy & Stem Cell Research.* 2001;10:369-383. DOI: 10.1089/152581601750288975

47. Callahan MK, Wolchok JD. At the bedside: CTLA-4- and PD-1-blocking antibodies in cancer immunotherapy. *J Leukoc Biol.* 2013;94:41-53. DOI: 10.1189/jlb.1212631

48. Johnson DB, Nebhan CA, Moslehi JJ et al. Immune-checkpoint inhibitors: long-term implications of toxicity. *Nature Reviews Clinical Oncology.* 2022;19:254-267. DOI: 10.1038/s41571-022-00600-w

49. Chamoto K, Hatae R, Honjo T. Current issues and perspectives in PD-1 blockade cancer immunotherapy. *International Journal of Clinical Oncology.* 2020;25:790-800. DOI: 10.1007/s10147-019-01588-7

50. Amatya C, Pegues MA, Lam N et al. Development of CAR T Cells Expressing a Suicide Gene Plus a Chimeric Antigen Receptor Targeting Signaling Lymphocytic-Activation Molecule F7. *Molecular Therapy.* 2021;29:702-717. DOI: https://doi.org/10.1016/j.ymthe.2020.10.008

51. Moghanloo E, Mollanoori H, Talebi M et al. Remote controlling of CAR-T cells and toxicity management: Molecular switches and next generation CARs. *Translational Oncology.* 2021;14:101070. DOI: https://doi.org/10.1016/j.tranon.2021.101070

52. Guo X, Mahlakõiv T, Ye Q et al. CBLB ablation with CRISPR/Cas9 enhances cytotoxicity of human placental stem cell-derived NK cells for cancer immunotherapy. *J Immunother Cancer.* 2021;9. DOI: 10.1136/jitc-2020-001975

53. Lu T, Chen L, Mansour AG et al. Cbl-b Is Upregulated and Plays a Negative Role in Activated Human NK Cells. *The Journal of Immunology.* 2021;206:677-685. DOI: 10.4049/jimmunol.2000177

54. Ruggeri L, Urbani E, André P et al. Effects of anti-NKG2A antibody administration on leukemia and normal hematopoietic cells. *Haematologica.* 2016;101:626-633. DOI: 10.3324/haematol.2015.135301

55. Nguyen S, Beziat V, Dhedin N et al. HLA-E upregulation on IFN-γ-activated AML blasts impairs CD94/NKG2A-dependent NK cytolysis after haplo-mismatched hematopoietic SCT. *Bone Marrow Transplantation.* 2009;43:693-699. DOI: 10.1038/bmt.2008.380

56. Brauneck F, Seubert E, Wellbrock J et al. Combined Blockade of TIGIT and CD39 or A2AR Enhances NK-92 Cell-Mediated Cytotoxicity in AML. International Journal of Molecular Sciences.

57. Zhang X, Zhang H, Chen L et al. TIGIT expression is upregulated in T cells and causes T cell dysfunction independent of PD-1 and Tim-3 in adult B lineage acute lymphoblastic leukemia. *Cellular Immunology.* 2019;344:103958. DOI: https://doi.org/10.1016/j.cellimm.2019.103958

58. Zeng T, Cao Y, Jin T et al. The CD112R/CD112 axis: a breakthrough in cancer immunotherapy. *Journal of Experimental & Clinical Cancer Research.* 2021;40:285. DOI: 10.1186/s13046-021-02053-y

59. Lutz-Nicoladoni C, Wolf D, Sopper S. Modulation of Immune Cell Functions by the E3 Ligase Cbl-b. *Frontiers in Oncology.* 2015 (Review);5. DOI: 10.3389/fonc.2015.00058

60. Kumar J, Kumar R, Kumar Singh A et al. Deletion of Cbl-b inhibits CD8⁺ T-cell exhaustion and promotes CAR T-cell function. *J Immunother Cancer.* 2021;9:e001688. DOI: 10.1136/jitc-2020-001688

61. Peer S, Baier G, Gruber T. Cblb -deficient T cells are less susceptible to PD-L1-mediated inhibition. *Oncotarget; Vol 8, No 26.* 2017.

62. Linger RM, Keating AK, Shelton Earp HG, Douglas K. TAM receptor tyrosine kinases: biologic functions, signaling, and potential therapeutic targeting in human cancer. *Adv Cancer Res.* 2008;100:35-83. DOI: 10.1016/S0065-230X(08)00002-X

63. Chirino LM, Kumar S, Okumura M et al. TAM receptors attenuate murine NK-cell responses via E3 ubiquitin ligase Cbl-b. *European Journal of Immunology.* 2020 (https://doi.org/10.1002/eji.201948204);50:48-55. DOI: https://doi.org/10.1002/eji.201948204

64. Kim HS, Das A, Gross CCB, Y. T. et al. Synergistic signals for natural cytotoxicity are required to overcome inhibition by c-Cbl ubiquitin ligase. *Immunity.* 2010;32:175-186. DOI: 10.1016/j.immuni.2010.02.004

65. Borst L, van der Burg SH, van Hall T. The NKG2A–HLA-E Axis as a Novel Checkpoint in the Tumor Microenvironment. *Clinical Cancer Research.* 2020;26:5549-5556. DOI: 10.1158/1078-0432.CCR-19-2095

66. Wang X, Xiong H, Ning Z. Implications of NKG2A in immunity and immune-mediated diseases. *Frontiers in Immunology.* 2022 (Review);13. DOI: 10.3389/fimmu.2022.960852

67. Bexte T, Alzubi J, Reindl LM et al. CRISPR-Cas9 based gene editing of the immune checkpoint NKG2A enhances NK cell mediated cytotoxicity against multiple myeloma. *OncoImmunology.* 2022;11:2081415. DOI: 10.1080/2162402X.2022.2081415

68. Kamiya T, Seow SV, Wong D et al. Blocking expression of inhibitory receptor NKG2A overcomes tumor resistance to NK cells. *The Journal of Clinical Investigation.* 2019;129:2094-2106. DOI: 10.1172/JCI123955

69. Chauvin J-M, Zarour HM. TIGIT in cancer immunotherapy. *J Immunother Cancer.* 2020;8:e000957. DOI: 10.1136/jitc-2020-000957

70. Carlsten M, Norell Hk, Bryceson YT et al. Primary Human Tumor Cells Expressing CD155 Impair Tumor Targeting by Down-Regulating DNAM-1 on NK Cells1. *The Journal of Immunology.* 2009;183:4921-4930. DOI: 10.4049/jimmunol.0901226

71. Chauvin J-M, Ka M, Pagliano O et al. IL15 Stimulation with TIGIT Blockade Reverses CD155-mediated NK-Cell Dysfunction in Melanoma. *Clinical Cancer Research.* 2020;26:5520-5533. DOI: 10.1158/1078-0432.CCR-20-0575

72. Ge Z, Peppelenbosch MP, Sprengers D et al. TIGIT, the Next Step Towards Successful Combination Immune Checkpoint Therapy in Cancer. *Frontiers in Immunology.* 2021 (Review);12.

73. Wang F, Hou H, Wu S et al. TIGIT expression levels on human NK cells correlate with functional heterogeneity among healthy individuals. *European Journal of Immunology.* 2015 (https://doi.org/10.1002/eji.201545480);45:2886-2897. DOI: https://doi.org/10.1002/eji.201545480

74. Mussolino C, Strouboulis J. Recent Approaches for Manipulating Globin Gene Expression in Treating Hemoglobinopathies. *Frontiers in Genome Editing.* 2021 (Review);3. DOI: 10.3389/fgeed.2021.618111

75. Kato GJ, Piel FB, Reid CD et al. Sickle cell disease. *Nature Reviews Disease Primers.* 2018;4:18010. DOI: 10.1038/nrdp.2018.10

76. Kassim AA, DeBaun MR. The case for and against initiating either hydroxyurea therapy, blood transfusion therapy or hematopoietic stem cell transplant in asymptomatic children with sickle cell disease. *Expert Opinion on Pharmacotherapy.* 2014;15:325-336. DOI: 10.1517/14656566.2014.868435

77. Kohne E. Hemoglobinopathies: clinical manifestations, diagnosis, and treatment. *Dtsch Arztebl Int.* 2011;108:31-32. DOI: 10.3238/arztebl.2011.0532

78. Magrin E, Semeraro M, Hebert N et al. Long-term outcomes of lentiviral gene therapy for the β-hemoglobinopathies: the HGB-205 trial. *Nat Med.* 2022;28:81-88. DOI: 10.1038/s41591-021-01650-w

79. White M, Whittaker R, Gándara C et al. A Guide to Approaching Regulatory Considerations for Lentiviral-Mediated Gene Therapies. *Human Gene Therapy Methods.* 2017;28:163-176. DOI: 10.1089/hgtb.2017.096

80. Lamsfus-Calle A, Daniel-Moreno A, Ureña-Bailén G et al. Hematopoietic stem cell gene therapy: The optimal use of lentivirus and gene editing approaches. *Blood Reviews.* 2020;40:100641. DOI: https://doi.org/10.1016/j.blre.2019.100641

81. Lamsfus-Calle A, Daniel-Moreno A, Ureña-Bailén G et al. Universal Gene Correction Approaches for β-hemoglobinopathies Using CRISPR-Cas9 and Adeno-Associated Virus Serotype 6 Donor Templates. *The CRISPR Journal.* 2021;4:207-222. DOI: 10.1089/crispr.2020.0141

82. Sankaran VG, Orkin SH. The Switch from Fetal to Adult Hemoglobin. *Cold Spring Harbor Perspectives in Medicine.* 2013;3.

83. Bauer DE, Orkin SH. Update on fetal hemoglobin gene regulation in hemoglobinopathies. *Current Opinion in Pediatrics.* 2011;23.

84. Frangoul H, Altshuler D, Cappellini MD et al. CRISPR-Cas9 Gene Editing for Sickle Cell Disease and β-Thalassemia. *New England Journal of Medicine.* 2020. DOI: 10.1056/NEJMoa2031054

85. CliniMACS Prodigy® Instrument, automated cell processing in a closed system. https://www.miltenyibiotec.com/DE-en/products/clinimacs-prodigy.html. (last accessed 26th January, 2023).

86. Zhu F, Shah N, Xu H et al. Closed-system manufacturing of CD19 and dual-targeted CD20/19 chimeric antigen receptor T cells using the CliniMACS Prodigy device at an academic medical center. *Cytotherapy.* 2018;20:394-406. DOI: https://doi.org/10.1016/j.jcyt.2017.09.005

87. Stroncek DF, Tran M, Frodigh SE et al. Preliminary evaluation of a highly automated instrument for the selection of CD34+ cells from mobilized peripheral blood stem cell concentrates. *Transfusion.* 2016 (https://doi.org/10.1111/trf.13394);56:511-517. DOI: https://doi.org/10.1111/trf.13394

88. Palani HK, Arunachalam AK, Yasar M et al. Decentralized manufacturing of anti CD19 CAR-T cells using CliniMACS Prodigy®: real-world experience and cost analysis in India. *Bone Marrow Transplantation.* 2022. DOI: 10.1038/s41409-022-01866-5

89. Wang K, Wei G, Liu D. CD19: a biomarker for B cell development, lymphoma diagnosis and therapy. *Experimental Hematology & Oncology.* 2012;1:36. DOI: 10.1186/2162-3619-1-36

90. Park JH, Geyer MB, Brentjens RJ. CD19-targeted CAR T-cell therapeutics for hematologic malignancies: interpreting clinical outcomes to date. *Blood.* 2016;127:3312-3320. DOI: 10.1182/blood-2016-02-629063

91. Liu S, Liang J, Liu Z et al. The Role of CD276 in Cancers. *Frontiers in Oncology.* 2021 (Review);11.

92. Guery T, Roumier C, Berthon C et al. B7-H3 protein expression in acute myeloid leukemia. *Cancer Medicine.* 2015 (https://doi.org/10.1002/cam4.522);4:1879-1883. DOI: https://doi.org/10.1002/cam4.522

93. Webber BR, Lonetree C-l, Kluesner MG et al. Highly efficient multiplex human T cell engineering without double-strand breaks using Cas9 base editors. *Nature Communications.* 2019;10:5222. DOI: 10.1038/s41467-019-13007-6

94. Lamsfus-Calle A, Daniel-Moreno A, Antony JS et al. Comparative targeting analysis of KLF1, BCL11A, and HBG1/2 in CD34+ HSPCs by CRISPR/Cas9 for the induction of fetal hemoglobin. *Scientific Reports.* 2020;10:10133. DOI: 10.1038/s41598-020-66309-x

95. Neri S, Mariani E, Meneghetti A et al. Calcein-Acetyoxymethyl Cytotoxicity Assay: Standardization of a Method Allowing Additional Analyses on Recovered Effector Cells and Supernatants. *Clinical Diagnostic Laboratory Immunology.* 2001;8:1131-1135. DOI: 10.1128/CDLI.8.6.1131-1135.2001

96. Homolya L, Holló Z, Germann UA et al. Fluorescent cellular indicators are extruded by the multidrug resistance protein. *Journal of Biological Chemistry.* 1993;268:21493-21496. DOI: https://doi.org/10.1016/S0021-9258(20)80566-3

97. Karimi MA, Lee E, Bachmann MH et al. Measuring Cytotoxicity by Bioluminescence Imaging Outperforms the Standard Chromium-51 Release Assay. *PLOS ONE.* 2014;9:e89357. DOI: 10.1371/journal.pone.0089357

98. Vivier E, Ugolini S, Blaise D et al. Targeting natural killer cells and natural killer T cells in cancer. *Nature Reviews Immunology.* 2012;12:239-252. DOI: 10.1038/nri3174

99. Chamberlain CA, Bennett EP, Kverneland AH et al. Highly efficient PD-1-targeted CRISPR-Cas9 for tumor-infiltrating lymphocyte-based adoptive T cell therapy. *Molecular Therapy - Oncolytics.* 2022;24:417-428. DOI: https://doi.org/10.1016/j.omto.2022.01.004

100. Komatsu F, Kajiwara M. Relation of natural killer cell line NK-92-mediated cytolysis (NK-92-lysis) with the surface markers of major histocompatibility complex class I antigens, adhesion molecules, and Fas of target cells. *Oncol Res.* 1998;10:483-489.

101. Guo Q, Mintier G, Ma-Edmonds M et al. 'Cold shock' increases the frequency of homology directed repair gene editing in induced pluripotent stem cells. *Scientific Reports.* 2018;8:2080. DOI: 10.1038/s41598-018-20358-5

102. Álvarez MM, Biayna J, Supek F. TP53-dependent toxicity of CRISPR/Cas9 cuts is differential across genomic loci and can confound genetic screening. *Nature Communications.* 2022;13:4520. DOI: 10.1038/s41467-022-32285-1

103. Zhang Z, Qiu S, Zhang X et al. Optimized DNA electroporation for primary human T cell engineering. *BMC Biotechnol.* 2018;18:4-4. DOI: 10.1186/s12896-018-0419-0

104. Spencer NY, Jacobi A, Roberts N. Stability of CRISPR reagents under different freezing, storage, and thawing conditions. https://eu.idtdna.com/pages/education/decoded/article/stability-of-crispr-reagents-under-different-freezing-storage-and-thawing-conditions. (last accessed 08.02.2023).

105. Giralt S, Costa L, Schriber J et al. Optimizing Autologous Stem Cell Mobilization Strategies to Improve Patient Outcomes: Consensus Guidelines and Recommendations. *Biology of Blood and Marrow Transplantation.* 2014;20:295-308. DOI: https://doi.org/10.1016/j.bbmt.2013.10.013

106. Wu Y, Zeng J, Roscoe BP et al. Highly efficient therapeutic gene editing of human hematopoietic stem cells. *Nature Medicine.* 2019;25:776-783. DOI: 10.1038/s41591-019-0401-y

107. Iancu EM, Kandalaft LE. Challenges and advantages of cell therapy manufacturing under Good Manufacturing Practices within the hospital setting. *Current Opinion in Biotechnology.* 2020;65:233-241. DOI: https://doi.org/10.1016/j.copbio.2020.05.005

108. Meneghel J, Kilbride P, Morris GJ. Cryopreservation as a Key Element in the Successful Delivery of Cell-Based Therapies—A Review. *Frontiers in Medicine.* 2020 (Review);7.

11. Appendix

PAPER 1

Preclinical evaluation of CRISPR-edited CAR-NK-92 cells for off-the-shelf treatment of AML and B-ALL

International Journal of
Molecular Sciences

MDPI

Article

Preclinical Evaluation of CRISPR-Edited CAR-NK-92 Cells for Off-the-Shelf Treatment of AML and B-ALL

Guillermo Ureña-Bailén [1], Jérôme-Maurice Dobrowolski [1], Yujuan Hou [1], Alicia Dirlam [1], Alicia Roig-Merino [2], Sabine Schleicher [1], Daniel Atar [1], Christian Seitz [1,3], Judith Feucht [1,3], Justin S. Antony [1], Tahereh Mohammadian Gol [1], Rupert Handgretinger [1] and Markus Mezger [1,*]

[1] Department of Hematology and Oncology, Children's Hospital, University Hospital Tuebingen, 72076 Tuebingen, Germany
[2] MaxCyte Inc., Rockville, MD 20850, USA
[3] Cluster of Excellence iFIT (EXC2180) "Image-Guided and Functionally Instructed Tumor Therapies", University of Tübingen, 72074 Tuebingen, Germany
* Correspondence: markus.mezger@med.uni-tuebingen.de

Abstract: Acute myeloid leukemia (AML) and B-cell acute lymphocytic leukemia (B-ALL) are severe blood malignancies affecting both adults and children. Chimeric antigen receptor (CAR)-based immunotherapies have proven highly efficacious in the treatment of leukemia. However, the challenge of the immune escape of cancer cells remains. The development of more affordable and ready-to-use therapies is essential in view of the costly and time-consuming preparation of primary cell-based treatments. In order to promote the antitumor function against AML and B-ALL, we transduced NK-92 cells with CD276-CAR or CD19-CAR constructs. We also attempted to enhance cytotoxicity by a gene knockout of three different inhibitory checkpoints in NK cell function (CBLB, NKG2A, TIGIT) with CRISPR-Cas9 technology. The antileukemic activity of the generated cell lines was tested with calcein and luciferase-based cytotoxicity assays in various leukemia cell lines. Both CAR-NK-92 exhibited targeted cytotoxicity and a significant boost in antileukemic function in comparison to parental NK-92. CRISPR-Cas9 knock-outs did not improve B-ALL cytotoxicity. However, triple knock-out CD276-CAR-NK-92 cells, as well as CBLB or TIGIT knock-out NK-92 cells, showed significantly enhanced cytotoxicity against U-937 or U-937 CD19/tag AML cell lines. These results indicate that the CD19-CAR and CD276-CAR-NK-92 cell lines' cytotoxic performance is suitable for leukemia killing, making them promising off-the-shelf therapeutic candidates. The knock-out of CBLB and TIGIT in NK-92 and CD276-CAR-NK-92 should be further investigated for the treatment of AML.

Keywords: NK-92; CD19-CAR; CD276-CAR; leukemia; AML; B-ALL; CRISPR-Cas9 knock-out; CBLB; NKG2A; TIGIT

Citation: Ureña-Bailén, G.; Dobrowolski, J.-M.; Hou, Y.; Dirlam, A.; Roig-Merino, A.; Schleicher, S.; Atar, D.; Seitz, C.; Feucht, J.; Antony, J.S.; et al. Preclinical Evaluation of CRISPR-Edited CAR-NK-92 Cells for Off-the-Shelf Treatment of AML and B-ALL. *Int. J. Mol. Sci.* **2022**, *23*, 12828. https://doi.org/10.3390/ijms232112828

Academic Editor: Anne-Catherine Prats

Received: 23 September 2022
Accepted: 21 October 2022
Published: 24 October 2022

1. Introduction

Acute leukemia comprises a group of heterogenous, progressive clonal disorders driven by genetic mutations in blood progenitor cells. Such genetic changes ultimately induce an unrestrained potential for self-renewal together with a developmental arrest of affected progenitor cells at a specific stage of their differentiation. The resulting immature cells (blasts) are likely to invade the bone marrow and the reticulo-endothelial system along with other extramedullary areas, thereby inhibiting various functions of the organism and eventually leading to death if not properly treated [1]. Among the various subsets of acute leukemia, acute lymphocytic leukemia (ALL) is the most frequent malignant disorder in children, whereas acute myeloid leukemia (AML) is the most prevalent blood disorder in adults [2,3].

In recent years, chimeric antigen receptor (CAR)-based immunotherapies have emerged for the treatment of leukemia. Effective CAR therapies against B-ALL have been approved by the FDA in late 2017 [4]. Nevertheless, there are key limitations that can compromise

the efficacy of the treatment. Drawbacks, such as immunosuppression, graft-versus-host disease (GvHD) and host-versus-graft effect (HvG), can be overcome by further genetic enhancement of CAR effector cells [5]. Iatrogenic effects such as cytokine release syndrome (CRS) and neurotoxicity are major hurdles in CAR-T cell therapies, which can be prevented by selecting a different suitable CAR carrier such as natural killer (NK) cells [6]. Additional concerns arise with regard to the highly costly, long-time manufacturing process of CAR cells derived from primary immune cells, where convenient off-the-shelf therapies can aid [6,7]. Taking these aspects into consideration, we have developed CAR-NK-92 cells and tested their cytotoxicity against different leukemic cell lines to assess their therapeutic efficacy against AML and B-ALL. Further CRISPR-Cas9-induced genetic improvements were also considered. The increasing number of clinical and preclinical studies reporting improved anticancer cytotoxicity after gene knock-out or antibody blockade of inhibitory checkpoints sets the grounds for a wider range of treatment options in the future [5,8–17]. However, critical questions may arise as to which strategy is more effective for treating a certain type of cancer. We have considered a side-by-side comparison of the knock-out of three important inhibitory checkpoints in NK cell effector function (CBLB, NKG2A, TIGIT) to assess their antileukemic efficacy in the presence or absence of the CAR. In addition, triple knock-outs were studied to corroborate potential additive or synergistic effects in the modulation of cytotoxic performance.

2. Results

2.1. Ligand Profile Characterization of Leukemia Cell Lines

AML and B-ALL cell lines were analyzed by flow cytometry to determine the expression of each target antigen (CD19 and CD276) as well as relevant ligands for inhibitory receptors including CTLA-4 (CD80 and CD86), NKG2A (HLA-E), PD-1 (CD273 & CD274), TIGIT (CD112 and CD155) and TIM-3 (CD66a and Gal-9) (Figure 1) [18]. B-ALL cell lines (KOPN-8, MHH-CALL-4, Nalm-6, Nalm-6 GFP/Luc) showed a high CD19 expression (expressed in 95–100% of the cells, Figure 1a) and a modest expression of inhibitory ligands, being Gal-9 the most abundantly expressed (50–100%, Figure 1a). Transgenic Nalm-6 GFP/Luc cell line reported a high expression of GFP (97.7%, Figure 1b). On the other hand, AML cell lines (NOMO-1, THP-1, U-937, U-937 CD19tag/Luc) expressed high levels of CD276 (80–100%, Figure 1c). AML cell lines exhibited a wider expression of inhibitory molecules, including CD155, Gal-9 and HLA-E (30–100%, 80–100% and 60–80%, respectively, Figure 1c). Transgenic U-937 CD19tag/Luc cell line showed high levels of CD19 (99.8%, Figure 1d).

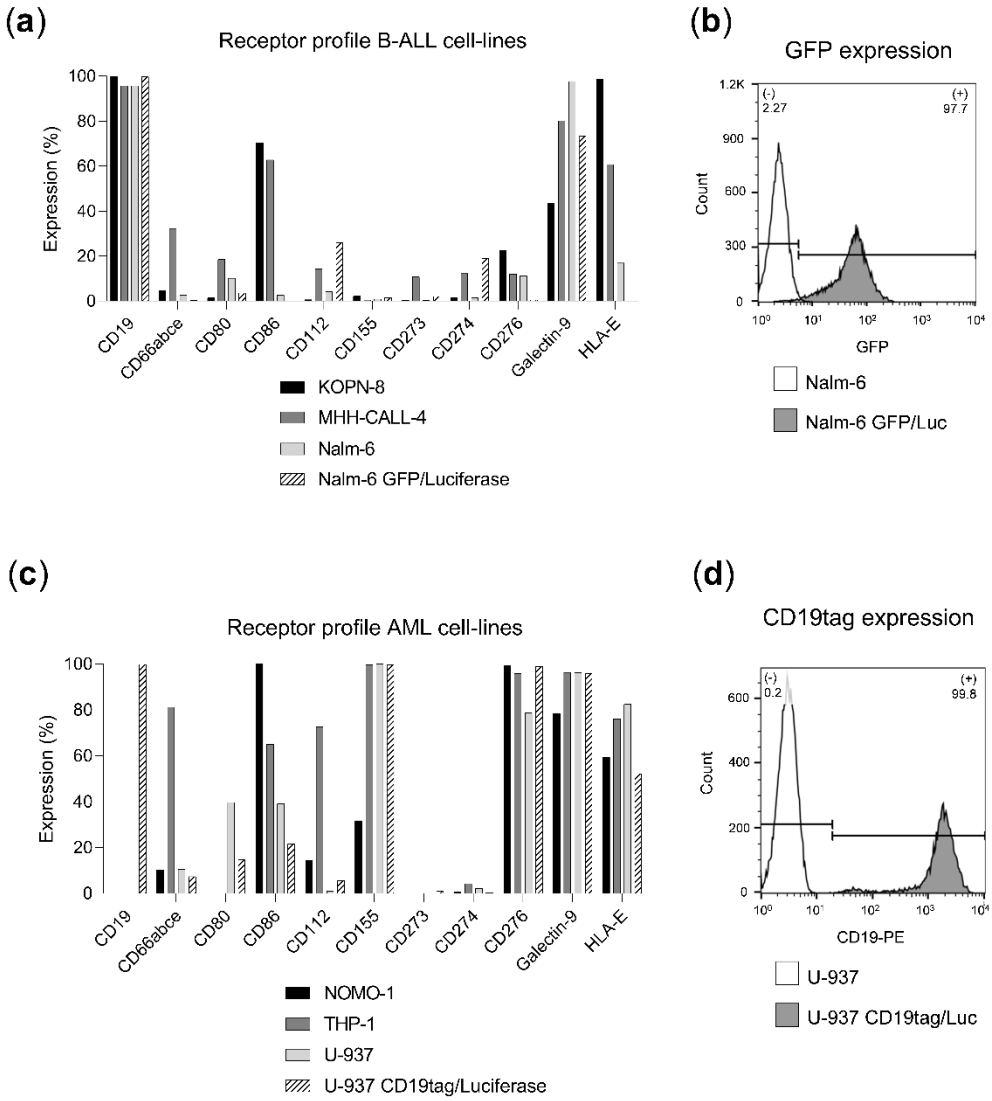

Figure 1. Ligand profile characterization of leukemia cell lines. Percentage of ligand or GFP-expressing cells was determined by flow cytometry. (**a**) Ligand expression in B-ALL cell lines (KOPN-8, MHH-CALL-4, Nalm-6 and Nalm-6 GFP/Luc). (**b**) GFP expression of Nalm-6 GFP/Luc (grey) in comparison to non-transduced Nalm-6 (white). (**c**) Ligand expression in AML cell lines (NOMO-1, THP-1, U-937 and U-937 CD19tag/Luc). (**d**) CD19 expression of U-937 CD19tag/Luc (grey) in comparison to non-transduced U-937 (white).

2.2. Receptor Profile Characterization of Effector Cell Lines

To verify the presence of the CAR in the transduced NK-92 cell lines, the staining of a reporter gene included in each CAR construct was studied: CD34 expression was correlated with CD276-CAR levels and expression of CD271 was an indicator of CD19-CAR expression (98% CD34 expression in CD276-CAR-NK-92 and 100% CD271 expression in CD19-CAR-NK-92, respectively, Figure 2a,b). The inhibitory checkpoints of CAR and parental NK-92 cells were further analyzed, showing a similar expression profile across all cell lines (Figure 2b). High levels of PD1, NKG2A and TIGIT were observed (90–100%, 99–100% and 95–100%, respectively, Figure 2b).

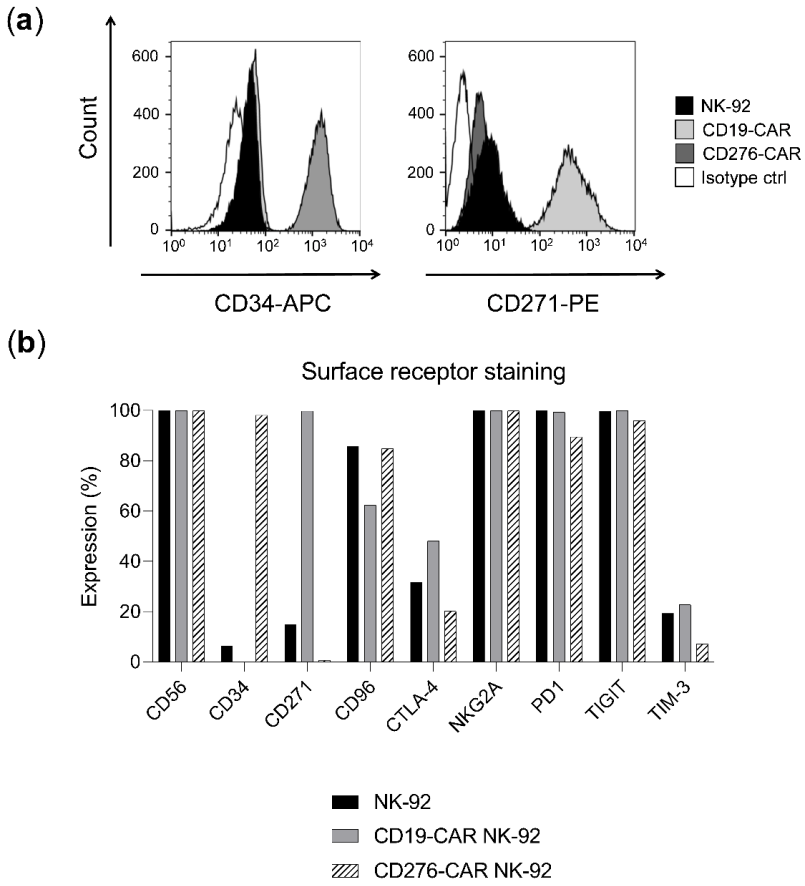

Figure 2. Receptor profile characterization of NK-92 cell lines. Percentage of receptor-expressing cells was determined by flow cytometry. (**a**) Expression of CAR reporter genes (CD34 and CD271) in NK-92 (black), CD19-CAR NK-92 (light grey), CD276-CAR NK-92 (dark grey) and NK-92 isotype control (white). (**b**) Receptor expression in NK-92 (black), CD19-CAR (grey) and CD276-CAR-NK-92 cell lines (white).

2.3. CAR-NK-92 Outperforms Parental NK-92 Antileukemic Activity

Both parental and CAR-NK-92 cells were tested in vitro with leukemia cell lines. Different effector-to-target ratios were investigated in calcein release assays and a time-course cytotoxicity study was analyzed in luciferase assays (Figure 3). CD19-CAR-NK-92 showed significantly improved specific lysis in calcein assays (40–60% against KOPN-8, MHH-CALL-4 and Nalm-6) in relation to their parental counterpart (up to 10% specific lysis) (Figure 3a–c). A similar effect was observed in luciferase assays, where CD19-CAR-NK-92 cytotoxicity (85% against Nalm-6 GFP/Luc after 6 h) greatly outperformed non-transduced NK-92 (8% specific lysis after 6 h) (Figure 3d). This enhanced cytolytic activity was also induced by CD276-CAR-NK-92 in AML cell lines (less than 5% of specific lysis in calcein assays for parental NK-92 vs. 30–40% in CD276-CAR-NK-92; 16% specific lysis in luciferase assays for NK-92 after 6 h vs. 95% for CD276-CAR-NK-92, Figure 3e–h). The cytotoxic performance of both CAR cell lines was specific and targeted as no antileukemic activity was observed in absence of their ligand (Figure 3a–h). CD276-CAR-NK-92 cytotoxicity against B-ALL was identical or decreased compared to parental NK-92 (Figure 3a–d). A similar activity could be observed for CD19-CAR against AML cell lines except for the transgenic luciferase-expressing U-937 cell line due to the high expression of CD19tag (up to 90% specific lysis after 6 h, Figure 3h).

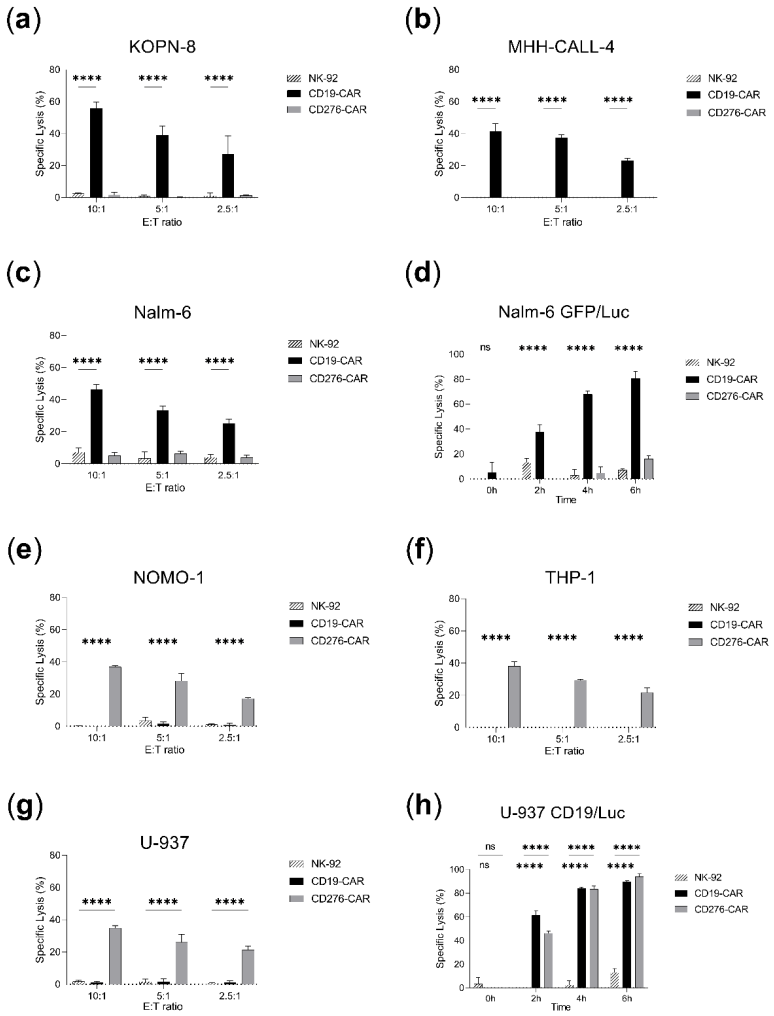

Figure 3. Cytotoxicity assays comparing NK-92 and CAR-NK-92 antileukemic performance. Specific lysis is shown as mean ± SD (n = 3). Calcein assays were incubated for 2 h and several effector-to-target (E:T) ratios were employed: 10:1, 5:1, 2.5:1. Luciferase assays were performed over a time span of 6 h in 5:1 E:T ratio. (**a**) KOPN-8 calcein assay. (**b**) MHH-CALL-4 calcein assay. (**c**) Nalm-6 calcein assay. (**d**) Nalm-6 GFP/Luc luciferase assay. (**e**) NOMO-1 calcein assay. (**f**) THP-1 calcein assay. (**g**) U-937 calcein assay. (**h**) U-937 CD19tag/Luc luciferase assay. **** $p < 0.0001$, ns, non-significant ($p > 0.05$).

2.4. CRISPR-Cas9 Knock-Out of CBLB, NKG2A and TIGIT

To further enhance the antileukemic activity of NK-92 and CAR-NK-92, three inhibitory molecules (CBLB, NKG2A, TIGIT) were knocked out by CRISPR-Cas9. Additionally, a sequential triple knock-out of all targets was generated in the same cell-line. The employed single-guide RNAs (sgRNAs) aimed at exonic regions of the aforementioned targets (Figure 4a). Sequencing results revealed high InDel (Insertion or Deletion) efficiency for all three targets (CBLB: 71–90%, NKG2A: 84–94%, TIGIT: 80–83%, Figure 4b) and flow cytometry analyses confirmed the knock-outs at the protein level for NKG2A and TIGIT (85–100% reduction for NKG2A and 60–75% for TIGIT, Figure 4c–f). Immunoblots showed a marked reduction in CBLB protein levels following CRISPR-Cas9 treatment, consistent with the high knock-out efficacy achieved (60–100% reduction in protein expression, Figure 4g,h).

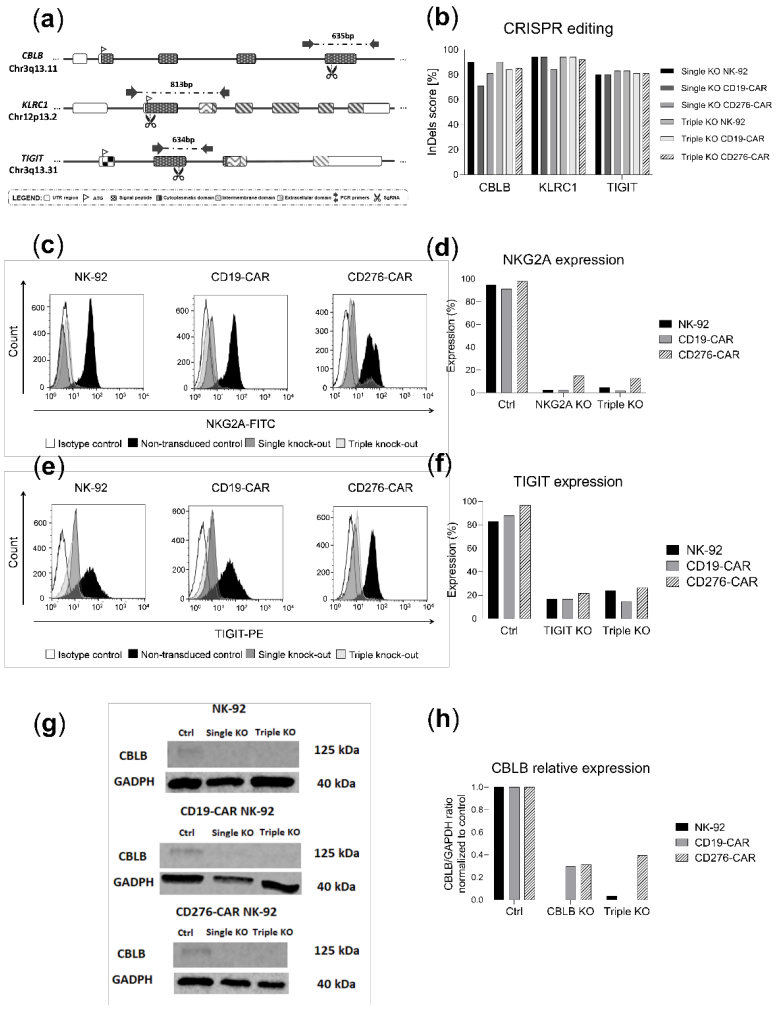

Figure 4. CRISPR-Cas9 editing of NK-92 and CAR-NK-92 cell lines. (**a**) Schematic illustration showing the cutting sites of CBLB, NKG2A and TIGIT gRNAs in their corresponding genes as well as depicting primers and PCR amplicon sizes for InDel analyses. (**b**) InDel score for CBLB, NKG2A and TIGIT in single and triple knock-out cell lines. (**c**) NKG2A histogram expression in parental cell line (black), single knock-out cell line (dark grey), triple knock-out cell line (light grey) and isotype control (white). (**d**) NKG2A protein levels in single and triple knock-out cell lines. (**e**) TIGIT histogram expression in parental cells (black), single knock-out cells (dark grey), triple knock-out cells (light grey) and isotype control (white). (**f**) TIGIT protein levels in single and triple knock-out cells. (**g**) Immunoblot of CBLB and GADPH in single and triple knock-out cells. (**h**) Normalized CBLB/GADPH ratio of band densitometry readings in single and triple knock-out cells.

2.5. Evaluation of the Effect of Inhibitory Checkpoint Knock-Out in Parental and CD19-CAR-NK-92 B-ALL Killing Assays

The generated effector cell lines were tested along with their parental counterpart in cytotoxicity assays (Figure 5). CBLB and TIGIT knock-out CD19-CAR-NK-92 showed comparable killing rates to unedited CD19-CAR-NK-92 (40–60% in 10:1 E:T ratios in calcein assays and up to 85% in luciferase assays, Figure 5b,d,f,h). Unexpectedly, the killing efficacy of CD19-CAR-NK-92 was reduced with NKG2A or triple knock-out against KOPN-8, MHH-CALL-4 and Nalm-6 but analysis at later time points (4–6 h) in luciferase assay against Nalm-6 GFP/Luc revealed similar performance to CD19-CAR-NK-92 (80.8 ± 4.5% for CD19-CAR, 75 ± 0.7% for NKG2A knock-out and 76 ± 2.3 for triple knock-out, Figure 5h). Overall, CBLB, NKG2A and TIGIT knock-out CD19-CAR cell lines did not improve the antileukemic activity of CD19-CAR cells (Figure 5b,d,f,h). Similarly, no enhancement of the effector

function could be observed in the knock-out NK-92 cell lines (Figure 5a,c,e,g). Irradiation of parental or CD19-CAR-NK-92 did not decrease the killing efficacy (Figure 5a–h).

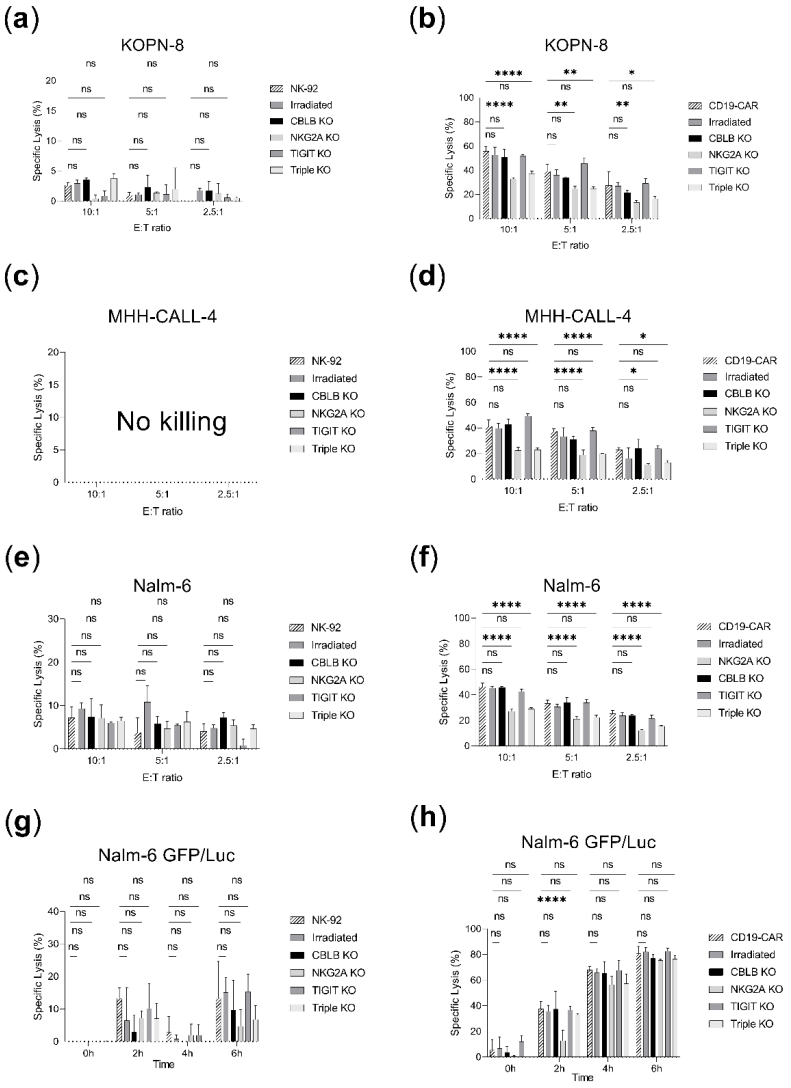

Figure 5. Cytotoxicity assays in B-ALL cell-lines comparing the cytotoxicity of parental NK-92 and CD19-CAR-NK-92 vs. irradiated, CBLB, NKG2A, TIGIT or triple knock-out cells. Specific lysis is shown as mean ± SD (n = 3). Calcein assays were incubated for 2 h and several effector-to-target (E:T) ratios were employed: 10:1, 5:1, 2.5:1. Luciferase assays were studied for a time span of 6 h at 5:1 E:T ratio. (**a**) NK-92 cell lines vs. KOPN-8 calcein assay. (**b**) CD19-CAR-NK-92 cell lines vs. KOPN-8 calcein assay. (**c**) NK-92 cell lines vs. MHH-CALL-4 calcein assay did not display cytotoxicity in the tested conditions (no killing). (**d**) CD19-CAR-NK-92 cell lines vs. MHH-CALL-4 calcein assay. (**e**) NK-92 cell lines vs. Nalm-6 calcein assay. (**f**) CD19-CAR-NK-92 cell lines vs. Nalm-6 calcein assay. (**g**) NK-92 cell lines vs. Nalm-6 GFP/Luc luciferase assay. (**h**) CD19-CAR-NK-92 cell lines vs. Nalm-6 GFP/Luc luciferase assay. * $p < 0.05$; ** $p < 0.01$; **** $p < 0.0001$; ns, non-significant ($p > 0.05$).

2.6. Evaluation of the Effect of Inhibitory Checkpoint Knock-Out in Parental and CD276-CAR-NK-92 AML Killing Assays

The antileukemic effect of CRISPR-modified NK-92 and CD276-CAR-NK-92 cells was assessed in cytotoxicity assays in AML cell lines (Figure 6). A significant boost of the cytotoxicity was observed for CBLB knock-out NK-92 against U-937, as well as CBLB and TIGIT knock-out NK-92 against U-937 CD19tag/Luc after 6 h (20–30% or 2.5 to 3-fold improvement, Figure 6e,g). CBLB knock-out in NK-92 also exhibited significant improvement against NOMO-1 and Nalm-6 in 5:1 and 2.5:1 E:T ratios, respectively, but no

benefit is observable in higher E:T ratios (Figure 6a,c). In contrast, CD276-CAR-NK-92 triple knock-out seemed to increase antileukemic activity in U-937 (20% increase in 10:1 E:T ratios, Figure 6f), but not U-937 CD19tag/Luc where the specific lysis was slightly lower (15% decrease at 6 h, Figure 6h). CBLB and TIGIT knock-outs underperformed against NOMO-1 and THP-1 (15% or 1.5 to 2-fold decrease, Figure 6b,d) but exhibited comparable killing to CD276-CAR vs. U-937 and its luciferase-expressing clone (25% in 5:1 E:T ratio and 90% at 6 h, respectively, Figure 6f,h). Killing rates were neither improved with NKG2A knock-out and remained comparable to parental CD276-CAR-NK-92 (40%, 20% and 25% specific lysis, respectively, Figure 6b,d,f) or lower (20–30% decrease at 6 h, Figure 6h). Irradiation of parental or CD276-CAR-NK-92 demonstrated similar cytotoxicity to its non-irradiated counterpart (Figure 6a–h).

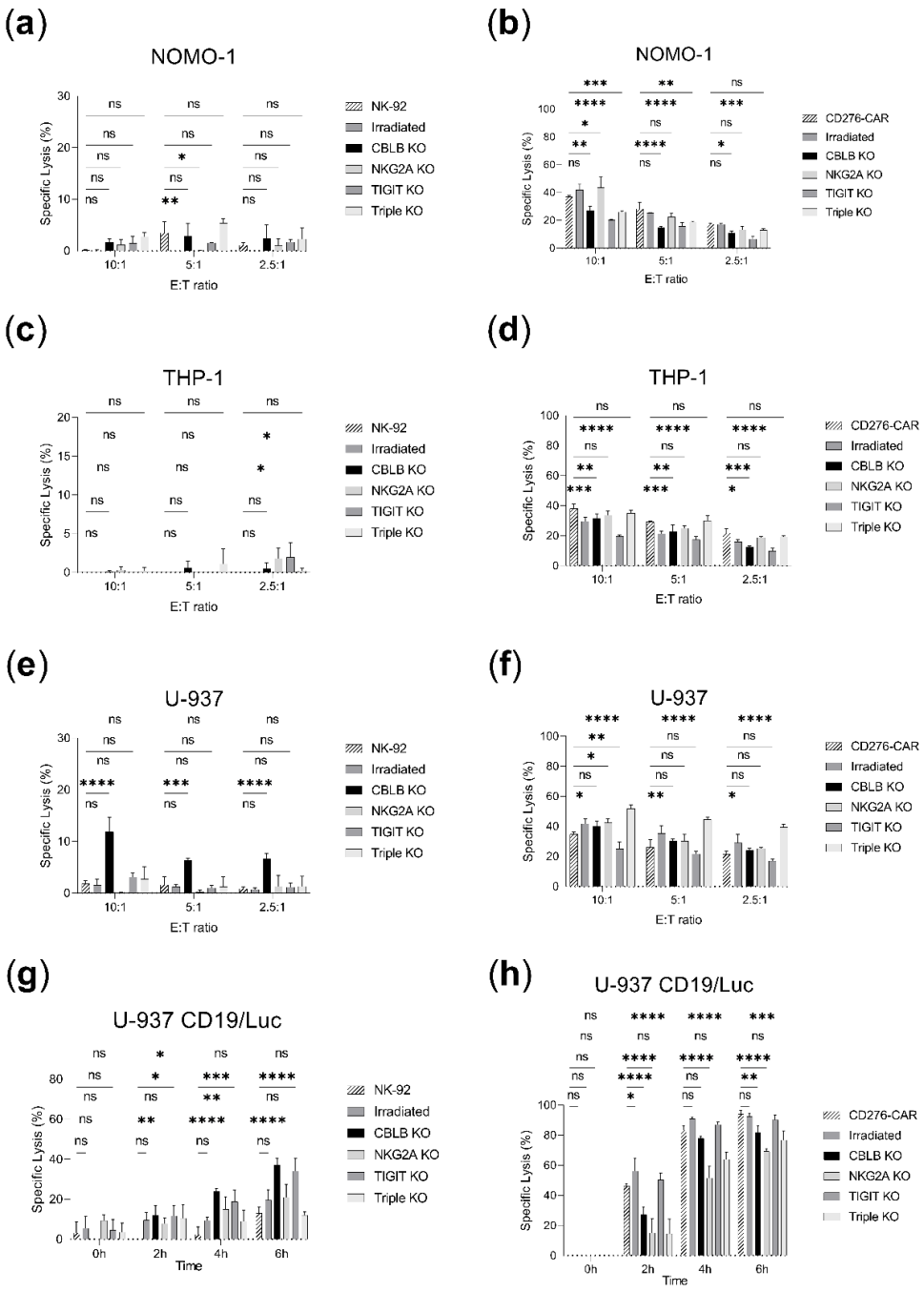

Figure 6. Cytotoxicity assays in AML cell lines comparing parental NK-92 and CD276-CAR-NK-92 vs. irradiated, CBLB, NKG2A, TIGIT or triple knock-out cells. Specific lysis is shown as mean ± SD

(n = 3). Calcein assays were incubated for 2 h and several effector-to-target (E:T) ratios were employed: 10:1, 5:1, 2.5:1. Luciferase assays were studied for a time span of 6 h at 5:1 E:T ratio. (**a**) NK-92 cell lines vs. NOMO-1 calcein assay. (**b**) CD276-CAR-NK-92 cell lines vs. NOMO-1 calcein assay. (**c**) NK-92 cell lines vs. THP-1 calcein assay. (**d**) CD276-CAR-NK-92 cell lines vs. THP-1 calcein assay. (**e**) NK-92 cell lines vs. U-937 calcein assay. (**f**) CD276-CAR-NK-92 cell lines vs. U-937 calcein assay. (**g**) NK-92 cell lines vs. U-937 CD19tag/Luc luciferase assay. (**h**) CD276-CAR-NK-92 cell lines vs. U-937 CD19tag/Luc luciferase assay. * $p < 0.05$; ** $p < 0.01$; *** $p > 0.001$; **** $p < 0.0001$; ns, non-significant ($p > 0.05$).

3. Discussion

CD19-CAR-NK-92 cell-based treatment was previously reported to exert potent and specific cytotoxicity in B-cell precursor cell lines and leukemic blasts [19]. There have been no previous studies on CD276-CAR-NK-92 cells for the treatment of AML, but their efficacy has been tested against other malignancies such as neuroblastoma or melanoma. Furthermore, earlier studies in T cells proved the effectiveness of CD276-CAR against AML cell lines and mouse models [20–23]. These observations are consistent with the results observed in the present study, where both CD19-CAR and CD276-CAR NK-92 cells exhibit a targeted and strong cytotoxic effect against B-ALL and AML cell lines, respectively, in comparison to the parental cell lines ($p < 0.0001$, Figure 3). This enhancement of the antileukemic performance, together with the unlimited source material and ease of expansion, makes CAR-NK-92 cells promising and affordable candidates for the off-the-shelf treatment of leukemia.

However, one of the main drawbacks of NK-92-based immunotherapy lies on their limited persistence in the host and thereby gradual loss of anticancer function [6]. This limitation originates from the necessary irradiation of the effector cells to ensure a safe therapeutic application. In the current study, both CD19 and CD276-CAR functionalities were not affected after 10Gy irradiation (up to 6 h of incubation, Figures 5 and 6). Nonetheless, a substantial loss of cytotoxicity in the days following the infusion is well described [24]. To overcome the loss of therapeutic efficacy due to the reduced lifespan and subsequent cytotoxicity decline of irradiated NK-92 cells, sequential transfusions of readily available effector cells are considered in the treatment scheme. Notwithstanding, this dosage strategy increases the risk of anti-HLA antibody formation against NK-92 and can negatively affect the outcome of the therapy [25,26]. Hence, it would be crucial to exert the maximum cytotoxic effect as quickly as possible to take advantage of the full antileukemic potential of each NK-92 infusion and reduce the number of doses.

Inhibitory ligands expressed by the leukemic blasts or their microenvironment can inhibit or delay the antileukemic response [27,28]. Since the expression of several inhibitory ligands was observed in both AML and B-ALL cell lines (Figure 1a,c), disrupting inhibitory checkpoints expressed on NK-92 could potentially improve their effector function. CBLB, NKG2A and TIGIT, three inhibitory checkpoints the suppression of which has been shown to boost antileukemic treatment, were selected as knock-out targets. CBLB ablation previously demonstrated cytotoxicity enhancement in placental stem-cell-derived NK cells against a HL-60 leukemia mouse model and was known to be expressed in the NK-92 cell line [9,29]. Furthermore, NKG2A blockade has been shown to induce tumor cell death in a leukemia mouse model [30]. Its expression was reported in the effector cell lines (Figure 2b) and its main ligand, HLA-E, was highly expressed in most of the target cell lines used in this work (Figure 1a,c). Finally, TIGIT was considered since its blockade in combination with other blocking antibodies resulted in enhanced NK-92 cytotoxicity against AML and its ligands CD112 and CD155 expressed in several target cell lines (Figure 1a,c) [31]. TIM-3 was initially considered as well, due to its relevance in AML immunosuppression and prominent expression of Gal-9 in the target cells but was eventually not evaluated due to its low expression in the effector NK-92 cell lines (Figure 2b) [32].

We also considered multiplexing knock-outs to favor the balance towards NK activation, which is highly dependent on the milieu of activatory versus inhibitory signals [18,27,33]. Previous research suggests that more effective strategies can be achieved when targeting several inhibitory checkpoints at the same time [31]. Accordingly, the triple knock-out of the target genes was pursued in a step-by-step approach consisting of a single target knock-out at a time, separated by at least two weeks of culture expansion to ensure proper cell recovery prior to a new transfection. This sequential method was preferred to one-shot multiplexing to avoid potential translocations or chromosomic rearrangements generated by multiple DSBs' induced at the same time [34].

Very high rates of protein knock-outs were attained for all targets (Figure 4). These efficient transfection protocols can be easily transferred to other targets of interest in NK-92 immunotherapy. Despite successful CRISPR-induced modifications, our results show no consistent improvement of the single or multiple knock-out of these inhibitory checkpoints in combination with CD19 or CD276-CAR constructs (Figures 5 and 6). This observation is in accordance with our previous study of NKG2A knock-out in CD276-CAR-NK-92 against melanoma, where no enhancement of the functionality could be reported [20]. Only in very specific set-ups, such as triple knock-out CD276-CAR versus U-937, did the knock-out approach seem to be significantly advantageous (Figure 6f). More importantly, we have reported the underperformance of NKG2A, CBLB, TIGIT or triple knock-out CAR-NK-92 cell lines, in both calcein and luciferase cytotoxicity assays (Figures 5 and 6). Since this effect is not observable in non-transduced NK-92, these unexpected findings could be attributed to loss of cellular fitness after multiple genetic manipulations of CAR-transduced NK-92. In addition, potential CRISPR-derived off-target modifications cannot be excluded. It seems that this negative effect delays the cytotoxic response but does not hamper effective cytotoxicity at later time points, as supported by the observation of a similar performance to CAR-NK-92 at 4–6 h in luciferase assays for most knock-out cell lines (Figures 5h and 6h).

It would seem that the potential benefit of the studied knock-outs in CAR-NK-92 effector function would be small and not worthy of implementation in CAR-NK-92-based antileukemic treatments. However, one of the main limitations of the current study lies in in vitro experimentation. Chamberlain et al. previously reported no benefit of PD-1 knock-out in the anticancer function of tumor-infiltrating T cells (TILs) in cytotoxicity assays [35], despite the fact that its effectiveness has been extensively proven in in vivo pre-clinical research and investigated in clinical trials [8,36]. Similarly, we cannot exclude a favorable outcome of the tested knock-outs under the complexity of in vivo models, where pro-leukemic elements such as the bone microenvironment can play a major role in cancer progression and immunosuppression [37,38]. We have shown significant benefits for CBLB and TIGIT knock-out in NK-92 cells against U-937 AML cell lines (Figure 6e,g). The CBLB knock-out in NK-92 also exhibited significant improvement against NOMO-1 and Nalm-6 in 5:1 and 2.5:1 E:T ratios, respectively, but being the reported cytotoxicity close to the detection level with no benefit presented in higher E:T ratios, we would assume this observation is likely to be an artifact and more time of incubation would be needed to assess the benefit (Figure 6a,c). The improvements observed for CBLB and TIGIT knock-outs in AML could be overshadowed in CD276-CAR-NK-92 cytotoxicity assays by the powerful CAR-driven activation, which almost reached complete lysis of leukemic cells after 6 h of co-culture (Figure 6h). We hypothesize that the CD276-CAR-NK-92 performance might be hindered by more adverse immunosuppressive conditions, where the checkpoint knock-outs could help to restore cytotoxicity or enhance it, as suggested by the significant improvement observed for the triple knock-out CD276-CAR-NK-92 against U-937 cells (Figure 6f). Further studies are needed to assess completely the effect of CBLB and TIGIT knock-outs in CD276-CAR-NK-92 immunotherapy, which are likely to exhibit therapeutic effects in the treatment of AML. We cannot conclude the same for CD19-CAR-NK-92, where the knock-out of CBLB, NKG2A and TIGIT did not improve the cytotoxic performance. Different inhibitory checkpoints should be targeted to enhance B-ALL NK-92-based immunotherapy.

4. Materials and Methods

4.1. Cell Lines and Culture Conditions

NK-92 parental cells were purchased from the American Type Culture Collection (ATCC) and were cultured with MEM Alpha Medium (1X) + GlutaMAX (Thermo Fisher Scientific, Waltham, MA, USA) supplemented with 20% *v/v* FBS, 1% *v/v* L-glu, 1% *v/v* P/S and 100 U/mL IL-2 (Miltenyi Biotec, Bergisch Gladbach, Germany). AML cell lines (NOMO-1, THP-1, U-937) and B-ALL cell lines (KOPN-8, MHH-CALL-4, Nalm-6) were obtained from the German Collection of Microorganisms and Cell Cultures GmbH (DSMZ, Braunschweig, Germany). Transgenic Nalm-6 GFP/Luciferase and U-937 CD19tag/Luciferase were generated as previously described [39,40]. Leukemia cell lines were cultured with RPMI medium supplemented with 10% *v/v* FBS, 1% *v/v* L-glu, 1% *v/v* P/S (Thermo Fisher Scientific, Waltham, MA, USA) except MHH-CALL-4 which was supplemented with 20% *v/v* FBS.

4.2. FACS Staining

Cells were washed with PBS and stained at room temperature using a 1:10 dilution of the indicated antibodies in 100 µL PBS for 10 min. Cells were washed once more to remove antibody excess and flow cytometry data was subsequently acquired with FACSCalibur (BD Biosciences, Franklin Lakes, NJ, USA). Live cells were gated based on forward and side scatter plots. Isotype staining's were performed as control conditions. Anti-CTLA-4 PE extracellular antibody, anti-Gal-9-PE and their corresponding isotype controls were purchased from Biolegend, San Diego, CA, USA. The rest of the antibodies (anti-CD276-PE, anti-CD80-PE, anti-CD86-APC, anti-CD273-PE, anti-CD274-APC, anti-HLA-E-APC, anti-CD112-PE, anti-CD66abce-APC, anti-CD155-PE, anti-CD19-APC or FITC, anti-PD1-PE, anti-TIM3-APC, anti-NKG2A-FITC, CD56-APC, CD96-APC, TIGIT-PE, CD34-APC, CD271-PE and corresponding isotype controls) were obtained from Miltenyi Biotec, Bergisch Gladbach, Germany. CD19-CAR and CD276-CAR expression on NK-92 cells was determined by CD271 and CD34 marker gene expression, respectively, whereas luciferase expression on target cells was correlated with GFP for Nalm-6 GFP/Luc and CD19 marker expression for U-937 CD19tag/Luc.

4.3. CAR Transduction

For CD19-CAR transduction, the 19–28z SFGγ retroviral vector employed in this work (kindly provided by Michel Sadelain (MSKCC) to J.F.) has been previously described [41,42]. Virus and transductions were performed as formerly reported (293Vec-RD114 packaging cells were kindly provided by BioVec Pharma Inc, Québec, Canada) [39]. Second-generation CD276-CAR lentiviral vector and transduction in NK-92 cells were described in an earlier publication [23].

4.4. CRISPR-Cas9 Transfection

Three different NK-cell inhibitory checkpoints (CBLB, NKG2A, TIGIT) were disrupted in effector NK-92 and CAR-NK-92 cell lines by the CRISPR-Cas9 system. The employed sgRNAs were previously tested or newly designed using CHOPCHOP v3 software (www.chopchop.cbu.uib.no (accessed on 27 May 2022), Table 1) [43].

Table 1. List of sgRNAs employed in this study.

Target Gene	gRNA Nucleotide Sequence	Reference
CBLB	TAATCTGGTGGACCTCATGA	Guo et al. [9]
KLRC1 (NKG2A)	GGTCTGAGTAGATTACTCCT	Grote et al. [20]
TIGIT	ACCCTGATGGGACGTACACT	Own design (CHOPCHOP)

KLRC1 (NKG2A) knock-out was generated by using the Neon transfection system (ThermoFisher, Scientific, Waltham, MA, USA) and knock-out cells were sorted and en-

riched, as formerly described. [20] CBLB and TIGIT knock-outs were generated employing MaxCyte GTx™ electroporator (MaxCyte Inc, Rockville, MD, USA). V3 Cas9 and sgRNA (IDT, Coralville, IA, USA) were incubated at a molar ratio of 1:2 (1.5 µmol to 3 µmol) for 15 min to favor RNP complexation. Two and a half million cells were washed and resuspended in 50 µL of MaxCyte® electroporation buffer, then mixed with the RNP and electroporated in R-50x3 processing assemblies using the NK-4 electroporation protocol (MaxCyte, Rockville, MD, USA). Cells were seeded in pre-warmed 12-wellplates after electroporation and were incubated for 30 min in the incubator. Next, fresh medium without antibiotics and interleukins was added at 2×10^6 cells/mL. After four hours, a culture medium with 2X IL-2 (200 U/mL) was added to have a final concentration of 1×10^6 cells/mL. For the generation of triple knock-out, NKG2A knock-out cells were expanded for two weeks before transfecting CBLB RNP with the same MaxCyte protocol as described in this section. The double knock-out cells were expanded again for two weeks and finally transfected with TIGIT RNP using the MaxCyte protocol (MaxCyte, Rockville, MD, USA).

4.5. Assessment of CRISPR-Cas9-Induced Knock-Out

On day 5 post-electroporation, the CRISPR-modified cells were harvested for DNA isolation with the NucleoSpin Tissue kit following the manufacturer's instructions (Macherey-Nagel, Düren, Germany) and were employed in PCR reactions to amplify the target region (primer sequences and PCR protocols described in Table S1). Samples were cleaned up of remaining reagents with QIAquick PCR purification kit (Qiagen, Hilden, Germany) and were sequenced by Sanger-sequencing (Eurofins Genomics, Ebersberg, Germany). CRISPR-induced insertions and deletions were analyzed by ICE v3 software (www.ice.synthego.com (accessed on 17 May to 2 August 2022), Synthego, Redwood, CA, USA). [44] NKG2A and TIGIT knock-outs were assessed by flow cytometry as aforementioned whereas CBLB knock-out was analysed by Western blot.

4.6. CBLB Western Blot

Three to five million cells were resuspended in RIPA Lysis and Extraction Buffer (ThermoFisher, Scientific, Waltham, MA, USA) supplemented with 1X Halt™ Protease and Phosphatase Inhibitor Cocktail (ThermoFisher, Scientific, Waltham, MA, USA) and incubated on ice for 20 min. The soluble fraction was recovered after 10 min of centrifugation at 10,000× *g* 4 °C. Protein concentration was determined by standard Bradford assay. A total of 20 µg of protein was loaded in a Mini-PROTEAN TGX gel (Bio-Rad, Hercules, CA, USA) and separated by electrophoresis. The gel was transferred to a Midi format 0.2 µm PVDF membrane using Trans-Blot Turbo Transfer System (Bio-Rad, Hercules, CA, USA). The membrane was blocked with EveryBlot Blocking Buffer (Bio-Rad, Hercules, CA, USA) and incubated for 1 h at room temperature (RT) or overnight at 4 °C with rabbit anti-CBLB (Cell Signaling Technologies, Danvers, MA, USA, clone: D3C12) diluted at 1:500 and rat anti-GAPDH (Biolegend, San Diego, CA, USA, clone: W17079A) diluted at 1:1000 in blocking buffer. After washing, the membrane was incubated for 1 h at room temperature with IRDye 800CW goat anti-rat and IRDye 680RD goat anti-rabbit (LI-COR Biosciences, Lincoln, NE, USA) at 1:15,000 in a blocking buffer. The membrane was developed using LI-COR Odyssey Fc and band intensity was quantified with Image Studio 4.0 (LI-COR Biosciences, Lincoln, NE, USA).

4.7. Calcein Release Assay

Calcein solution (Calcein AM, Biolegend, San Diego, CA, USA) was prepared at 1 µg/µL in DMSO. Target cells were washed and resuspended in PBS at 10^6 cells/mL, then incubated at 37 °C 5% CO_2 in the incubator with 10 µL of calcein solution per mL of cell suspension for 1 h with gentle swirls every 10 min. Next, target cells were washed three times with assay medium (RPMI 10% FBS) to remove calcein excess. The target cell solution was prepared at 10^5 cells/mL in assay medium and 100 µL was added to a 96 well-plate.

100 µL of effector cells were added to the target cells at indicated ratios in technical triplicates. Two controls were prepared in the same plate: spontaneous lysis (SL, target cells in assay medium) and maximum killing (MK, target cells in assay medium with Tryton X-100). The plate was placed in the incubator for 2 h before taking fluorometric measurements of the supernatant in a TECAN Spark reader (TECAN, Männedorf, Switzerland) to measure calcein release. Effector-specific lysis (ESL) was calculated as below:

$$\text{ESL} = (\text{measured value} - \text{SL})/(\text{MK} - \text{SL}) \times 100 \quad (1)$$

4.8. Luciferase Assay

Nalm6-expressing Luc-GFP and U937 CD19tag/Luc served as target cells for luciferase cytotoxicity assay protocols. In brief, 1×10^4 target cells were resuspended in 100 µL of assay medium (RPMI 10% FBS) and co-cultured with 5×10^4 effector cells in 50 µL of assay medium for different time points in the incubator (0–6 h) and in technical triplicates. D-luciferin (Gold-Bio, St. Louis, MO, USA) was dissolved in pure water to a final concentration of 15 mg/mL and stored at −20 °C. To generate the working assay solution, a stock aliquot was mixed 1:4 in RPMI 10% FBS and 50 µL were added to each assay well (final volume 200 µL) immediately before the luminescence measurement in TECAN Spark reader (TECAN, Männedorf, Switzerland). Effector-specific lysis (ESL) was calculated according to spontaneous lysis (SL, target cells in assay medium with luciferin) and maximum killing controls (MK, target cells in assay medium with Tryton X-100 and luciferin) using Formula (1).

4.9. Data Analysis

All graphical and statistical analyses were performed with GraphPad Prism 9 software (GraphPad Software Inc., San Diego, CA, USA). Two-way ANOVA analyses were performed for gaussian distributed datasets. Multiple non-parametric *t*-tests were performed when the Shapiro–Wilk test for normal distribution was not passed. Flow cytometry data were analyzed using FlowJo software (FlowJo LLC., BD Biosciences, Franklin Lakes, NJ, USA).

Supplementary Materials: The following supporting information can be downloaded at: https://www.mdpi.com/article/10.3390/ijms232112828/s1.

Author Contributions: Conceptualization, G.U.-B. and M.M.; methodology, G.U.-B., A.R.-M., J.F. and M.M.; software, G.U.-B. and T.M.G.; validation, G.U.-B. and M.M.; formal analysis, G.U.-B.; investigation, G.U.-B., J.-M.D., Y.H., A.D. and T.M.G.; resources, A.R.-M., S.S., D.A., C.S., J.F., R.H. and M.M.; data curation, G.U.-B.; writing—original draft preparation, G.U.-B.; writing—review and editing, G.U.-B., J.F., A.D., C.S., J.S.A. and M.M.; visualization, G.U.-B.; supervision, J.S.A., T.M.G. and M.M. All authors have read and agreed to the published version of the manuscript.

Funding: This work was supported by Stefan Morsch Stiftung, Clinician Scientist Program (N°. 440-0-0), MaxCyte Inc. and the University Children's Hospital of Tübingen. We acknowledge support by Open Access Publishing Fund of University of Tübingen.

Institutional Review Board Statement: The study was conducted according to the guidelines of the Declaration of Helsinki, and approved by ethics committee at the Medical Faculty of the Eberhard Karls University and the University Hospital Tuebingen (reference number 008/2014BO2).

Informed Consent Statement: Not applicable.

Data Availability Statement: The data presented in this study are available from the corresponding author upon reasonable request.

Acknowledgments: We thank our colleagues Carmen Julia Pastor-Maldonado and Mary Elisabeth Carter for their thorough language revision of the manuscript. We also acknowledge the support of Evi Schmid's group in Children's Hospital of Tuebingen with the performance of standard Bradford assays for protein quantification.

Conflicts of Interest: The authors declare no conflict of interest.

References

1. Davis, A.S.; Viera, A.J.; Mead, M.D. Leukemia: An overview for primary care. *Am. Fam. Physician* **2014**, *89*, 731–738. [PubMed]
2. Seth, R.; Singh, A. Leukemias in Children. *Indian J. Pediatr.* **2015**, *82*, 817–824. [CrossRef] [PubMed]
3. Shallis, R.M.; Wang, R.; Davidoff, A.; Ma, X.; Zeidan, A.M. Epidemiology of acute myeloid leukemia: Recent progress and enduring challenges. *Blood Rev.* **2019**, *36*, 70–87. [CrossRef]
4. Liu, Y.; Chen, X.; Han, W.; Zhang, Y. Tisagenlecleucel, an approved anti-CD19 chimeric antigen receptor T-cell therapy for the treatment of leukemia. *Drugs Today* **2017**, *53*, 597–608. [CrossRef] [PubMed]
5. Ureña-Bailén, G.; Lamsfus-Calle, A.; Daniel-Moreno, A.; Raju, J.; Schlegel, P.; Seitz, C.; Atar, D.; Antony, J.S.; Handgretinger, R.; Mezger, M. CRISPR/Cas9 technology: Towards a new generation of improved CAR-T cells for anticancer therapies. *Brief. Funct. Genom.* **2020**, *19*, 191–200. [CrossRef]
6. Fabian, K.P.; Hodge, J.W. The emerging role of off-the-shelf engineered natural killer cells in targeted cancer immunotherapy. *Mol. Ther. Oncolytics* **2021**, *23*, 266–276. [CrossRef] [PubMed]
7. Boissel, L.; Campbell, K.; Toneguzzo, F.; Nichols, K.; Klingemann, H. NK-92: An "off the shelf" target-specific cytotoxic cell therapeutic. *Cytotherapy* **2015**, *17*, S19. [CrossRef]
8. McGowan, E.; Lin, Q.; Ma, G.; Yin, H.; Chen, S.; Lin, Y. PD-1 disrupted CAR-T cells in the treatment of solid tumors: Promises and challenges. *Biomed. Pharmacother.* **2020**, *121*, 109625. [CrossRef]
9. Guo, X.; Mahlakõiv, T.; Ye, Q.; Somanchi, S.; He, S.; Rana, H.; DiFiglia, A.; Gleason, J.; van der Touw, W.; Hariri, R.; et al. CBLB ablation with CRISPR/Cas9 enhances cytotoxicity of human placental stem cell-derived NK cells for cancer immunotherapy. *J. Immunother. Cancer* **2021**, *9*, e001975. [CrossRef]
10. Zhu, H.; Blum, R.H.; Bernareggi, D.; Ask, E.H.; Wu, Z.; Hoel, H.J.; Meng, Z.; Wu, C.; Guan, K.L.; Malmberg, K.J.; et al. Metabolic Reprograming via Deletion of CISH in Human iPSC-Derived NK Cells Promotes In Vivo Persistence and Enhances Anti-tumor Activity. *Cell Stem Cell* **2020**, *27*, 224–237. [CrossRef]
11. Giuffrida, L.; Sek, K.; Henderson, M.A.; Lai, J.; Chen, A.X.Y.; Meyran, D.; Todd, K.L.; Petley, E.V.; Mardiana, S.; Mølck, C.; et al. CRISPR/Cas9 mediated deletion of the adenosine A2A receptor enhances CAR T cell efficacy. *Nat. Commun.* **2021**, *12*, 3236. [CrossRef] [PubMed]
12. Jung, I.Y.; Kim, Y.Y.; Yu, H.S.; Lee, M.; Kim, S.; Lee, J. CRISPR/Cas9-Mediated Knockout of DGK Improves Antitumor Activities of Human T Cells. *Cancer Res.* **2018**, *78*, 4692–4703. [CrossRef] [PubMed]
13. Huang, R.S.; Shih, H.A.; Lai, M.C.; Chang, Y.J.; Lin, S. Enhanced NK-92 Cytotoxicity by CRISPR Genome Engineering Using Cas9 Ribonucleoproteins. *Front. Immunol.* **2020**, *11*, 1008. [CrossRef] [PubMed]
14. Morimoto, T.; Nakazawa, T.A.-O.; Matsuda, R.; Nishimura, F.; Nakamura, M.A.-O.; Yamada, S.A.-O.; Nakagawa, I.A.-O.; Park, Y.S.; Tsujimura, T.; Nakase, H.A.-O. CRISPR-Cas9-Mediated TIM3 Knockout in Human Natural Killer Cells Enhances Growth Inhibitory Effects on Human Glioma Cells. *Int. J. Mol. Sci.* **2021**, *22*, 3489. [CrossRef]
15. Wang, Y.; Mohseni, M.; Grauel, A.; Diez, J.E.; Guan, W.; Liang, S.; Choi, J.E.; Pu, M.; Chen, D.; Laszewski, T.; et al. SHP2 blockade enhances anti-tumor immunity via tumor cell intrinsic and extrinsic mechanisms. *Sci. Rep.* **2021**, *11*, 1399. [CrossRef]
16. Afolabi, L.O.; Adeshakin, A.O.; Sani, M.M.; Bi, J.; Wan, X. Genetic reprogramming for NK cell cancer immunotherapy with CRISPR/Cas9. *Immunology* **2019**, *158*, 63–69. [CrossRef]
17. Dimitri, A.; Herbst, F.; Fraietta, J.A. Engineering the next-generation of CAR T-cells with CRISPR-Cas9 gene editing. *Mol. Cancer* **2022**, *21*, 78. [CrossRef]
18. Souza-Fonseca-Guimaraes, F.; Cursons, J.; Huntington, N.D. The Emergence of Natural Killer Cells as a Major Target in Cancer Immunotherapy. *Trends Immunol.* **2019**, *40*, 142–158. [CrossRef]
19. Romanski, A.; Uherek, C.; Bug, G.; Seifried, E.; Klingemann, H.; Wels, W.S.; Ottmann, O.G.; Tonn, T. CD19-CAR engineered NK-92 cells are sufficient to overcome NK cell resistance in B-cell malignancies. *J. Cell. Mol. Med.* **2016**, *20*, 1287–1294. [CrossRef]
20. Grote, S.; Ureña-Bailén, G.; Chan, K.C.; Baden, C.; Mezger, M.; Handgretinger, R.; Schleicher, S. In Vitro Evaluation of CD276-CAR NK-92 Functionality, Migration and Invasion Potential in the Presence of Immune Inhibitory Factors of the Tumor Microenvironment. *Cells* **2021**, *10*, 1020. [CrossRef]
21. Lichtman, E.I.; Du, H.; Shou, P.; Song, F.; Suzuki, K.; Ahn, S.; Li, G.; Ferrone, S.; Su, L.; Savoldo, B.; et al. Preclinical Evaluation of B7-H3-specific Chimeric Antigen Receptor T Cells for the Treatment of Acute Myeloid Leukemia. *Clin. Cancer Res.* **2021**, *27*, 3141–3153. [CrossRef]
22. Zhang, Z.; Jiang, C.; Liu, Z.; Yang, M.; Tang, X.; Wang, Y.; Zheng, M.; Huang, J.; Zhong, K.; Zhao, S.; et al. B7-H3-Targeted CAR-T Cells Exhibit Potent Antitumor Effects on Hematologic and Solid Tumors. *Mol. Ther. Oncolytics* **2020**, *17*, 180–189. [CrossRef]
23. Grote, S.; Chan, K.C.-H.; Baden, C.; Bösmüller, H.; Sulyok, M.; Frauenfeld, L.; Ebinger, M.; Handgretinger, R.; Schleicher, S. CD276 as a novel CAR NK-92 therapeutic target for neuroblastoma. *Adv. Cell Gene Ther.* **2021**, *4*, e105. [CrossRef]
24. Navarrete-Galvan, L.; Guglielmo, M.; Cruz Amaya, J.; Smith-Gagen, J.; Lombardi, V.C.; Merica, R.; Hudig, D. Optimizing NK-92 serial killers: Gamma irradiation, CD95/Fas-ligation, and NK or LAK attack limit cytotoxic efficacy. *J. Transl. Med.* **2022**, *20*, 151. [CrossRef] [PubMed]
25. Arai, S.; Meagher, R.; Swearingen, M.; Myint, H.; Rich, E.; Martinson, J.; Klingemann, H. Infusion of the allogeneic cell line NK-92 in patients with advanced renal cell cancer or melanoma: A phase I trial. *Cytotherapy* **2008**, *10*, 625–632. [CrossRef] [PubMed]
26. Klingemann, H.; Boissel, L.; Toneguzzo, F. Natural Killer Cells for Immunotherapy—Advantages of the NK-92 Cell Line over Blood NK Cells. *Front. Immunol.* **2016**, *7*, 91. [CrossRef] [PubMed]

27. Wolf, N.K.; Kissiov, D.U.; Raulet, D.H. Roles of natural killer cells in immunity to cancer, and applications to immunotherapy. *Nat. Rev. Immunol.* **2022**. [CrossRef]
28. Daher, M.; Rezvani, K. Next generation natural killer cells for cancer immunotherapy: The promise of genetic engineering. *Curr. Opin. Immunol.* **2018**, *51*, 146–153. [CrossRef]
29. Paolino, M.; Choidas, A.; Wallner, S.; Pranjic, B.; Uribesalgo, I.; Loeser, S.; Jamieson, A.M.; Langdon, W.Y.; Ikeda, F.; Fededa, J.P.; et al. The E3 ligase Cbl-b and TAM receptors regulate cancer metastasis via natural killer cells. *Nature* **2014**, *507*, 508–512. [CrossRef]
30. Ruggeri, L.; Urbani, E.; André, P.; Mancusi, A.; Tosti, A.; Topini, F.; Bléry, M.; Animobono, L.; Romagné, F.; Wagtmann, N.; et al. Effects of anti-NKG2A antibody administration on leukemia and normal hematopoietic cells. *Haematologica* **2016**, *101*, 626–633. [CrossRef]
31. Brauneck, F.; Seubert, E.; Wellbrock, J.; Schulze Zur Wiesch, J.; Duan, Y.; Magnus, T.; Bokemeyer, C.; Koch-Nolte, F.; Menzel, S.; Fiedler, W. Combined Blockade of TIGIT and CD39 or A2AR Enhances NK-92 Cell-Mediated Cytotoxicity in AML. *Int. J. Mol. Sci.* **2021**, *22*, 12919. [CrossRef]
32. Gonçalves Silva, I.; Yasinska, I.M.; Sakhnevych, S.S.; Fiedler, W.; Wellbrock, J.; Bardelli, M.; Varani, L.; Hussain, R.; Siligardi, G.; Ceccone, G.; et al. The TIM-3-galectin-9 Secretory Pathway is Involved in the Immune Escape of Human Acute Myeloid Leukemia Cells. *EBioMedicine* **2017**, *22*, 44–57. [CrossRef] [PubMed]
33. Anel, A.; Aguiló, J.I.; Catalán, E.; Garaude, J.; Rathore, M.G.; Pardo, J.; Villalba, M. Protein Kinase C-θ (PKC-θ) in Natural Killer Cell Function and Anti-Tumor Immunity. *Front. Immunol.* **2012**, *3*, 187. [CrossRef] [PubMed]
34. Webber, B.R.; Lonetree, C.-L.; Kluesner, M.G.; Johnson, M.J.; Pomeroy, E.J.; Diers, M.D.; Lahr, W.S.; Draper, G.M.; Slipek, N.J.; Smeester, B.A.; et al. Highly efficient multiplex human T cell engineering without double-strand breaks using Cas9 base editors. *Nat. Commun.* **2019**, *10*, 5222. [CrossRef] [PubMed]
35. Chamberlain, C.A.; Bennett, E.P.; Kverneland, A.H.; Svane, I.M.; Donia, M.; Met, Ö. Highly efficient PD-1-targeted CRISPR-Cas9 for tumor-infiltrating lymphocyte-based adoptive T cell therapy. *Mol. Ther. Oncolytics* **2022**, *24*, 417–428. [CrossRef]
36. Zhao, Z.; Shi, L.; Zhang, W.; Han, J.; Zhang, S.; Fu, Z.; Cai, J. CRISPR knock out of programmed cell death protein 1 enhances anti-tumor activity of cytotoxic T lymphocytes. *Oncotarget* **2018**, *9*, 5208–5215. [CrossRef]
37. Pimenta, D.B.; Varela, V.A.; Datoguia, T.S.; Caraciolo, V.B.; Lopes, G.H.; Pereira, W.O. The Bone Marrow Microenvironment Mechanisms in Acute Myeloid Leukemia. *Front. Cell Dev. Biol.* **2021**, *9*, 3164. [CrossRef]
38. Gnoni, A.; Brunetti, O.; Longo, V.; Calabrese, A.; Argentiero, A.L.; Calbi, R.; Solimando Antonio, G.; Licchetta, A. Immune system and bone microenvironment: Rationale for targeted cancer therapies. *Oncotarget* **2020**, *11*, 480–487. [CrossRef]
39. Feucht, J.; Sun, J.; Eyquem, J.; Ho, Y.-J.; Zhao, Z.; Leibold, J.; Dobrin, A.; Cabriolu, A.; Hamieh, M.; Sadelain, M. Calibration of CAR activation potential directs alternative T cell fates and therapeutic potency. *Nat. Med.* **2019**, *25*, 82–88. [CrossRef]
40. Seitz, C.M.; Mittelstaet, J.; Atar, D.; Hau, J.; Reiter, S.; Illi, C.; Kieble, V.; Engert, F.; Drees, B.; Bender, G.; et al. Novel adapter CAR-T cell technology for precisely controllable multiplex cancer targeting. *Oncoimmunology* **2021**, *10*, 2003532. [CrossRef]
41. Brentjens, R.J.; Santos, E.; Nikhamin, Y.; Yeh, R.; Matsushita, M.; La Perle, K.; Quintás-Cardama, A.; Larson, S.M.; Sadelain, M. Genetically targeted T cells eradicate systemic acute lymphoblastic leukemia xenografts. *Clin. Cancer Res.* **2007**, *13*, 5426–5435. [CrossRef] [PubMed]
42. Rivière, I.; Brose, K.; Mulligan, R.C. Effects of retroviral vector design on expression of human adenosine deaminase in murine bone marrow transplant recipients engrafted with genetically modified cells. *Proc. Natl. Acad. Sci. USA* **1995**, *92*, 6733–6737. [CrossRef] [PubMed]
43. Labun, K.; Montague, T.G.; Krause, M.; Torres Cleuren, Y.N.; Tjeldnes, H.; Valen, E. CHOPCHOP v3: Expanding the CRISPR web toolbox beyond genome editing. *Nucleic Acids Res.* **2019**, *47*, W171–W174. [CrossRef] [PubMed]
44. Conant, D.; Hsiau, T.; Rossi, N.; Oki, J.; Maures, T.; Waite, K.; Yang, J.; Joshi, S.; Kelso, R.; Holden, K.; et al. Inference of CRISPR Edits from Sanger Trace Data. *CRISPR J.* **2022**, *5*, 123–130. [CrossRef]

PAPER 2

Automated good manufacturing practice-compatible CRISPR-Cas9 editing of hematopoietic and progenitor stem cells for clinical treatment of β-hemoglobinopathies

The CRISPR Journal
Volume XX, Number X, 2023

DOI: 10.1089/crispr.2022.0086

The CRISPR Journal

ORIGINAL ARTICLE

Automated Good Manufacturing Practice-Compatible CRISPR-Cas9 Editing of Hematopoietic Stem and Progenitor Cells for Clinical Treatment of β-Hemoglobinopathies

Guillermo Ureña-Bailén,[1,†] Milena Block,[2,†] Tommaso Grandi,[2] Faidra Aivazidou,[2] Jona Quednau,[2] Dariusz Krenz,[2] Alberto Daniel-Moreno,[1] Andrés Lamsfus-Calle,[1] Thomas Epting,[3] Rupert Handgretinger,[1,4] Stefan Wild,[2,‡] and Markus Mezger[1,*,‡]

Cellular therapies hold enormous potential for the cure of severe hematological and oncological disorders. The forefront of innovative gene therapy approaches including therapeutic gene editing and hematopoietic stem cell transplantation needs to be processed by good manufacturing practice to ensure safe application in patients. In the present study, an effective transfection protocol for automated clinical-scale production of genetically modified hematopoietic stem and progenitor cells (HSPCs) using the CliniMACS Prodigy® system including the CliniMACS Electroporator (Miltenyi Biotec) was established. As a proof-of-concept, the enhancer of the *BCL11A* gene, clustered regularly interspaced short palindromic repeat (CRISPR) target in ongoing clinical trials for β-thalassemia and sickle-cell disease treatment, was disrupted by the CRISPR-Cas9 system simulating a large-scale clinical scenario, yielding 100 million HSPCs with high editing efficiency. *In vitro* erythroid differentiation and high-performance liquid chromatography analyses corroborated fetal hemoglobin resurgence in edited samples, supporting the feasibility of running the complete process of HSPC gene editing in an automated closed system.

Introduction

Gene editing approaches are currently used to develop therapies for the treatment of severe hematological disorders. Among other technologies, the clustered regularly interspaced short palindromic repeat (CRISPR)-Cas9 system has proven to be one of the most versatile and affordable technologies for gene therapy. Its applications include disruption, addition, and correction of genes of interest in a great variety of clinically relevant cells.[1–6] Recently, an important improvement in the health and life quality of two patients treated by a CRISPR-based gene therapy suffering from β-thalassemia and sickle-cell disease (SCD), respectively, was reported.[7] The strategy consisted in targeting *BCL11A*, a gene involved in the negative regulation of fetal hemoglobin (HbF), to promote the resurgence of HbF expression as previously demonstrated in preclinical studies.[8–10] These results encourage the expansion of CRISPR-based protocols for the treatment of β-hemoglobinopathies and other hematological disorders.

For the implementation of these therapies, it is common to perform genetic engineering of effector cells *ex vivo,* before their infusion into the patient. In this context, electroporation is a valuable option for the delivery of the CRISPR-Cas9 components into the cells. The electric field exerted in the cellular membrane during the electroporation process increases the permeability and allows efficient transfer of the cargo into the cells.[11,12]

The CliniMACS Prodigy system (Miltenyi Biotec) offers fully automated cell culture and expansion in a closed, good manufacturing practice (GMP)-compatible system. The CliniMACS Electroporator was recently implemented into

[1]*Department of General Pediatrics, Oncology and Hematology, University Children's Hospital, Tübingen, Germany;* [2]*Miltenyi Biotec B.V. & Co. KG, Bergisch Gladbach, Germany;* [3]*Institute for Clinical Chemistry and Laboratory Medicine, University Hospital, Freiburg, Germany; and* [4]*Abu Dhabi Stem Cells Center, Abu Dhabi, United Arab Emirates.*
[†]*These authors have contributed equally to this work and share the first authorship.*
[‡]*These authors have contributed equally to this work and share the senior authorship.*

*Address correspondence to: *Markus Mezger, Department of General Pediatrics, Oncology and Hematology, University Children's Hospital, Hoppe-Seyler-Straße 1, Tübingen DE 72076, Germany,* E-mail: markus.mezger@med.uni-tuebingen.de

the platform design, enabling additional gene-editing protocols using a single process within one closed tubing set. In this publication, we propose an optimized transfection protocol for editing $CD34^+$ hematopoietic stem and progenitor cells (HSPCs) at a clinical production scale that facilitates translation to patient treatment.

Materials and Methods

Ethics statement

All leukapheresis samples were obtained following standard collection procedures in accordance with the guidelines of the certified collection centers (Cytocare).

HSPC isolation and culture

$CD34^+$ HSPCs were magnetically isolated from mobilized leukapheresis products from healthy donors using the CliniMACS Plus or CliniMACS Prodigy (Miltenyi Biotec). The isolation was performed using the CliniMACS $CD34^+$ reagent (Miltenyi Biotec).

HSPCs were used freshly after isolation or were thawed and recovered from frozen aliquots. They were cultured at a concentration of 1×10^6 cells/mL in an HSC medium 1 day before electroporation at 37°C 5% CO_2 in 24-well plates in the incubator (Heracell; Thermo Fisher) or the CliniMACS Prodigy cell culture unit (Miltenyi Biotec). The HSC medium consisted of HSC-Brew GMP Basal Medium (Miltenyi Biotec) supplemented with 1% HSC-Brew GMP Supplement (Miltenyi Biotec), 2% human serum albumin (HSA) (Octapharma), MACS® GMP Recombinant Human stem cell factor (SCF) (100 ng/mL), MACS® GMP Recombinant Human thrombopoietin (TPO) (20 ng/mL), and MACS® GMP Recombinant Human Flt-3 ligand (100 ng/mL; Miltenyi Biotec).

Small-scale HSPC electroporation

$CD34^+$ cells were transfected in CliniMACS Electroporation Buffer (Miltenyi Biotec) at a concentration of 5×10^6 to 1.5×10^7 cells/mL using the CliniMACS Prodigy electroporator with 1 μg DsRed mRNA (*in vitro* transcribed as previously described).[8] One hundred microliters of cell suspension was electroporated in 0.2 cm electrode distance Ingenio® electroporation cuvettes (Mirus Bio LLC) using the test cuvette adapter (TCA) and the respective software on the CliniMACS Prodigy. The used electroporation parameters are indicated in the Results section. For all experiments, two consecutive electroporation pulses with defined voltage and time were applied. In addition, interrupted (burst) as well as bipolar pulses were tested with 8 μs burst duration. After electroporation, cells were transferred to a 24-well plate for recovery in HSC medium at 37°C or 32°C, 5% CO_2.

Upscale HPSC electroporation

The cuvette of the CliniMACS Prodigy EP-2 was manually filled with 600 μL of $CD34^+$ cells in the CliniMACS Electroporation Buffer (Miltenyi Biotec) at a concentration of 5×10^6 to 1.5×10^7 cells/mL with either 30 μg/mL eGFP mRNA (Miltenyi Biotec) or 150–900 pmol ribonucleoprotein (RNP) complex per million cells. The cuvette was placed into the CliniMACS Electroporator and cells were electroporated using the TCA software on the CliniMACS Prodigy. Unless indicated otherwise, the following electroporation parameters were used:

- Pulse 1 (high voltage): 600 V 104 μs burst/bipolar—8 μs burst duration.
- Pulse 2 (low voltage): 200 V 5000 μs square.

After electroporation, the electroporated cell suspension was added to 6 mL of HSC medium and transferred to a 24-well plate for overnight recovery culture at 37°C or 32°C, 5% CO_2.

Automated generation of edited $CD34^+$ HPSCs (Prodigy sample)

$CD34^+$ HSPCs were manufactured using the T cell engineering (TCE) process on the CliniMACS Prodigy platform. Process parameters were defined by the operator and saved in the activity matrix of the process. The separated $CD34^+$ HSPCs were connected to the tubing set, after evaluation of the viability and total cell number. The cells were automatically transferred to the CentriCult Unit (CCU) of the CliniMACS Prodigy TS 520 (Miltenyi Biotec) and cultivated using the same medium, temperature, and CO_2 concentration used for the small-scale experiments. On day 1, $CD34^+$ cells were electroporated using the CliniMACS Prodigy EP-2 tubing set on the CliniMACS electroporator: cells were rebuffered in the CliniMACS Electroporation Buffer (Miltenyi Biotec); the RNP was transferred to the nucleic acid bag, and electroporation was started using the optimized pulse previously described in the upscale electroporation.

After each electroporation cycle, the edited cells were automatically transferred back to the cultivation chamber and cultured in HSC medium for 24 h including shaking (shaker type 2). On day 2, the cells were formulated in NaCl supplemented with 0.5% HSA and cells were harvested in the target cell bag. The final cell product was directly used for functional analysis or frozen until further use.

CRISPR-Cas9 transfection and analysis

To prove the efficacy of the electroporation settings, a previously designed sgRNA targeting *BCL11A* was used (Table 1). Unless indicated otherwise, the sgRNA

Table 1. Sequences of BCL11A gRNA and primers used in this work

	Sequence	*Ref.*
BCL11A gRNA	CTAACAGTTGCTTTTATCAC	8
BCL11A forward primer	GTGTATGTGCTGATTGAGGGC	
BCL11A reverse primer	GGACAGCCCGACAGATGAAA	

and Cas9 V3 ribonucleoprotein (Integrated DNA Technologies) were incubated for 20 min at room temperature at a 1:2 molar ratio, complexing 450 pmol of Cas9 and 900 pmol of sgRNA per million cells, respectively. $CD34^+$ HSPCs were harvested 24 h postelectroporation and DNA was isolated using the NucleoSpin Tissue kit following the manufacturer's instructions (Macherey-Nagel). Polymerase chain reaction (PCR) amplification targeting the region susceptible to CRISPR-Cas9 editing was performed (primer sequences available in Table 1). After corroboration in 1% agarose gel, samples were purified using the QIAquick PCR Purification Kit (Qiagen) and Sanger sequenced (Eurofins Genomics).

The obtained results were analyzed and the InDel score was quantified by the ICE online tool (Inference of CRISPR Edits; Synthego). If applicable, Mann–Whitney nonparametric tests were performed to assess the difference in editing efficiency.

Flow cytometry

Flow cytometric measurements to monitor the cell viability, transfection efficiency, and phenotype of $CD34^+$ HSPCs were performed on day 2 after transfection using the MACSQuant analyzer 10 (Miltenyi Biotec). To determine cell viability, 7-aminoactinomycin (Miltenyi Biotec) or propidium iodide (Miltenyi Biotec) was added. The transfection efficiency was determined by measuring the mean fluorescent intensity of the $DsRed^+$ control cells. HSPCs were characterized by staining with two panels comprising anti-CD34-PE/Vio770 (REA1164), anti-CD133/1-APC (AC133), anti-CD45-VioBlue (5B1), or anti-CD34-PE/Vio770 (REA1164), anti-CD45RA-APC/Vio770 (T6D11), CD90-APC (REA897).

During erythroid differentiation, cells were analyzed by staining with three different panels: Panel I: CD34-VioBlue (REA1164) and CD36-APC (platelet glycoprotein 4, REA760). Panel II: CD235a-VioBlue (glycophorin A, REA175) and CD71-APC (transferrin receptor, REA902). Panel III: CD233-APC (Band3, REA368) and CD49d-FITC (α-4 integrin, MY18-24A9). All antibodies were obtained from Miltenyi Biotec. Data were analyzed using MACSQuantify software (Miltenyi Biotec).

In addition, for the automated process, cell recovery was determined for the $CD34^+$ HPSCs by quantification of viable cells on day 2 after electroporation. Where appropriate, nonparametric Mann–Whitney tests were performed to assess the difference in cell viability.

Colony-forming unit assay

The clonal ability of the edited and nonedited $CD34^+$ HSPCs was determined by performing a colony-forming unit (CFU) assay. Five hundred live cells resuspended in 300 μL of IMDM were added to 3 mL of StemMACS™ HSC-CFU complete with erythropoietin, human medium (Miltenyi Biotec) and equally distributed among two 35 mm wells (six-well plates). The plates were incubated for 14 days at 37°C and the resulting colonies were counted using a light microscope.

HSPC differentiation to the erythroid lineage

Erythroid *in vitro* differentiation of the transfected HSPCs was performed according to established protocols.[8,13,14] Briefly, $CD34^+$ HSPCs were cultured at a starting concentration of 10^4/mL in StemMACS HSC expansion medium supplemented with 2 mM of L-glutamine, 100 ng/mL of SCF (Miltenyi Biotec), 10 ng/mL of IL-3 (Miltenyi Biotec), 0.5 U/mL of human EPO (eBiosciences), 200 μg/mL of holo transferrin (Sigma Aldrich), and 100 U/mL of Pen/Strep for 7 days. For the second phase, the cells were seeded at a starting concentration of 10^5/mL in StemMACS HSC expansion medium supplemented as above, but with 3 U/mL of EPO and cultured for another 4 days. Cells were finally cultured at a starting concentration of 10^5/mL as in phase 1, but with 3 U/mL of EPO and 1 mg/mL of holo transferrin until day 21. Erythroid differentiation and maturation were monitored by flow cytometry on days 7, 14, and 21.

HbF quantification

For high-performance liquid chromatography (HPLC), cell pellets after 21 days of erythroid differentiation were frozen for further analysis. The frozen pellets were treated and processed as previously described.[8] The analysis was performed on a LaChrom Elite HPLC-system (Merck-Hitachi) using a gradient elution mode with a bis-tris buffer system (buffer A: bis-tris 20 mM, NH_4-acetate 13 mM, KCN 1 mM, and buffer B: bis-tris 20 mM, Na-acetate 38 mM, KCN 1 mM, NaCl 200 mM). Hemoglobin proteins were detected by absorbance measurements at 415 nm. Intracellular HbF was also determined on day 21 of erythroid differentiation utilizing intracellular anti-HbF-FITC staining according to the intracellular flow cytometry staining protocol (Miltenyi Biotec).

Analysis of thawed material

Cell pellets from the resulting sample of automated large-scale gene editing and its corresponding controls were resuspended in a freezing medium composed of 90% fetal bovine serum and 10% dimethyl sulfoxide (DMSO) as a cryoprotectant. The cryovials were stored at −80°C in a liquid nitrogen tank for 6 months. Then, samples were gently thawed in a warm water bath (37°C) and were subsequently washed with StemMACS HSC expansion medium (Miltenyi Biotec) without supplements to remove DMSO. Cells were counted and seeded at 1×10^6 cells/mL of culture using a prewarmed HSC maintenance medium (StemMACS HSC expansion medium supplemented with 100 ng of SCF, 20 ng of TPO, and 100 ng of Flt-3 ligand per milliliter of medium; Miltenyi Biotec) in a 24-well plate. The plate was placed in the incubator (37°C 5% CO_2) and 1 million cells' aliquots were taken at different time points for viability and genetic analyses (0, 1, 2, 4, and 24 h).

Results

Adaption of electroporation parameters for large-scale processing

A prescreening was performed to investigate the effect of different electroporation pulses on the transfection efficiency and viability of HSPCs. Small-scale electroporations using the TCA were performed to transfect DsRed mRNA as a reporter of transfection efficiency. Three different electroporation modes were compared: *square, burst,* and *bipolar burst* (*flip*). The *burst* pulse comprises a series of short 8 μs pulses. The pulse duration is given as the sum of the individual bursts. In bipolar mode, the field directions change after each burst.

The direct comparison using 600 V and 104 μs for the first pulse and 250 V for 2 ms for the second pulse indicates the highest transfection rate of nearly 80% for the *square* pulse, closely followed by the *flip* and the *burst* mode. Increasing the voltage of the first pulse decreased the viability of the cells for *square* pulses, whereas the bipolar mode gave comparable viabilities even when applying 800 V (Fig. 1A). Increasing the time for the second pulse enhanced the transfection efficiency. Higher second pulse voltages up to 300 V also improved the efficiency, but at the cost of lower viability. However, 400 V combined with a shorter duration of 0.75 ms is also a reasonable combination (Fig. 1A).

To mimic a clinical treatment scenario, the electroporation cuvette included in the CliniMACS Prodigy® EP-2 tubing set was manually filled with magnetically isolated $CD34^+$ HSPCs (94.2% ± 2% viable $CD34^+$ HSPCs among all viable white blood cells [WBCs]) to test the upscale of the electroporation conditions. In this context, *square* and *flip* settings with 600 V as the first pulse were selected to transfect HSPCs with BCL11A RNP as they proved to be highly efficient in the small-scale optimization (Fig. 1A). However, the observed editing performance was moderate (48–54%, Fig. 1B), indicating that further optimization was needed to achieve higher InDel rates. To proceed with the upscale screening of the most efficient electroporation settings, the *flip* protocol was set as it previously led to the highest *BCL11A* editing (54% InDel rate, Fig. 1B). For the first pulse, 600 V 104 μs burst/bipolar—8 μs burst, was applied.

FIG. 1. Study and optimization of electroporation conditions using CliniMACS Prodigy electroporator. **(A)** Small-scale pulse optimization using DsRed mRNA to determine the transfection efficiency (gray) and viability (white), $n = 2$. **(B)** Upscale *BCL11A* transfection using two of the most suitable electroporation settings in small-scale optimization led to moderate InDel efficiencies, $n = 1$. **(C)** Upscale comparison of different conditions to further optimize transfection efficiency. *BCL11A* editing is provided in InDel rate after Sanger sequencing of the PCR product (gray). Viability was determined by flow cytometry 2 days post-transfection (white), $n = 2$. Nonsignificant differences were observed for editing efficiencies in Mann–Whitney tests ($p > 0.05$). **(D)** Influence of different RNP concentrations (2250 pmol/mL, light gray; 4500 pmol/mL, dark gray; 6750 pmol/mL, black) with increasing cell concentrations (5×10^6 to 1.5×10^7 cells/mL) on the *BCL11A* editing rate, $n = 1$. **(E)** Same data as in **(D)**, but displayed as editing rate in relation to RNP concentration per 10^6 cells, $n = 1$. **(F)** Effect of the electroporation volume in CliniMACS Prodigy EP-2 cuvette on the editing performance (gray) and viability (white), $n = 2$. Nonsignificant differences were observed for editing efficiencies and viabilities in Mann–Whitney tests ($p > 0.05$). **(G)** RNP stability controlling freshly prepared RNP (control) versus RNP recovered after a process run and storage time of 60 min, $n = 1$. **(H)** Effect of the RNP incubation time on the editing rate (light gray) and viability (white), $n = 2$. Nonsignificant differences were observed for editing efficiencies and viabilities in Mann–Whitney tests ($p > 0.05$). **(I)** Average editing rate for thawed HSPCs from different donors, $n = 4$. **(J)** Comparison of *BCL11A* transfection efficiency after cultivation in the CliniMACS Prodigy system versus a classical cell incubator, $n = 1$. HSPCs, hematopoietic stem and progenitor cells; PCR, polymerase chain reaction; RNP, ribonucleoprotein.

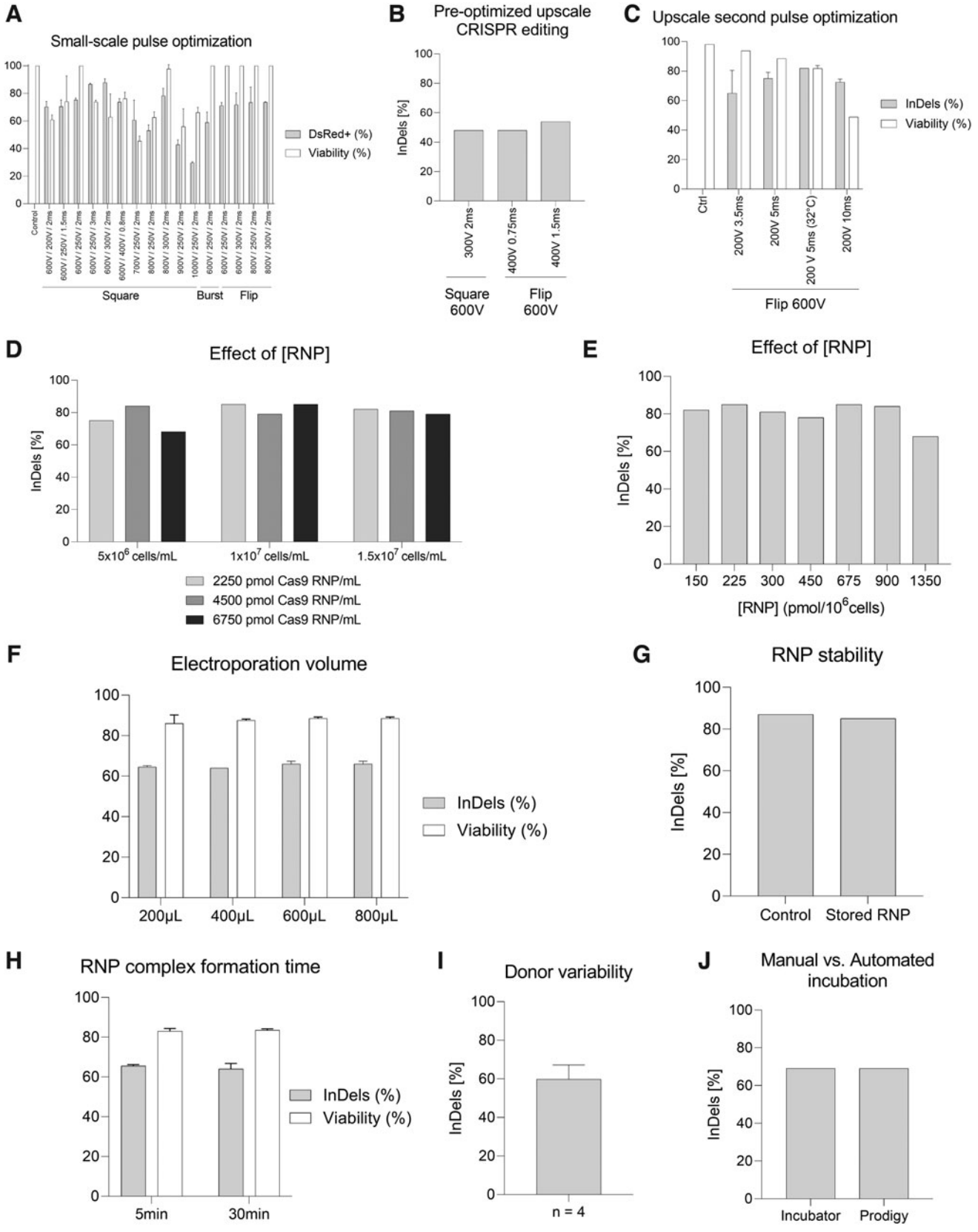
A
Small-scale pulse optimization
DsRed+ (%)
Viability (%)
Square
Burst
Flip
B
Pre-optimized upscale CRISPR editing
InDels [%]
300V 2ms
400V 0.75ms
400V 1.5ms
Square 600V
Flip 600V
C
Upscale second pulse optimization
InDels (%)
Viability (%)
Ctrl
200V 3.5ms
200V 5ms
200 V 5ms (32°C)
200V 10ms
Flip 600V
D
Effect of [RNP]
InDels [%]
5x10^6 cells/mL
1x10^7 cells/mL
1.5x10^7 cells/mL
2250 pmol Cas9 RNP/mL
4500 pmol Cas9 RNP/mL
6750 pmol Cas9 RNP/mL
E
Effect of [RNP]
InDels [%]
150 225 300 450 675 900 1350
[RNP] (pmol/10^6cells)
F
Electroporation volume
InDels (%)
Viability (%)
200µL
400µL
600µL
800µL
G
RNP stability
InDels [%]
Control
Stored RNP
H
RNP complex formation time
InDels (%)
Viability (%)
5min
30min
I
Donor variability
InDels [%]
n = 4
J
Manual vs. Automated incubation
InDels [%]
Incubator
Prodigy

To promote suitable viability, it was decided to decrease the voltage of the second pulse to 200 V since higher voltages, such as 300 V, have been shown to reduce viability (Fig. 1A). In addition, it was considered to increase the duration of the second pulse to promote efficient gene editing. By increasing the length of the second 200 V pulse from 3.5 to 5 ms, the efficiency of *BCL11A* editing was boosted (InDel rate from 65% ± 15.6% to 75% ± 4.3%, Fig. 1C). Further improvement was achieved by postincubation of the electroporated cells at 32°C (InDel score 82%, Fig. 1C). This ''cold shock'' has proven to increase InDels derived from nonhomologous end joining repair.[15] Further increase of the second pulse to 10 ms drastically harmed the viability of the samples (from ≈80% to 50%, Fig. 1C).

BCL11A editing is effective in a wide range of RNP and cell concentrations

Different RNP and cellular concentrations were tested to identify the most suitable composition during electroporation (Fig. 1D, E). Cells in the electroporation buffer were mixed with RNP and manually filled into the cuvette of the CliniMACS Prodigy EP-2 tubing set to simulate upscale conditions. The editing rate appeared robust within the range of tested RNP and cell concentrations with a slight tendency to lower editing rates for the low cell concentration of 5×10^6 cells/mL (Fig. 1D). Considering the RNP-to-cell ratio, as depicted in Figure 1E, comparable InDel rates of 78–85% were observed for 150–900 pmol of RNP per million cells. For the high RNP-to-cell ratio (1350 pmol per million cells), respectively, a cell concentration of 5×10^6 cells/mL combined with a high RNP concentration of 6750 pmol/mL, the editing rate dropped (InDel rate 68%, Fig. 1E).

A cell concentration of 1×10^7 cells/mL and an RNP concentration of 2250–6750 pmol/mL (225–675 pmol per million cells) during electroporation were depicted as the most effective condition for further experiments (Fig. 1D, E).

The selected transfection conditions work for different electroporation volumes

The typical filling volume during automated large-scale electroporation in the CliniMACS Prodigy electroporator is 600–650 μL. To investigate the potential impact of different electroporation volumes, a range of 200–800 μL was tested. Independent of the volume, the editing efficiency was consistent between all tested samples (InDel rate 64–66%, Fig. 1F).

CRISPR RNP complex stability is not a limiting factor in the editing process

The CliniMACS Prodigy electroporator sequentially electroporates 600–650 μL of cells per cycle with a cycle time of ≈30 s. The duration of the electroporation process will depend on the total volume to be processed. More specifically, we used 25 mL of cell suspension for the large-scale electroporation with an approximate duration of 40 min. We considered that the RNP might be degraded over time. To investigate the effect of storage at a defined room temperature (22°C), the remaining RNP complex of a large-scale electroporation was used in a small-scale electroporation using the TCA after a storage time of 1 h. The InDel rate was comparable with freshly prepared RNP (85% InDel rate, Fig. 1G).

In a different experiment, the RNP complex was additionally incubated at room temperature (22°C) for 5 and 30 min, showing similar results in the editing performance (InDel rate 65.5% ± 0.5% and 64% ± 2%, respectively, Fig. 1H). Within the tested time scale of up to 1 h, storage of the RNP complex has no impact on the editing efficiency.

Comparable editing rates can be reached for different donors

Cells from different donors can affect the experimental outcome. To assess the effect of individual variability of cellular fitness along the process, $CD34^+$ HSPCs from four different donors were thawed and processed. Although slightly different efficiencies can be observed, the editing was consistent in all samples (*BCL11A* InDel rate: 60 ± 7.3, Fig. 1I).

Culture conditions can be scaled up without impacting the cell product

The post-transfection recovery is crucial for gene editing and cell survival. The manual cultivation in the incubator was compared with the cultivation in the CCU of the CliniMACS Prodigy system. The editing performance was equivalent, indicating optimal conditions of the automated culture for transfection efficiency (69% InDel rate, Fig. 1J).

BCL11A knockout in $CD34^+$ HSPCs is efficient in a large-scale scenario with clinically relevant cell numbers

After the identification of the most suitable electroporation parameters and conditions for efficient *BCL11A* editing, a large-scale run was performed. $CD34^+$ HSPCs were isolated from a mobilized leukapheresis using the CliniMACS CD34 enrichment. 2.1×10^8 $CD34^+$ HSPCs

(94.7% viable $CD34^+$ HSPCs among all viable WBCs) were further processed using the TCE process on the CliniMACS Prodigy. On day 2, 1.1×10^8 cells were harvested (52% recovery, Fig. 2A) and further analyzed. The editing efficiency of the upscale control and large-scale samples was 80–86% and 71–74%, respectively, with a viability of 76.9% and 80.8%, which was similar to 85% viable cells observed for nontransfected control (NTC) (Fig. 2A).

The differentiation potential of $CD34^+$ HSPCs is not compromised after *BCL11A* knockout and HbF resurgence is independent of the production scale

CFU assays were conducted to determine the proliferation and differentiation potential of the electroporated cells and therefore assess whether the cells remained functional. Cells were seeded immediately after separation (baseline, day 0) and compared with the samples with cells after electroporation and cultivation in the CliniMACS Prodigy on day 2 (Fig. 2B). The cells developed into the typical myeloid colonies exhibiting very similar total colony counts, as well as distributions of colony types among the samples.

To corroborate that the differentiation potential of the edited HSPCs is not compromised and to investigate the induced expression of HbF in the edited cells, an *in vitro* erythroid differentiation protocol was performed. The expression of relevant differentiation markers was assessed during the differentiation on days 7, 14, and 21 (Fig. 2C). Whereas the purity of $CD34^+$ cells was typically more than 95% after separation and 2 days of culture, the expression decreased during the differentiation below the detection limit at day 14 (Fig. 2C and Supplementary Fig. S1A). Along the differentiation, CD36 (an early marker for erythroid differentiation)[16] increased from day 7 to 14 and decreased until day 21. CD233 and CD235a erythrocyte markers[17] increased their positive population from below 20% and 5% to roughly 90% and 75% on day 21 as described during erythropoiesis (Fig. 2C and Supplementary Fig. S1B, C).

High expression of CD49d was reported on day 14, but it dropped below 5% on day 21 as expected in the late stage of erythroid differentiation (Fig. 2C and Supplementary Fig. S1C).[14] More than 80% of the cells expressed CD71 on day 7, maintaining high expression levels until day 21. This observation correlates with the development of proerythroblasts to basophilic and polychromatophilic erythroblasts and finally late-stage orthochromatic erythroblasts[17] (Fig. 2C and Supplementary Fig. S1). Both upscale and large-scale samples reported similar receptor expression levels to those observed in the NTC. $CD34^-$, $CD235a^+$, $CD71^+$ cells indicate hemoglobin-expressing, mature differentiated erythrocytes as required for the analysis of HbF expression.[18]

Concerning HbF resurgence after *BCL11A* disruption, flow cytometry and HPLC analyses revealed an upregulation of HbF in upscale and large-scale samples (Fig. 2D–F). The HbF staining and flow cytometry analyses indicate HbF induction in the differentiation control sample, increasing from 16% on day 7 to 64% and 67% on days 14 and 21, respectively (Fig. 2D). However, the rate of HbF expressing cells appeared higher for the edited cells with 19%, 97%, and 84% for the upscale control sample and 21%, 83%, and 83% for the large-scale sample processed on the CliniMACS Prodigy (Fig. 2D).

FIG. 2. Large-scale *BCL11A* editing of HSPCs using CliniMACS Prodigy system with electroporator compared with NTC, NTCe, and upscale controls using the CliniMACS Prodigy EP-2 cuvette. **(A)** *BCL11A* editing at the genomic level ($n = 1$ with technical replicates), cellular viability, and recovery at day 2 after electroporation ($n = 1$). **(B)** CFU assay of large-scale samples compared with upscale samples. Total colonies counted for 250 seeded HSPCs (left) and proportion of different colonies, $n = 1$ with technical replicates. **(C)** Erythroid differentiation staining on days 7, 14, and 21. Positive rate by flow cytometry for CD34, CD36, CD235a, CD71, CD233, and CD49d, mock electroporated cells (NTCe) (dark gray), upscale control electroporation (light gray), and cells electroporated by the CliniMACS Prodigy process (white), $n = 1$. **(D)** HbF levels of electroporated samples measured by flow cytometry on days 7, 14, and 21. **(E)** HbF/(HbF+HbA_0) ratio as determined by HPLC analysis of normal control cells, HbF expressing control cells, and processed cells after additional erythroid differentiation: mock electroporated cells (NTCe), upscale control electroporated cells, and cells electroporated by the CliniMACS Prodigy process, $n = 1$. **(F)** HPLC chromatograms of HbF expressing control cells and electroporated samples after *in vitro* erythroid differentiation. BFU-E, burst-forming unit-erythroid; CFU, colony-forming unit; CFU-G, CFU-granulocyte; CFU-GEMM, CFU-granulocyte erythrocyte macrophage megakaryocyte; CFU-GM, CFU-granulocyte macrophage; CFU-M, CFU-macrophage; HbF, fetal hemoglobin; HPLC, high-performance liquid chromatography; NTC, nontransfected controls; NTCe, electroporated nontransfected controls.

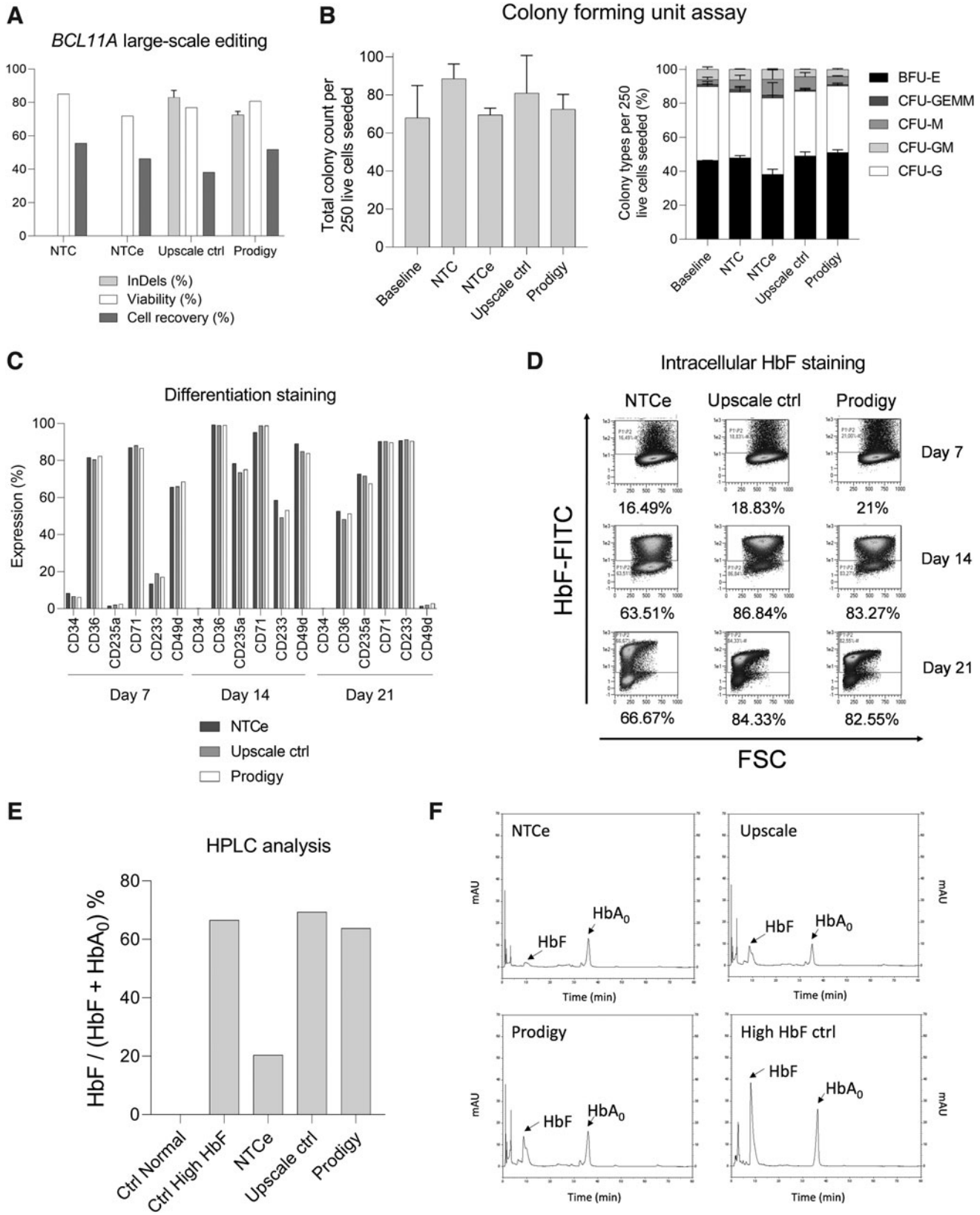
A
BCL11A large-scale editing
100
80
60
40
20
0
NTC
NTCe
Upscale ctrl
Prodigy
InDels (%)
Viability (%)
Cell recovery (%)
B
Colony forming unit assay
Total colony count per 250 live cells seeded
Baseline
NTC
NTCe
Upscale ctrl
Prodigy
Colony types per 250 live cells seeded (%)
BFU-E
CFU-GEMM
CFU-M
CFU-GM
CFU-G
C
Differentiation staining
Expression (%)
CD34
CD36
CD235a
CD71
CD233
CD49d
Day 7
Day 14
Day 21
NTCe
Upscale ctrl
Prodigy
D
Intracellular HbF staining
NTCe
Upscale ctrl
Prodigy
Day 7
Day 14
Day 21
16.49%
18.83%
21%
63.51%
86.84%
83.27%
66.67%
84.33%
82.55%
HbF-FITC
FSC
E
HPLC analysis
HbF / (HbF + HbA0) %
Ctrl Normal
Ctrl High HbF
NTCe
Upscale ctrl
Prodigy
F
NTCe
Upscale
Prodigy
High HbF ctrl
HbF
HbA0
mAU
Time (min)

The HPLC analysis corroborates the cytometry data with an HbF to HbF plus HbA ratio of 20.4% for the electroporated but nontransduced control, 69.3% for the upscale, and 63.8% for the large-scale electroporation sample (Fig. 2E, F). The HbF expression, besides the spontaneous or differentiation-induced HbF expression in the control sample, resembles the editing rate on the genomic level.

Freeze and thawing of edited HSPCs decreased the *BCL11A* knockout population

After the large-scale run, samples were frozen and stored at −80°C for 6 months to analyze the InDel score and evaluate the recovery of the cells after thawing. Unexpectedly, there was a reduction in *BCL11A* editing for both upscale control and large-scale electroporation samples (from 86% to 67% and 74% to 54%, respectively, Fig. 3A). Genetic analyses were performed with the large-scale sample at different time points after thawing to assess this observation, revealing a similar InDel score (54–59% at 0–4 h, Fig. 3B) that was moderately increased after 24 h (66% InDels, Fig. 3B). The thawed cells showed high viability (82–86%, Fig. 3B) and consistent cellular numbers during the first few hours after thawing (9.4×10^5–1.12×10^6 cells/mL at 0–4 h, Fig. 3C), whereas a decline was observed after 24 h (7.6×10^5 cells/mL, Fig. 3C).

Discussion

Hemoglobinopathies are among the most common human genetic disorders worldwide.[19] Besides hematopoietic stem cell transplantation (HSCT), there has been no curative transfusion-dependent β-thalassemia (TDT) and SCD. However, gene therapies either using viral vectors or genome editing strategies could overcome this shortcoming. In this context, the first gene therapy based on *ex vivo* transduced HPSCs to integrate a modified form of the β-globin gene has just recently been approved by the FDA.[20]

We investigated different gene editing approaches and considered *BCL11A* a promising target.[8] In a proof-of-principle investigation, editing of the *BCL11A* locus has shown clinical benefit for β-thalassemia (TDT) and SCD patients.[7] As for other individualized cell therapies, safe and cost-efficient production is crucial for the future availability of these treatments. Therefore, in parallel to clinical developments, we were aiming to improve traditional GMP gene editing approaches and implement the whole cell engineering protocol in an automated closed system. Predefined electroporation pulses are often used and the respective parameters such as voltage or pulse duration cannot be adapted. As shown in this work, optimizing the used conditions enables to balance transfection efficiency and cell survival.

Traditionally, different devices are used, for example, for cell concentration, culture, and electroporation. Accordingly, the respective instruments need to be operated individually and cells have to be transferred in between. Reducing manual and open steps is important to minimize risks during production. In this way, the impact of different operators is also diminished and reproducibility can be improved.[21]

Apart from that, scalability will be a prerequisite to serving patients, especially for prevalent diseases such

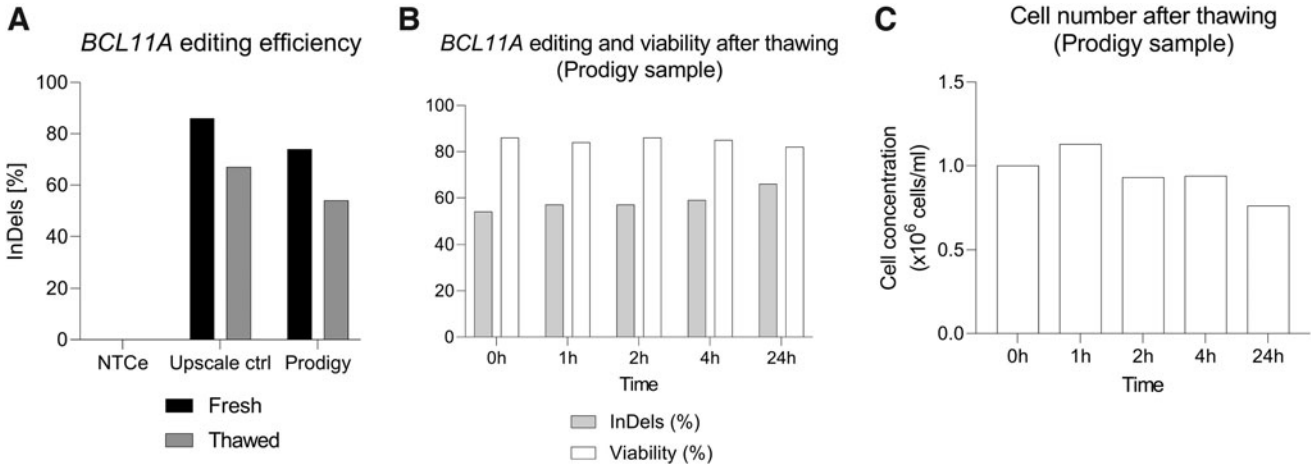

FIG. 3. Effect of freezing/thawing cycle in gene editing and viability. **(A)** *BCL11A* editing efficiency comparison of freshly edited HSPCs versus thawed edited HSPCs after freezing storage at −80°C for 6 months, $n=1$. **(B)** Time course analysis of *BCL11A* editing efficiency and cellular viability after thawing for large-scale Prodigy sample. **(C)** Time course analysis of cell number after thawing for large-scale Prodigy sample.

as hemoglobinopathies. As discussed during the annual ISCT meeting, the availability of trained staff can be a challenge for sophisticated cell products.[22] Simplified procedures and automation will relieve some of the tasks, allowing to focus on monitoring the production processes. As personnel costs have been addressed for up to 47% of the total costs,[23] lowering the workload is expected to also substantially contribute to cost-effectiveness.

Another considerable cost factor is the necessary clean room facilities. In this study, using a closed system for the production of cellular therapies could overcome the limitation of a single-cell product manufactured per clean room.[23] Thereby, the fixed costs for the facility could be reduced by parallel production. Considering reliable production procedures and cost-effectiveness is not only relevant for late clinical trials or commercial manufacturing, but can be critical already during early developments.

With our work, we tackled some challenges related to different scales and automations. To achieve reasonable throughput, the electroporation volume is increased compared with the manual electroporation systems. The raised conductivity bears the risks of impaired transfection efficiency. To address this issue, we adapted the electroporation pulse (Fig. 1C) and confirmed the reproducible performance for increasing electroporation volumes (Fig. 1F).

The electroporation process on the CliniMACS Prodigy system performs cyclic electroporations until all cells are processed. The volume of cells that can be processed during electroporation (25–200 mL) with a recommended concentration of up to 5×10^7 cells/mL represents a feasible scale for clinical applications. The system has been designed to store the material to be electroporated, that is, the RNP, in a separate bag. Thereby, the risk of RNA degradation is minimized as the two fractions are mixed for each cycle just before the electroporation. However, deviations in the mixing ratio could impair the editing efficiency. We have shown that the CRISPR editing efficiency is sustained in a wide range of RNP and cellular concentrations (Fig. 1D, E).

Another concern had been the storage of the RNP during the processing time. Material loss, for example, by nonspecific binding to the storage bag or dissociation of the RNP complex could lead to a decreased efficiency over time. The editing efficiency was shown to be robust after the common duration of clinical-scale electroporation (storage time of 1 h, Fig. 1G).

Besides the electroporation itself, also the culture conditions might influence the results. In a direct comparison, we observed no differences between the automated process in the CentriCult Unit (CCU) of the CliniMACS Prodigy and cells cultured under standard incubation conditions in an incubator (Fig. 1J).

To assess the effect of individual variability of cellular fitness along the process, frozen HSPCs from four different healthy donors were tested. The editing efficiencies were very similar (Fig. 1I). Moderate editing could be a result of the use of thawed cellular material, which is also observable for the thawed cell samples used in other experiments reported in this publication (Fig. 1F, H, J) and is consistent with previous research conducted in the immunotherapy field.[8]

After the optimization screenings, we performed a clinical-scale production run. For this purpose, purified HSPCs (94.7% viable $CD34^+$ HSPCs among all viable WBCs) were processed in the CliniMACS Prodigy with the electroporator system using the CliniMACS Prodigy TS 520 and CliniMACS Prodigy EP-2 set. Posterior genomic studies revealed high disruption in *BCL11A* enhancer (Fig. 2A). Normal HSPC functionality and increased HbF levels were observed after CRISPR treatment, thereby proving the success of the strategy and feasibility of the overall process (Fig. 2B–F). With a yield of 52% (Fig. 2A), a clinically relevant cell number of about 1×10^8 cells were harvested from the isolated $CD34^+$ cells.

According to the American Society for Blood and Marrow Transplant (ASBMT), the minimum recommended stem cell dose for autologous HSCT is 2×10^6 $CD34^+$ cells/kg.[24] Accordingly, the cell product of 1×10^8 $CD34^+$ cells would be sufficient for the treatment of a 50 kg patient. Taking the recommended stem cell collection target of $3–5 \times 10^6$ $CD34^+$ cells per kilogram into account, we demonstrated the feasibility of the process for future clinical use.[24] As in our experiments, the cell number is typically limited by mobilization of HSPCs and the apheresis. Due to the additional manipulation steps for cell engineering and the related cell losses, mobilization, apheresis, and the production process need to be well balanced with the potential cell doses. The clinical-scale run had been intended as proof-of-principle experiment and further technical runs will be needed to confirm the reproducibility of the performance and suitability for routine use.

Finally, one of the most critical processes in HSPC gene therapy lies in the logistics from the manufacturing to the clinical site and the maintenance of the so-called cryochain.[25] As common clinical procedures involve gene editing, expansion, and freezing of the cellular material in specialized centers for subsequent transportation, thawing, and administration to the patient in the clinic,[7] the large-scale processed sample was frozen for 6 months

and thawed for genetic and viability analyses up to 24 h. While cell numbers were properly maintained with high viability during the first hours, it was observed a reduction in the *BCL11A* knockout population right after thawing in comparison with freshly edited cells (Fig. 3).

We hypothesize that this result could be explained by the superior cellular resilience of unedited cells compared with the CRISPR-edited ones against freezing stress. More runs would be needed to assess this potential negative effect derived from freezing and thawing cycles in clinical-scale gene editing efficiency. In addition, the freezing and thawing process was performed with conventional laboratory protocols, and thereby a different outcome can be expected following clinical standard procedures. Nonetheless, the use of thawed material has been associated with higher risks of cell loss during therapy development and graft failure.[25–28] On-site automated production by CliniMACS Prodigy can facilitate the usage of fresh material, suitably bypassing the challenging cryochain and favoring timely treatment availability. Still, it is important to remark that the use of fresh material can interfere with necessary quality controls and gene editing assessments as it would require a much faster application to the patient than cryopreserved cells.

As a consequence, the use of fresh cells for human therapy is mainly suspended in Europe since 2007 due to the adoption of the European Union Tissues and Cells Directive (EUTCD).[28] The routine use of fresh material, despite being highly desirable, still needs the optimization of quality assessments and GMP-compliant protocols to make it feasible in the clinic.

Conclusions

The large-scale run results indicate that efficient editing could be obtained at the clinical scale using CRISPR-Cas9 transfection in the CliniMACS Prodigy system with electroporator. Gene-edited HSPC generation and the subsequent cultivation for the treatment of β-hemoglobinopathies can be performed in a closed and automated system, enabling feasible on-site production that could potentially translate into clinical trials similar to NCT03655678 and NCT03745287. In addition, the generated protocol can be transferred to other diseases whose treatment is based on HSCT. In this way, we hope to contribute to accelerating cellular gene therapy accessibility in the near future and support the development of novel treatments for patient care.

Authors' Contributions

G.U.-B.: Conceptualization, investigation, visualization, data curation, writing—original draft, and writing—review and editing (equal). M.B.: Conceptualization, investigation, visualization, data curation, writing—original draft, and writing—review and editing (equal). T.G.: Investigation. F.A. Investigation. J.Q.: Investigation. D.K.: Investigation. A.D.-M.: Investigation. A.L.-C.: Investigation. T.E.: Investigation, resources, and supervision. R.H.: Conceptualization, resources, and supervision. S.W.: Conceptualization, resources, supervision, and writing—review and editing (equal). M.M.: Conceptualization, resources, supervision, and writing—review and editing (equal).

Author Disclosure Statement

M.B., T.G., F.A., J.Q., D.K., and S.W. are employed at Miltenyi Biotec. The rest of the authors declare no conflict of interest.

Funding Information

This work was supported by Miltenyi Biotec, Clinician Scientist Program (No. 440-0-0), Stefan Morsch Stiftung, and the University Children's Hospital of Tübingen.

Supplementary Material

Supplementary Figure S1

References

1. González-Romero E, Martínez-Valiente C, García-Ruiz C, et al. CRISPR to fix bad blood: A new tool in basic and clinical hematology. Haematologica 2019;104:881–893; doi: 10.3324/haematol.2018.211359
2. Liang X, Potter J, Kumar S, et al. Rapid and highly efficient mammalian cell engineering via Cas9 protein transfection. J Biotechnol 2015;208:44–53; doi: 10.1016/j.jbiotec.2015.04.024
3. Grote S, Ureña-Bailén G, Chan KC-H, et al. In vitro evaluation of CD276-CAR NK-92 functionality, migration and invasion potential in the presence of immune inhibitory factors of the tumor microenvironment. Cells 2021;10:1020; doi: 10.3390/cells10051020
4. Mandal PK, Ferreira LMR, Collins R, et al. Efficient ablation of genes in human hematopoietic stem and effector cells using CRISPR/Cas9. Cell Stem Cell 2014;15:643–652; doi: 10.1016/j.stem.2014.10.004
5. Brunetti L, Gundry MC, Kitano A, et al. Highly efficient gene disruption of murine and human hematopoietic progenitor cells by CRISPR/Cas9. J Vis Exp 2018134:57278; doi: 10.3791/57278
6. Liu X, Zhang Y, Cheng C, et al. CRISPR-Cas9-mediated multiplex gene editing in CAR-T cells. Cell Res 2017;27:154–157; doi: 10.1038/cr.2016.142
7. Frangoul H, Altshuler D, Cappellini MD, et al. CRISPR-Cas9 gene editing for sickle cell disease and β-thalassemia. N Engl J Med 2020;384:252–260; doi: 10.1056/NEJMoa2031054
8. Lamsfus-Calle A, Daniel-Moreno A, Antony JS, et al. Comparative targeting analysis of KLF1, BCL11A, and HBG1/2 in CD34+ HSPCs by CRISPR/Cas9 for the induction of fetal hemoglobin. Sci Rep 2020;10:10133; doi: 10.1038/s41598-020-66309-x
9. Daniel-Moreno A, Lamsfus-Calle A, Raju J, et al. CRISPR/Cas9-modified hematopoietic stem cells—Present and future perspectives for stem cell transplantation. Bone Marrow Transplant 2019;54:1940–1950; doi: 10.1038/s41409-019-0510-8
10. Bauer DE, Kamran SC, Orkin SH. Reawakening fetal hemoglobin: Prospects for new therapies for the β-globin disorders. Blood 2012;120:2945–2953; doi: 10.1182/blood-2012-06-292078
11. Lino CA, Harper JC, Carney JP, et al. Delivering CRISPR: A review of the challenges and approaches. Drug Deliv 2018;25:1234–1257; doi: 10.1080/10717544.2018.1474964

12. Glass Z, Lee M, Li Y, et al. Engineering the delivery system for CRISPR-based genome editing. Trends Biotechnol 2018;36:173–185; doi: 10.1016/j.tibtech.2017.11.006
13. Dever DP, Bak RO, Reinisch A, et al. CRISPR/Cas9 β-globin gene targeting in human haematopoietic stem cells. Nature 2016;539:384–389; doi: 10.1038/nature20134
14. Dulmovits BM, Appiah-Kubi AO, Papoin J, et al. Pomalidomide reverses γ-globin silencing through the transcriptional reprogramming of adult hematopoietic progenitors. Blood 2016;127:1481–1492; doi: 10.1182/blood-2015-09-667923
15. Guo Q, Mintier G, Ma-Edmonds M, et al. 'Cold shock' increases the frequency of homology directed repair gene editing in induced pluripotent stem cells. Sci Rep 2018;8:2080; doi: 10.1038/s41598-018-20358-5
16. Hu J, Liu J, Xue F, et al. Isolation and functional characterization of human erythroblasts at distinct stages: Implications for understanding of normal and disordered erythropoiesis in vivo. Blood 2013;121:3246–3253; doi: 10.1182/blood-2013-01-476390
17. Chen K, Liu J, Heck S, et al. Resolving the distinct stages in erythroid differentiation based on dynamic changes in membrane protein expression during erythropoiesis. Proc Natl Acad Sci U S A 2009;106:17413–17418; doi: 10.1073/pnas.0909296106
18. Romero Z, Urbinati F, Geiger S, et al. β-globin gene transfer to human bone marrow for sickle cell disease. J Clin Invest 2013;123:3317–3330; doi: 10.1172/JCI67930
19. Mussolino C, Strouboulis J. Recent approaches for manipulating globin gene expression in treating hemoglobinopathies. Front Genome Ed 2021;3:618111; doi: 10.3389/fgeed.2021.618111
20. FDA Approves First Cell-Based Gene Therapy to Treat Adult and Pediatric Patients with Beta-thalassemia Who Require Regular Blood Transfusions. Available from: https://www.fda.gov/news-events/press-announcements/fda-approves-first-cell-based-gene-therapy-treat-adult-and-pediatric-patients-beta-thalassemia-who (Last accessed: August 25, 2022).
21. Sarah Callens JH, McCoy R, Ward S. Cell and gene therapy manufacturing: The necessity for a cost-based development approach. Cell Gene Ther Insights 2016;2:115–120; doi: 10.18609.cgti.2016.014
22. ISCT provided post-pandemic venue for the entire cell and gene therapy sector to generate solutions to the major barriers to providing therapies to patients. Available from: https://www.isctglobal.org/telegrafthub/blogs/audrey-le/2022/07/24/isct-publishes-conclusions-and-consensus-from-its [Last accessed: November 1, 2022].
23. ten Ham RMT, Hövels AM, Hoekman J, et al. What does cell therapy manufacturing cost? A framework and methodology to facilitate academic and other small-scale cell therapy manufacturing costings. Cytotherapy 2020;22:388–397; doi: 10.1016/j.jcyt.2020.03.432
24. Giralt S, Costa L, Schriber J, et al. Optimizing autologous stem cell mobilization strategies to improve patient outcomes: Consensus guidelines and recommendations. Biol Blood Marrow Transplant 2014;20:295–308; doi: 10.1016/j.bbmt.2013.10.013
25. Meneghel J, Kilbride P, Morris GJ. Cryopreservation as a key element in the successful delivery of cell-based therapies—A review. Front Med (Lausanne) 2020;7:59222.
26. Dholaria B, Malki MMA, Artz A, et al. Securing the graft during pandemic: Are we ready for cryopreservation for all? Biol Blood Marrow Transplant 2020;26:e145–e146; doi: 10.1016/j.bbmt.2020.04.009
27. Hornberger K, Yu G, McKenna D, et al. Cryopreservation of hematopoietic stem cells: Emerging assays, cryoprotectant agents, and technology to improve outcomes. Transfus Med Hemother 2019;46:188–196; doi: 10.1159/000496068
28. Cottle C, Porter AP, Lipat A, et al. Impact of cryopreservation and freeze-thawing on therapeutic properties of mesenchymal stromal/stem cells and other common cellular therapeutics. Curr Stem Cell Rep 2022;8:72–92; doi: 10.1007/s40778-022-00212-1

Received: August 26, 2022
Accepted: December 9, 2022
Online Publication Date: January 20, 2023